Improved Extraction of Natural Fibers for Sustainable Polymer Composites

by

Anshul Singhal

A dissertation submitted in partial fulfillment
of the requirements for the degree of
Doctor of Philosophy
(Materials Science and Engineering)
in the University of Michigan
2023

Doctoral Committee:

Professor Alan I. Taub, Chair
Professor Mihaela Banu
Professor Nicholas A. Kotov
Professor Brian J. Love

Anshul Singhal

ansinghl@umich.edu

ORCID iD: 0000-0002-4762-5062

DEDICATION

This dissertation is dedicated to my family, my mentors, and my friends.

I couldn't have done this without you!

ACKNOWLEDGEMENTS

Pursuing a doctorate degree perhaps the most difficult thing I did in my life, and it not only shaped me academically but at the personal level too. While rest of this dissertation may be the result of my intellect, but here from my heart I am expressing my gratitude for the support I got from all the people during this journey.

To begin with, I would like to thank my advisor, Prof. Alan Taub, for giving me this opportunity and his constant support through all these years. Thank you for bringing the best in me, while giving me the space to improve over my weak areas and always motivating me to take the right path, even if it is the difficult one. From you, I learn the essence of true problem solving that as a scientist or an engineer, one must possess, which helped me taking on the challenges during different phases of the research in this dissertation, when I did not have the background or any prior knowledge to begin with.

I am grateful to my committee members- Prof. Mihaela Banu, Prof. Brian Love and Prof. Nicholas Kotov for their creative ideas, insightful feedback, support, and direction. I am especially thankful to Prof Banu, for coaching me on the mechanics part of this dissertation and providing me the computational resources for developing finite element models seen in Chapter 3.

I want to acknowledge the funding support for this research - University of Michigan-Global CO_2 Initiative under Blue Sky Initiatives and Ford Motor Company. I am thankful to our industry collaborators from Ford- Dr. Deborah Mielewski and Dr. Alper Kiziltas for their insights and direction during our weekly meetings.

Further, I am grateful to our collaborators at University of Michigan: Prof Judy Jin and Jin-Yang Hu from IOE for the statistical support seen in Chapter 2; Prof Ellen Aruda and Andrea Poli from ME for the DMA instrument support in bending tests seen in Chapter 3; and Prof. Henry Sodano and Dr. Kelsey Steinke from MS&E for providing the composite sample design seen in Chapter 4.

I am thankful to the Materials Science & Engineering, Van Vlack Laboratory Staff- Keith McIntyre, Ying Qi, Dr. Tim Chambers and Dr. Sahar Farjami, for training me on testing equipment and providing me timely support to solve any small to big equipment related issues for smooth running of my experiments, without whom I simply cannot imagine this dissertation possible. I am thankful to the Materials Science and Engineering department's administrative staff- Renee Hilgendorf, Shelley Fellers, Debbie Johnson, Patti Vogel, and Ellen Kampf for all the support from ordering supplies to solving any admin issues in between.

Now, I can't be thankful enough to the Taub group, a family I found away from home. Thank you, Dr. Caleb Reese, for convincing me to join the group and your mentorship all these years. Thank you, Dr. Avi Bregman, Dr. Wesley Chapkin, Dr. Yipeng He, Dr. Maya Nath, and Dr. Xun Liu for welcoming me to the lab and the project at that time. Probably the greatest strength of Taub group is the diversity of knowledge people possess here that really helped me in solving problems from time to time and for that I am grateful to you all- Dr. Aaron Gradstein, Dr. Dandan Zhang, Kanat Anurakparadorn, Randy Cheng, Jon Goettsch, Amy Langhorst, Anita Luong, Allison Podnar, and Xingkang She. Further, I am thankful to the natural fiber team, specially Amy Langhorst for being my support in this project all these years and contributing good ideas with valuable feedback time to time, that really helped me improve the quality of my research. I am

also thankful to the undergraduate student researchers- Jonah Chad and Jonah Berman for their support during fiber tensile tests.

I would like to thank my undergraduate mentors in India- Dr. Roli Purwar (Professor - Delhi Technological University) and Dr. DK Chattopadhyay (General Manager - R&D, HIL Limited) for introducing me to the field of research and developing the scientific curiosity towards technical innovation, that led me here.

I am grateful to my friends I found here, that have been an emotional support and the source for my laughter & fun times. Thank you for making my stay in Michigan memorable, Dandan, Kat, Aaron, Randy, Akshay, Rajan, Puneet, Ripu, to name but a few. Also, I am thankful to my lifelong best friends scattered around the globe but doesn't seem too far- Himanshu Goel, Kshitiz, Ankit, Himanshu Jain and Himanshi.

Lastly, I want to express my gratitude to my parents, Anita Singhal & Sanjay Singhal, and my sister, Arushi Singhal, for their unconditional love and support. I am grateful to all they have sacrificed for me and without whom none of this would be possible.

TABLE OF CONTENTS

LIST OF TABLES

LIST OF FIGURES

ABSTRACT

With increasing amount of global CO_2 levels, the demand of carbon negative materials has significantly increased. Natural fibers such as flax which are found on the outer bast region of the plant stem, are gaining importance due to their high specific mechanical properties as a sustainable replacement to glass fiber in polymer composites. But implementing these fibers in industry scale structural composite applications is limited by the high variability in their properties since the composite must be designed to the lower bound of mechanical properties. Besides being inherent, the current process of extraction is a major reason for this variability, which is a mechanized version of a traditional process being used for hundreds of years for textile use of these fibers and has not been optimized for production of high-quality natural fibers for composite application.

During processing, the stems initially go through a process called dew retting, where the bonding of the bast fiber layer with the stem's woody core is degraded by microbial activity in the field, which is inconsistent, limited to conditions of weather and results in fibers with non-uniform diameters. The next mechanical breaking step, where these retted stems are crushed between the rotating gear rollers to separate the bast fiber layer, further induces fiber damage under high bending strains leading to degradation & high variation in mechanical properties of these fibers.

The research in this dissertation is aimed at improving natural fiber quality and reducing variability in mechanical properties by elucidating the cause and eliminating the fiber damage occurring through various steps in the natural fiber extraction process. Here, first a lab scale-controlled retting is established using specific enzymes to overcome the limitations of the conventional dew retting for uniform fiber debonding within the plant stem. In this enzymatic

retting process, the effect of enzyme concentration & retting duration on the bast-woody core bond strength and resulting fiber diameters is studied by developing mechanical fiber peel tests and microscopy coupled with statistical analysis. It is observed that while the resulting fiber diameters are only affected by retting duration, the bond strength between the bast-woody core interphase is significantly affected by both enzyme concentration and duration of retting. Moreover, from single fiber tensile tests conducted on fibers resulting from different retting conditions, an optimal enzyme retting condition is chosen for later mechanical extraction.

To further understand the underlying mechanism of fracturing of these stems during the mechanical breaking step leading to fiber damage, compression and bending tests of retted flax stems is done along with visual observation of the fracture occurring inside the woody core. Finite element modeling (FEM) is implemented for bending analysis of stems under a range of tool geometries and is used as a guide to design an improved roller profile for a lab scale stem breaker. Further, significant improvement in tensile properties of extracted fibers from this improved breaking process is seen when compared to fibers extracted under high bending strains.

Finally, long continuous fibers from multiple stems at a time is extracted from the improved extraction process and the fiber yield is evaluated at each step. These fibers are then used to make unidirectional fiber composites. Longitudinal tensile tests are conducted on these composite samples and fiber properties are back calculated using composite's rule of mixtures. These back calculated fiber properties are found comparable to fibers properties evaluated using single fiber tensile tests. A systematic approach in this dissertation elucidates the effect of retting conditions and fiber property evaluation methods to guide the optimization of extraction process at larger scale for producing high quality natural fibers for sustainable composites.

Chapter 1
Introduction

1.1 Motivation

Natural fibers, earlier known for their use in clothing, structural and building applications, has gained more attention over the last decade as a composite reinforcement in polymers by both academia and industries over the world due to their environmental, economic and social benefit [1–5]. The automotive industry is now seeing natural fibers as viable alternative to synthetic fibers in polymer composites due to their potential in light weight applications [4,6–8]. Beside advantages like low production cost with low density and high specific strength [6,9–12] when compared to synthetic alternatives like glass fibers; CO_2 neutrality of natural fibers is particularly attractive to aid greenhouse effect and world's climate change [13]. However, composite performance directly depends upon the reinforcement and currently, these natural fibers face limitation to implement at industrial scale in high performance composite applications due to the high variability in properties (as seen in **Table 1.1**), partly being inherent in the plant and also from the process of extraction [6,9].

Table 1.1 Plant fiber properties found in literature compared to industry extracted flax and E-glass [5,14,23,15–22]

Properties	**Bamboo**	**Hemp**	**Flax**	**Flax[a]**	**E-Glass**
Density (ρ) [g/cm^3]	1	1.48	1.45	1.45	2.55
Tensile strength (TS) [MPa]	100-860	150-1110	200-1400	200-750	2400
Modulus (M) [GPa]	6-46	10-60	20-80	20-40	73
Specific Modulus [M/ρ]	6-46	7-40	14-55	14-28	29
Specific Strength [TS/ρ]	100-860	100-750	138-965	138-517	940

[a] industry extracted fibers by Fibrevolution™

Flax plant fibers as seen from **Table 1.1** have been extensively studied in previous literature due to their superior mechanical properties when compared to other plant fiber crops, and hence are chosen during various studies in this dissertation. Furthermore, upon putting flax and glass modulus values to evaluate composite's modulus with varying volume fraction of fibers using simple rule of mixtures in **Figure 1.1**, we can see the upper and lower bound of flax fiber composite modulus, where the upper bound modulus is higher than glass fiber composite values. However, the flax fibers from the current industry extraction process, as the case of our current collaborator in Oregon- Fibrevolution™, when used in this example shows composite modulus in the range lower than the average. Also, the composite design for structural application is limited to lower bound of fiber mechanical properties. Hence, the goal of the research in this dissertation is to increase this mean and lower bound of fiber properties.

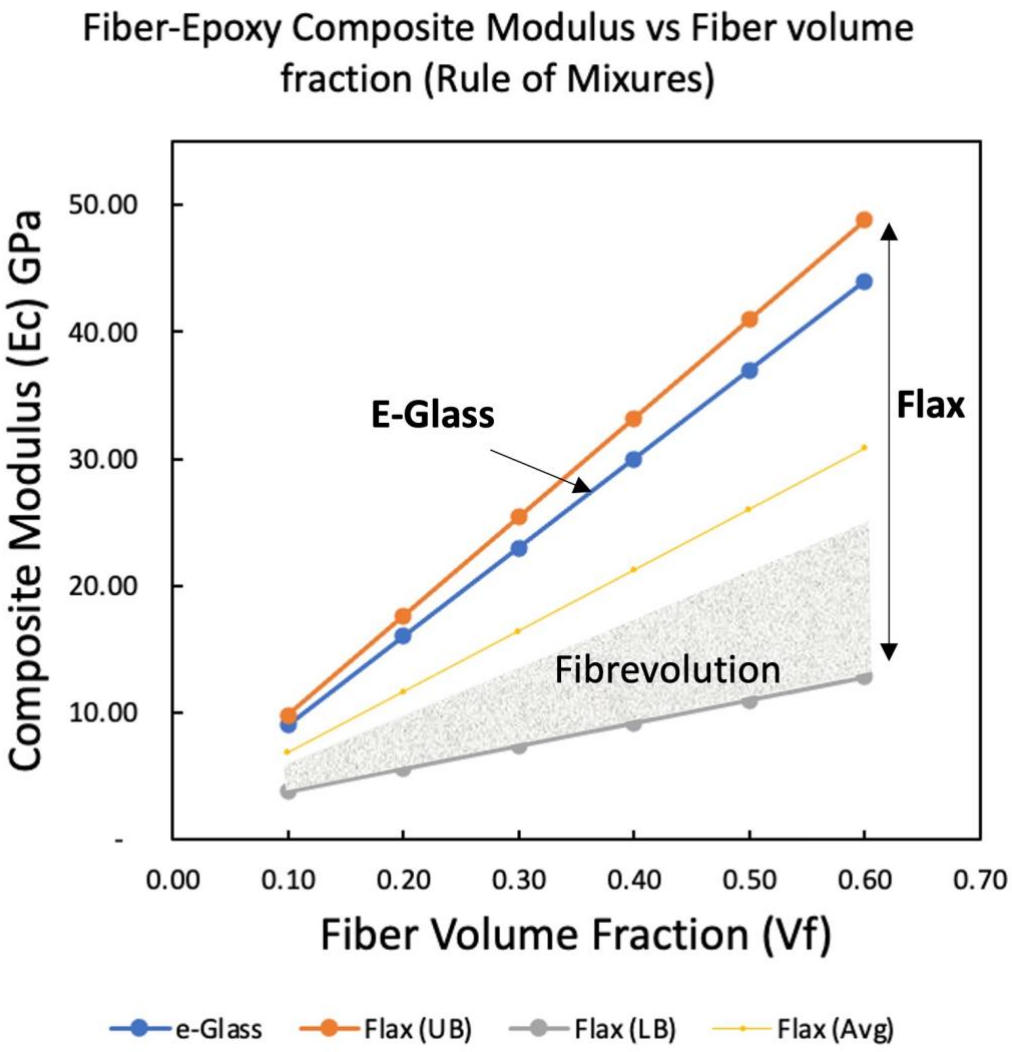

Figure 1.1 Fiber-composite modulus using simple rule of mixture

1.2 Plant Physiology and Natural Fibers

Natural fibers can be classified according to the extracted location from within different plants, including stems, leaves, and roots for use in composites [24–26]. These fibers exhibit different structural and mechanical properties due to their specific functions at the location in plants. For instance, coir fibers around coconut play the role of shock absorbance upon fall and

have a large lumen (hollow space) but less stiffness [26–28], whereas flax fibers are the supporting tissues of the stem and have high modulus and stiffness [26,29].

Figure 1.2 shows the location of flax fibers that form the outer bast region of the plant stem and are generally extracted in form of bundles of single fiber cells for industrial use, also called "technical fibers". Plant fiber literature defines the single plant fiber cells as "elementary fibers" adhered to each other by middle lamella interphase and when viewed through cross-section, technical fibers consist of around 10-40 elementary fibers which generally overlap along the length of the technical fiber as seen in **Figure 1.2(b)** [24]. The elementary flax fibers can be 10-25 um in diameter and 2-5 cm in length. The diameter of technical fibers depends on the number of elementary fibers and can vary from 50-300 um [24,26].

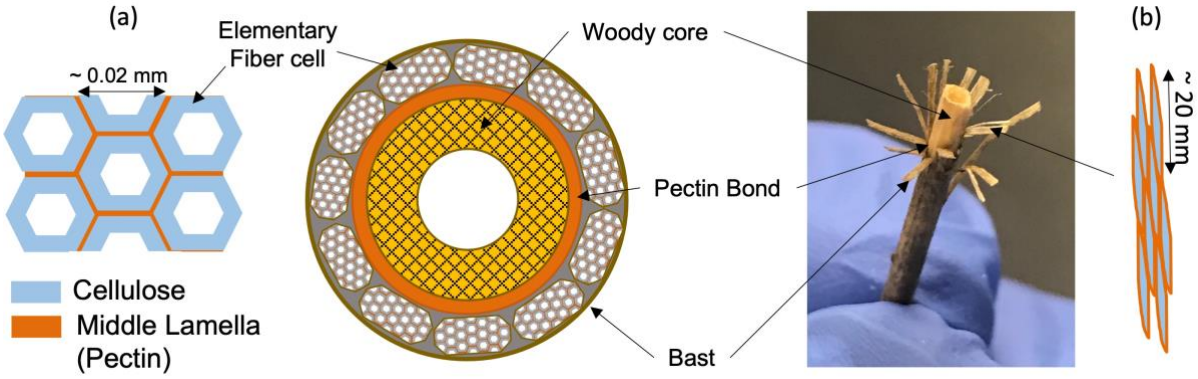

Figure 1.2 Flax stem cross-section schematic with (a) cross section and (b) vertical view of fiber cells arrangement

Among the different types of tissues that constitutes a plant, the elementary fiber cells are sclerenchyma tissue cells, whose diameter are dominated by thick cell walls to provide more permanent support [24,25,29–31] than other tissue cells. Also, these elementary cells are elongated cells with tapered ends and are generally dead upon maturity thereby forming a central cavity called "lumen" [24,32]. Also, their cell wall is itself a composite in nature, where the primary

component cellulose (~80-85 %) forms microfibrils of linear packed (1-4)-linked b-D-glucose chains, that are embedded in a matrix of lignin and hemicellulose [33]. These microfibrils are highly aligned in flax fibers, a reason for their superior tensile strengths among other natural fibers [4,6]. Furthermore, the middle lamella at the junction where the walls of neighboring cells come into contact is high in pectin [34] and contains different proteins compared with the bulk of the wall [35,36]. The similar pectin rich interphase also binds the bast layer to the plant woody core [37,38], as shown in **Figure 1.2**.

1.3 Natural Fiber Extraction Process

Extraction processes differ for different natural fibers according to plant species. However, extraction methods for all types of natural fibers are not well studied in the literature, except for bast fibers. Also, over hundreds of years, major use of these flax fibers is found in textile clothing application and the same commercial extraction process is currently used for extracting fiber for their use in composites. This extraction of fibers from flax plants takes place mainly through two steps: retting and mechanical extraction.

1.3.1 Retting and its types

Retting is an essential initial step in the process of fiber extraction and aims to degrade the bonding of the bast layer with the woody core, thus reducing the energy to separate the bast fibers in later mechanical steps [24,38]. Conventionally, plant stems are colonized by fungi and bacteria aiming to isolate fiber bundles by degrading the pectin rich cortical parenchyma surrounding fibers, the epidermis and the xylem through the enzymes secreted by them [24,26]. Water retting used to be the traditional method of isolating fiber bundles for ages, where stalks of the stem are submerged into water, allowing anaerobic bacteria to degrade the stems. However, water retting is

a major cause of water pollution and illegal in many countries. To overcome this issue, dew retting was started, where stem stalks are spread evenly on grass fields and are soaked overnight in heavy dews, allowing natural bacterial degradation to take place. Dew retting for flax stems by our collaborator Fibrevolution is shown in **Figure 1.3** along with the bast bundle division observed under scanning electron microscopy (SEM) (taken from Chapter 2). This method is again limited to certain climate conditions in certain regions [26].

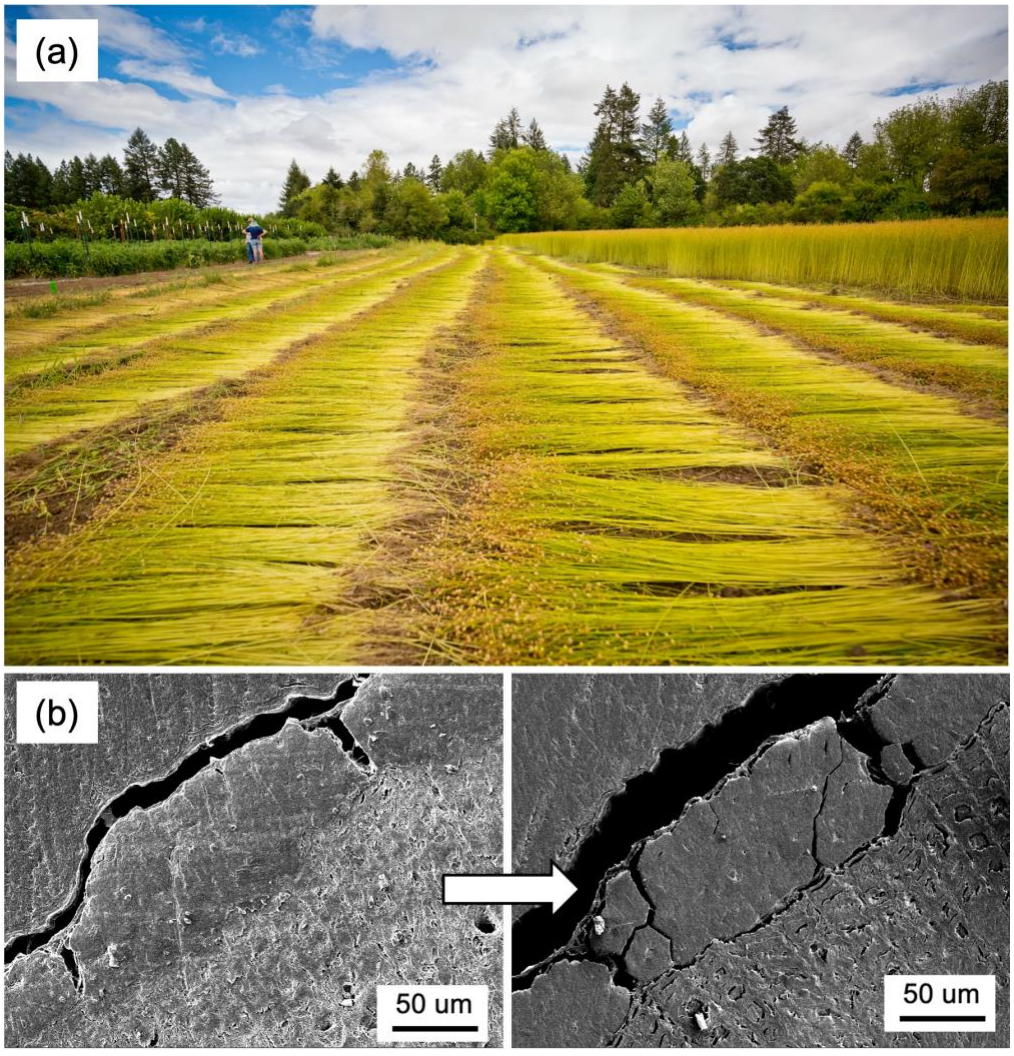

Figure 1.3 (a) Dew retting of flax stems in the field at Oregon by Fibrevolution and (b) morphological changes in the bast bundle during retting observed under Scanning Electron Microscopy (SEM)

Other retting methods explored by other researchers that haven't been implemented at industrial scale yet include microbial retting with a controlled colony of microbes such as fungi, chemical retting using chemicals like NaOH, EDTA and enzymatic retting [26,39–41]. Enzymatic retting has become popular in overcoming limitations of dew retting in recent studies, where using specific enzymes under mild controllable reaction conditions can produce fibers with more consistent properties in an environment friendly way [42–44] and hence are explored further in this dissertation.

1.3.2 Mechanical extraction

After retting, fibers are extracted through a series of mechanical processes namely, breaking, scutching and hackling. The most critical of these is breaking, where the retted stems are crushed between the gear teeth or flute profile of rotating rollers, to break and separate the inside brittle woody core from the bast fiber layer [24,26]. The schematic and an example of fluted breaker for breaking plant stems is shown in **Figure 1.4**. The broken woody core inside falls as shives. Here, the dimension and flutes depend upon the amount of plant breaking to achieve maximum throughput.

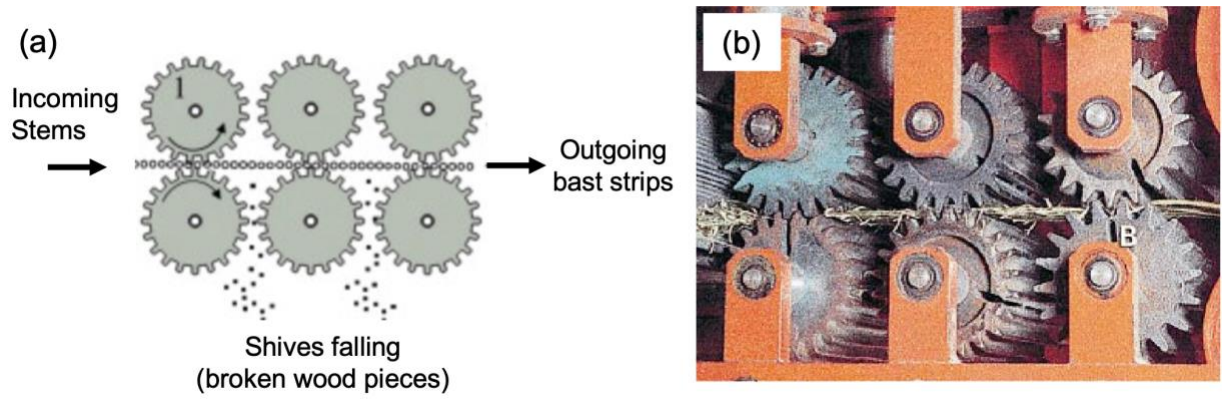

Figure 1.4 (a) Schematic of breaking process and (b) an example of commercial plant breaker [45,46]

After breaking, extracted bast fiber layers or strips then goes through cleaning and refining steps. Here, the incoming bast strips first undergoes scutching as shown in **Figure 1.5**, where the scraping action by blades of fast rotating scutching turbine further removes any undesired material like woody core (shives) and short fibers.

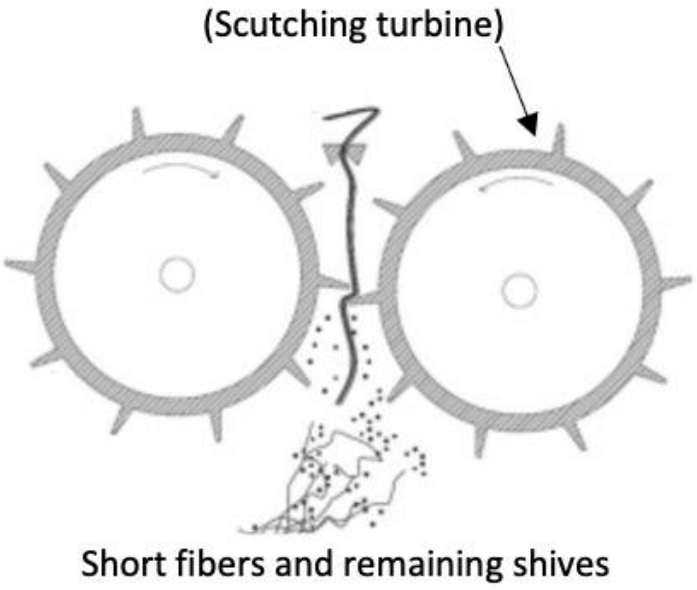

Figure 1.5 Schematic of scutching turbines [45]

The bast fiber strips coming out from breaking and scutching are thick and coarse and undergo a process called hackling to obtain efficient fiber individualization. Here the bast fiber strips are put into combing action between pins to align and divide the bast strips into finer technical fibers as shown in **Figure 1.6** [47,48]. During hackling the bundles of fibers besides being further divided are uniformly aligned as well by removing undesired shives or seeds. Furthermore, hackled fibers are continuous with respect to discontinuous scutched fibers [24,26,49–51].

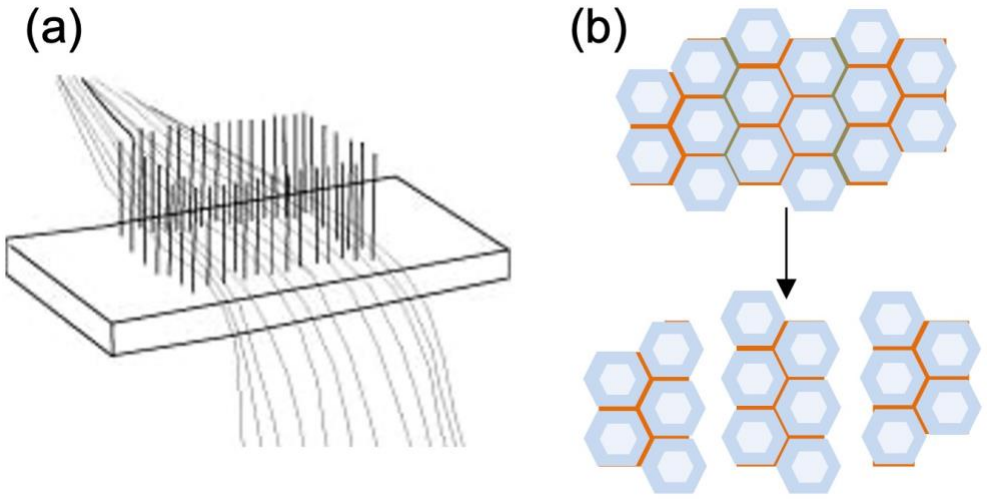

Figure 1.6 (a) Schematic of hackling step [47,48] and (b) division of bast fiber bundle into finer technical fibers

Scutching and hackling may be common for flax but not for extraction of all bast fibers. For instance, hemp fibers are separated using milling tools such as hammer mill, roller mill or beater and cleaning systems (also called decortication). Similarly, jute or kenaf fiber extraction is done by similar extraction units called jute mills or kenaf mills [26,52]. The bast fiber yield ranges from 10-40 % of dry stalk weight from these mechanical processes. Yield for long flax fibers is around 15 % of the total biomass from current industrial extraction [53].

1.4 Effect of Current Extraction Process on Fiber Properties and Gap in Literature

While this current commercial fiber extraction method is commercially viable for textile application, it degrades the natural fiber quality a lot from its original potential [54]. Defects can be originally present in the fibers due to misorientations of cellulose fibrils which occurred during fiber growth, dislocations, sliding planes or knees caused by bending of stems by wind or during lodging for processing. Besides these defects, the process of extraction significantly affects fiber morphology, chemical properties, and tensile strength [55,56].

1.4.1 Current retting method limitations

Different retting methods and the degree of retting can impact the fiber properties. Retting should be homogenous for production of fine technical fibers for uniform properties. However, the current commercial process of dew retting is weather dependent and inconsistent, where the microorganisms also degrade structural component of fibers (cellulose) and produce technical fibers with non-uniform diameters as seen in **Figure 1.7** [26,57]. Also, over-retting can affect the quality of technical fibers due to degradation of cellulose and pectin bonds between elementary fibers [26,58], whereas under-retted fibers may contains non-cellulosic impurities like surface wax that can cause stress concentrations in the composite and early failure [39]. Farmers use subjective observations and sensory judgement along with indirect methods to define end point or degree of dew retting [26], which makes it difficult to maintain a standard quality standard for natural fibers.

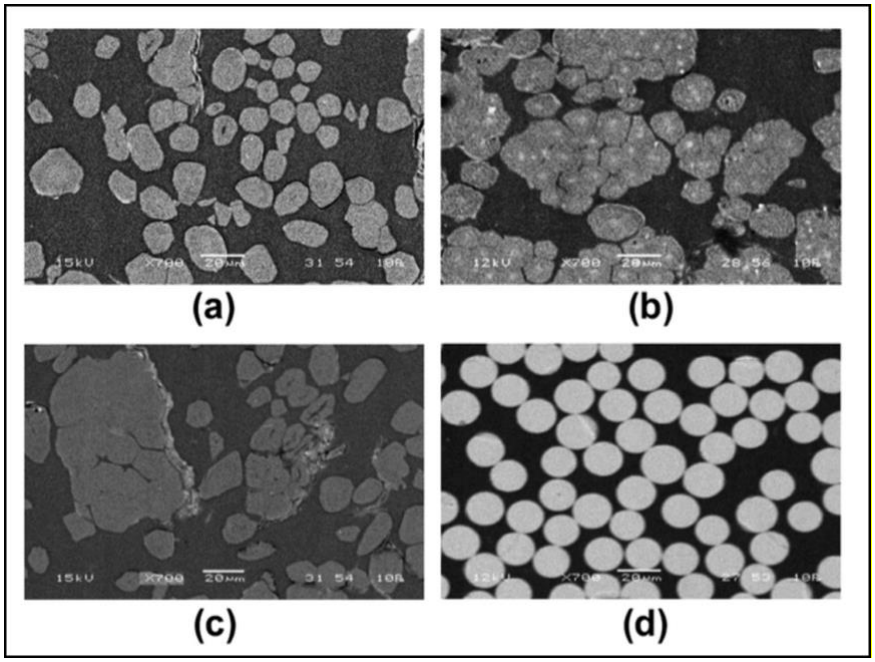

Figure 1.7 Differences into fiber individualization for flax fibers having different retting degrees (a, b, and c) compared to glass fibers (d) [59]

Additionally, two important phenomenon take place during retting as shown in **Figure 1.8**. First bast separation from woody core and second bast bundle differentiation into finer technical fibers. While current studies generally evaluate fineness and mechanical properties of resulting technical fibers as retting degree measures [43,60], there are limited reports on the bond strength of bast-woody core interphase, whose degradation is the primary goal of retting process. A reason for this is the absence of effective quantitative measures for evaluating retting degree. Current indicators of retting degree include qualitative tests such as user based ranking system in fried test [61], or indirect indicators like fiber fineness, change in stem weight or chemical composition after retting [39,43,57,62–64]. Mechanical peel test is commonly used to characterize the strength of adhesive tapes and has the potential to characterize the bast-woody core bond strength. A preliminary study on peeling hemp fibers by Réquilé et al. showed the impact of increasing dew retting degree on decreasing peeling force [62], which can be used as an effective retting degree measure, and explored in detail in Chapter 2 of this dissertation.

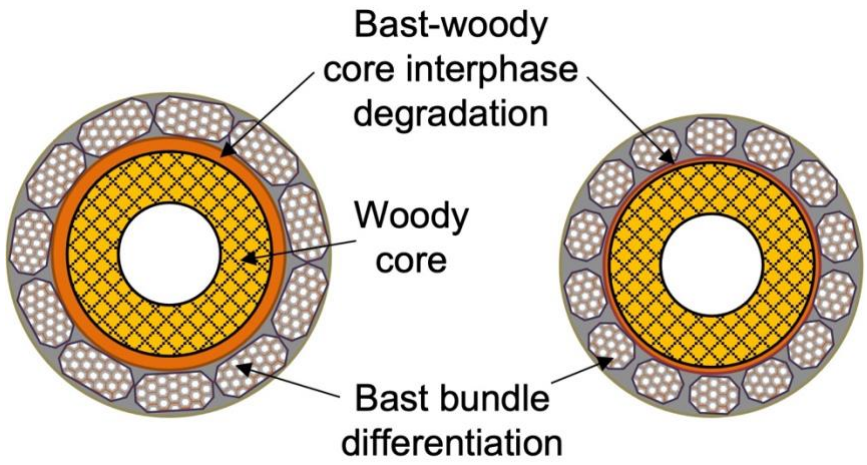

Figure 1.8 Flax schematic (not to scale) showing general retting effect of bast-woody core interphase degradation and bast bundle differentiation

1.4.2 Current mechanical extraction limitations

Besides retting, mechanical processing of fibers can cause extreme damage to fibers, reducing the fiber mechanical properties. Here, particularly during breaking step, many prior literature studies report the fiber damage and defects such as kink bands (as seen in **Figure 1.9**) occurring under excessive bending strains, leading to degradation and high variation in mechanical properties of these fibers [54]. Compared to breaking, scutching & hackling tend to have lower impact on fiber damage. However, high scutching rates have shown to decrease mechanical performance of natural fibers in literature studies [24,26]. Also, hackling after scutching improves tensile properties in the case of flax if compared to scutched alone fibers [39]. This can be attributed to the fact that fiber becomes more refined as hackling breaks the non-continuous fiber bundles at their weak points into finer technical fibers of reduced diameter and length [39,65,66].

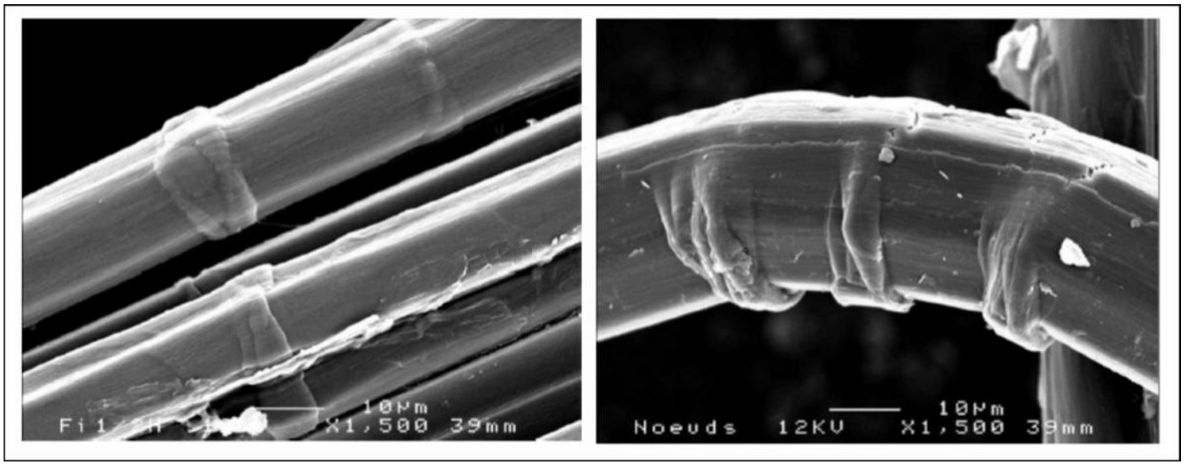

Figure 1.9 Kink-band defects on flax fibers before or after bending (Scale Bar: 10μm) [67]

Prior studies include characterization of these defects and its effect on fiber properties. Beaugrand et al. studied these damage mechanisms at the submicron level using X-ray tomography [68]. Hänninen et al. and Estrada et al. characterized bending defects in flax and hemp

fibers using polarized light microcopy and acid hydrolysis methods [69,70]. Also, several studies have been conducted on improving mechanical extraction equipment, such as a helical geared design of breaking rollers by Wang et al. [71], lab scale pilot plant for flax processing by Akin et al. [63], virtual environment studies of hemp fiber production line using TRIZ by Xu et al. [72] and finite element modeling of processing equipment by Olan et al. [73]. While most of these studies focus on either studying defects or improving the breaking with change in equipment configuration, limited studies were found to elucidate the fracture mechanism occurring during breaking of these stems at the fundamental level that can guide the process and equipment design for mechanical extraction of natural fibers with minimal damage and defects.

1.4.3 Current mechanical testing methods limitations for evaluating fiber properties

The current testing standard for evaluating the mechanical properties of single technical fibers assumes uniform cross section and homogenous material which adds variability in results and at times incapable to estimate correct mechanical properties of these fibers [74–77]. In addition, the effect of tensile testing of technical fibers at different gauge lengths is well studied by Bos et al., where flax fibers tested at shorter clamping length showed an increase in tensile strength [24], as seen in **Figure 1.10** [24]. A single elementary fiber has a greater tensile strength than a technical fiber. And testing at longer gauge lengths consider the fracture through the weak interphase between elementary fibers within the technical fiber as opposed to shorter gauge lengths where technical fiber failure occurs mainly through the elementary fibers.

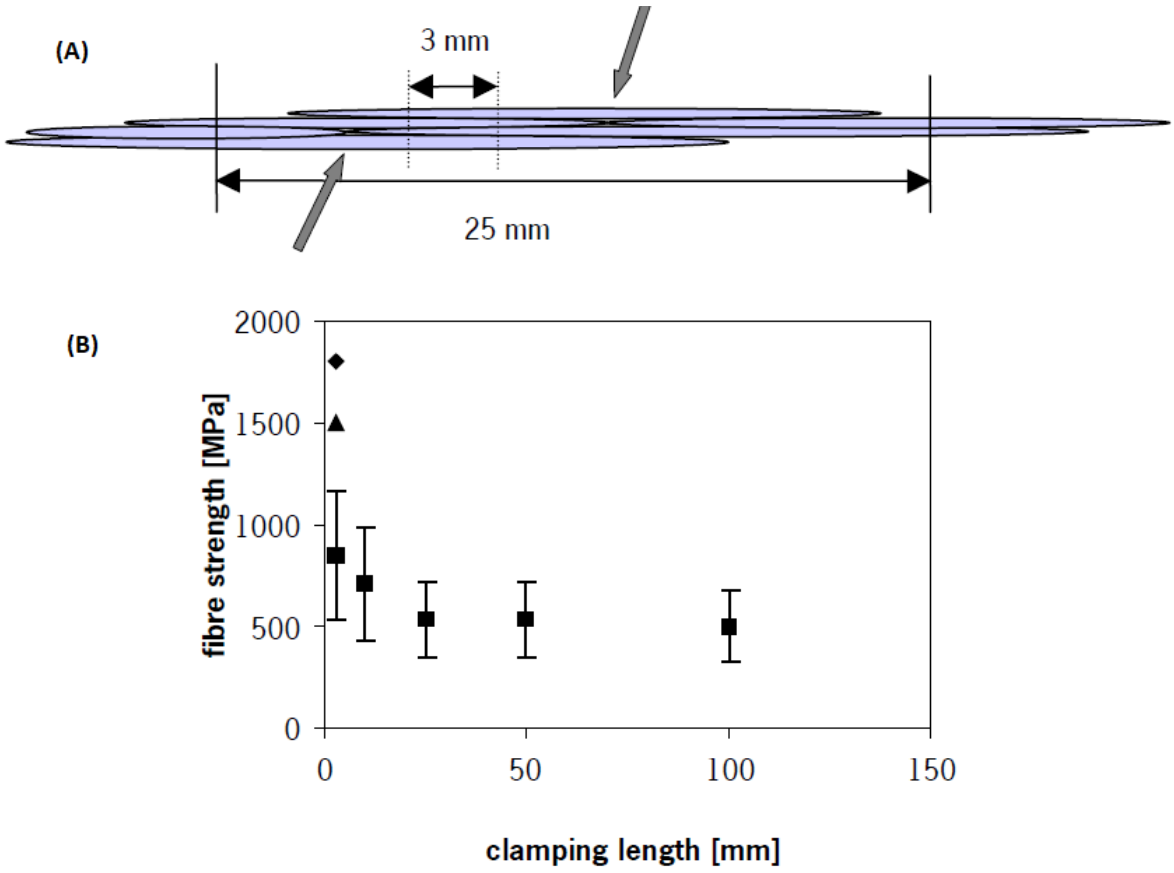

Figure 1.10 (A) Schematic representation of the way the Flax fibers break (B) Fiber tensile strength versus clamping length. ■ Technical fibers, ▲ elementary fibers [24].

Studies also show that technical fiber properties are inversely proportional to their cross-sectional area or diameter [14,66,78,79]. For instance, **Figure 1.11** shows graph between modulus vs fiber diameter in case of flax by Bourmaud et al. [79], where inverse dependence between the jute fiber tensile strength and the corresponding fiber diameter was shown through statistical analysis. This is due to the fact that finer fibers tend to orient the elementary fibers well and a reduction in defects or weak interphases. However, the data reported in these studies typically has high variability and a poor correlation coefficient. Also, the importance of gauge length in this

inverse correlation hasn't been clearly stated. Additionally, most of the prior studies on diameter effect are for dew retting, where both pectin interphase and elementary fibers are degraded [78,79].

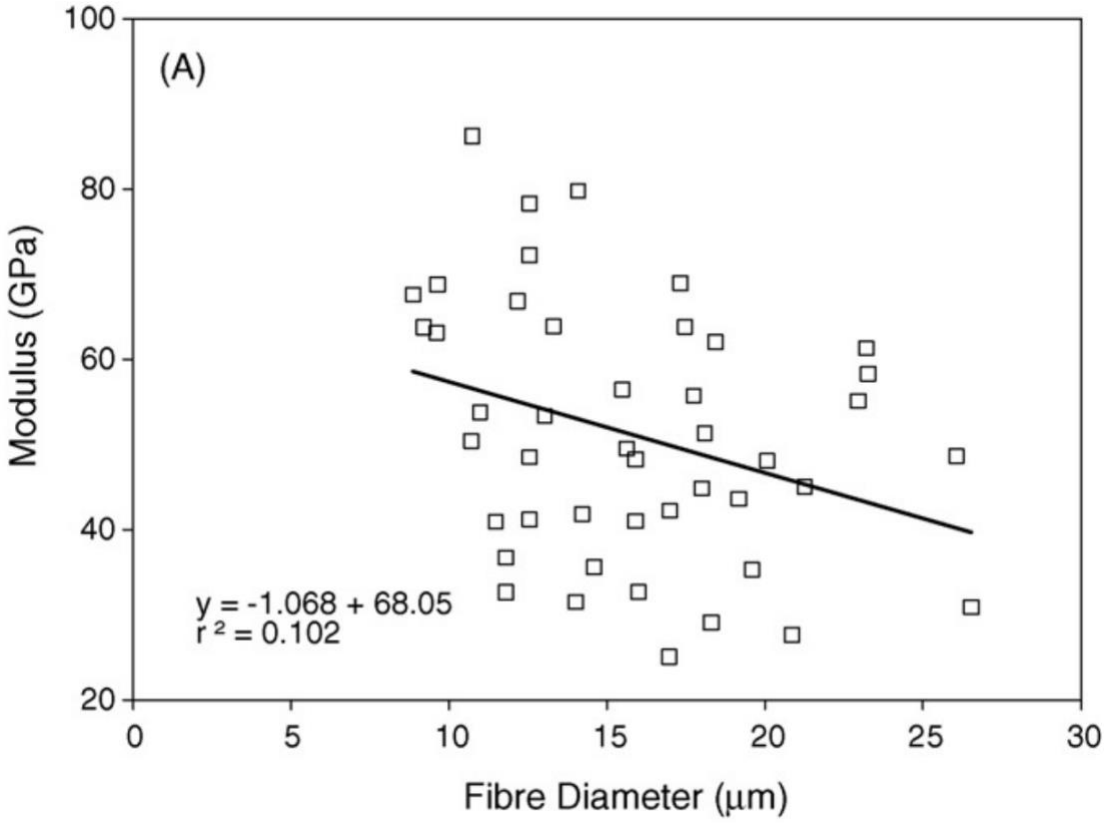

Figure 1.11 Variation of the modulus with the fiber diameter [79]

1.5 Thesis Outline and Research Objectives

The aim of this dissertation is to improve natural fiber quality and reduce variability in mechanical properties by elucidating the cause and eliminating the fiber damage occurring through various steps in natural fiber extraction process, particularly retting and breaking. Also, we aim to develop methods to provide a rapid evaluation of these fibers' performance in composites with the limited amount of fiber materials available for lab scale trials. The rest of this dissertation consists

of three main chapters (2-4) to explore these research goals in depth, concluding with the key findings' summary & future work directions in Chapter 5. Their outline is as follows:

⇒ *Chapter 2: Retting Condition Effect on Fiber Separation and Properties*

This chapter aims at controlling the retting process for uniform fibers properties through enzymatic retting and improving the reliability of current fiber testing methods. Here, improvements in single fiber testing are proposed along with the development of mechanical peel testing method for quantitative evaluation of retting degree. Furthermore, a systematic experimental approach is developed to answer major key questions here, first, "how dew retting and enzyme retting differently effect fiber properties?", then second, "How parameters like enzyme concentrations and retting duration effect the fiber properties?". Impact of over-retting on fiber properties for enzymatic retting is discussed and a retting condition is chosen to use for improved extraction studies in later chapters.

⇒ *Chapter 3: Mechanical Stem Breaking and Process Improvement Considerations*

This chapter aims at evaluating the fiber damage occurring at single stem level during mechanical breaking and develop better practices for high quality natural fiber mechanical extraction. Major key questions answered here are, "how compression and bending impact on fracturing of these stems?", and "what are the process and roller design parameters to consider for preventing over bending of the plant stems during extraction?". Here, finite element modelling (FEM) is done along with mechanical tests to study and improve breaking process with an improved roller profile. Lastly, impact of this improved stem breaking process on extracted fiber properties is evaluated.

⇒ *Chapter 4: Improved Fiber Extraction and Composite Fabrication*

This chapter aims first at extracting fibers from bulk stems using the retting condition and improved mechanical extraction developed in Chapter 2 and 3 respectively. Here, the fiber yield is evaluated at each level in the extraction process and compared with literature. Further, this chapter explores evaluating fiber performance in lab scale fabrication of small unidirectional composite samples. Key questions answered here are, "Is whether fabrication of small composite samples with low fiber amount can provide good estimation of fiber performance in composites?" and, "Can the back-calculated fiber tensile properties be used in place of the tedious single fiber testing method for evaluating fiber properties for composite applications?". Lastly, improvements and troubleshooting of composites are suggested for reducing the variability in fabricating small composite samples and evaluating tensile properties.

Chapter 2
Retting Condition Effect on Fiber Separation and Properties

2.1 Introduction

The retting process has been shown to effect the technical fiber mechanical properties, particularly on how uniformly it divides the bast fiber bundles into fine technical fibers. Also, as the elementary fibers are held together by similar glue holding them to the rest of the plant stem, the higher the degree of retting the finer is the division of bast fiber bundles into finer technical fibers [63,80,81]. Enzymatic retting has become popular in overcoming limitations of dew retting in recent studies, where using specific enzymes under mild controllable reaction conditions can produce fibers with more consistent properties in an environment friendly way [42–44]. Researchers have studied the effect of enzyme retting on fiber properties from plants such as flax [64,82–84], hemp [85,86], kenaf [40], alfa [44] and jute [87].

Additionally, the effect of combinations of specific enzymes for degrading specific bio matter like cellulose (cellulases), pectin (pectinases), lignin (laccase) and hemicellulose (xylanases) on flax fiber properties has been extensively studied by Prez et al. [43,57,82]. Here, pectin digesting enzymes or pectinases, particularly polygalacturonase, was found to be very efficient in fiber extraction while preserving the mechanical properties of the fibers [57,82]. Research has also been reported aimed at improving the enzyme retting through either the introduction of new combination of enzymes [82] or an improvement in process through introducing radio frequency pretreatment [60,61] and spraying [88]. Less emphasis has been

given to study the effect of enzyme concentration and incubation time. In the case of dew retting, retting degree depends mainly upon time as it is difficult to control the microbiology to change enzyme concentration [26,89,90]. In comparison, enzyme retting can provide an opportunity in scaling at industrial level by shortening the retting duration with an increase in enzyme concentration. Hence, it is important to study the effect of both time and concentration on fiber properties.

This chapter aims at improving both the reliability of current fiber testing methods and find the optimum enzyme retting conditions for effective bast separation without degrading technical fiber properties. Here, first improvements in single fiber testing are done and the developed testing methods for quantitative evaluation of retting degree are discussed. Further, a systematic approach is used to evaluate the effect of enzyme concentration and incubation time on bast separation along with bast differentiation and the properties of resulting fibers.

2.2 Experimental Approach

For specifically degrading pectin rich interphases without affecting cellulose component in flax fibers, a high pectin digesting enzyme Pectinex ultra-SPL was used for enzymatic retting. Fibers were hand extracted to eliminate the damage occurring from mechanical extraction steps. Mechanical peeling experiments were conducted to characterize the bond strength between bast-woody core interphase and correlated with chemical analysis of reducing sugar concentration in the retting liquid. Technical fiber cross-section area was evaluated through optical microscopy and scanning electron microscopy of flax stems was used to study bast differentiation into technical fibers from different conditions of retting. Single fiber tensile tests were conducted, where improvement in compliance and initial slack corrections were carried out over current ASTM standards to determine elongation and modulus correctly during tensile tests. Additionally, a

rigorous statistical analysis was performed for evaluating the effect of enzyme concentration and time over each property in the study.

2.2.1 Plant material and preliminary comparison studies between dew and enzymatic retting

Both Dew-retted and non-retted flax stems of Agatha variety used in this research were supplied by Fibrevolution^{TM}. These stems were grown under uniform conditions at Oregon State University research farm in spring of 2019 and retted in the field for 10 weeks in case of dew retting. Non-retted stems were used for enzyme retting in the lab. For uniformity in experiments, samples in current study were taken from the middle section (25 cm long) of these stems with diameter 1.5 ± 0.15 mm as shown in **Figure 2.1**, where maximum fiber content of consistent and superior quality is located according to previous studies [38,91,92].

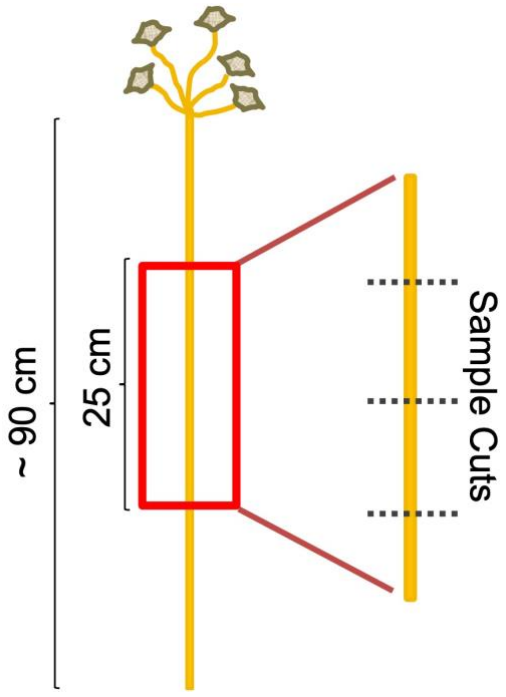

Figure 2.1 Schematic of a dried flax stem and sampling location in current studies

For comparing the effect of dew and enzymatic retting on fiber properties, five stems were randomly selected each from dew and enzyme retted stems for hand extraction of fibers. Here, enzyme retting of flax stems was done at 0.5% (v/v) enzyme to buffer concentration and 14-hour incubation time. Forty technical fibers were randomly selected from both fibers extracted from dew and enzyme retted stems for microscopy and tensile testing. Optical microscopy data was used for morphology and dimensional analysis of fibers for qualitative assessment and area measurement. Also, dew and enzyme retted fibers were formed into loop of similar radius of curvature, also known as *loop test*, a qualitative measure of compressive strength of a fiber [20,93].

2.2.2 Single stem enzymatic retting experimental design

For comparison of effects of various retting conditions, a systematic testing approach was developed here using a single stem for exposure to different retting conditions**. Table 2.1** summarizes the retting conditions used in this chapter. Here, besides dew retting taken for baseline comparisons, four enzymatic retting conditions were chosen according to full factorial design of experiments, where the low and high point for incubation time was chosen as 6 hours and 24 hours. The low and high point for enzyme concentration was chosen as 0.5 % (v/v) and 2 % (v/v).

Table 2.1 Sample overview used in the current study

Sample	Retting Degree	Retting Condition
Dew	Medium	Field Retted, 10 weeks
S_0	/	Buffer, 24 h, 40 °C, 4.5 pH
S_{L6}	Low	0.5 % Enzyme-Buffer (v/v), 6 h, 40 °C, 4.5 pH
S_{L24}	Medium	0.5 % Enzyme-Buffer (v/v), 24 h, 40 °C, 4.5 pH
S_{H6}	Medium	2 % Enzyme-Buffer (v/v), 6 h, 40 °C, 4.5 pH
S_{H24}	High	2 % Enzyme-Buffer (v/v), 24 h, 40 °C, 4.5 pH

Samples from a single stem for different retting conditions and characterizations in this chapter is summarized in **Figure 2.2**. Five sections (5 cm each) were cut and marked from the 25 cm long middle section of a single flax stem. It has been shown earlier that the fibers from the middle section of the plant stem have best mechanical properties and are comparable when sampled from sections closer to each other as the case where 5 cm sections were sampled within the 25 cm middle section of flax stem [38,91,92]. Here, one section was used as control (S_0) without any enzyme in the solution during the retting process and rest four were subjected to different degree of retting as summarized in **Table 2.1**. Stems were randomly selected and numbered to sample stems for various characterizations after enzyme retting as shown in **Figure 2.2**. Middle section from a new single dew retted stem was selected for each comparison with enzyme retted stem in a particular characterization.

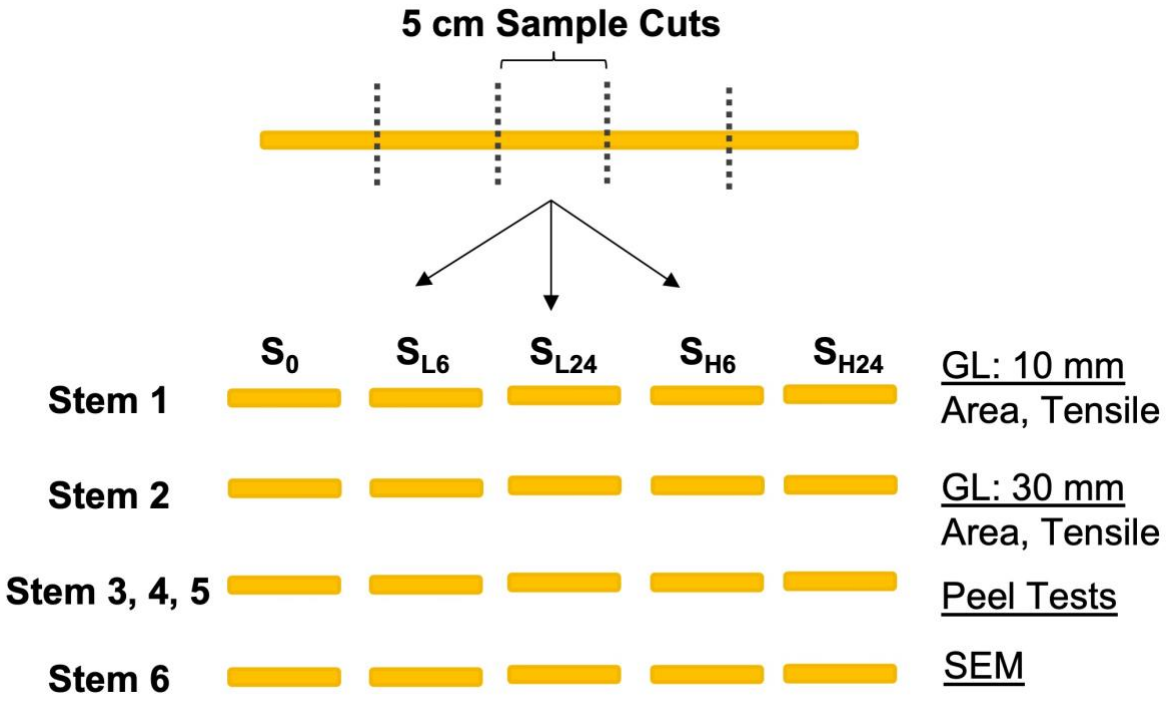

Figure 2.2 Single stem sampling for different enzyme retting conditions and characterization (GL: gauge length)

2.3 Lab Scale Enzymatic Retting Process and Fiber Extraction

To specifically degrade the pectin glue holding the fiber bundles to stem, enzyme retting was carried out with Pectinex® Ultra SPL (procured from Sigma Aldrich), a high pectin hydrolysis enzyme with enzymatic activity of greater than 3,800 units/mL according to product data sheet. The schematic for enzymatic retting is shown in **Figure 2.3**. Here, cut pieces of flax stems were first oven dried at 80°C for 6 hour to remove any moisture for correct initial weight analysis and enzyme concentrations ranging from 0.5-2% (v/v) were prepared with sodium acetate buffer (0.05M, 4.5pH) for various experiments in this study. Then, flax stems were taken with prepared enzyme solution at 1:25 ratio (gm:ml) into test tubes that were shaken horizontally at 100 rpm at 40°C inside the oven. After incubation for time ranging from 6-24 hours in different experiments, the retting liquid is collected for analysis and the enzyme retted stems were gently washed under distilled water five times followed by oven drying at 100°C for 24 hours before extraction of fibers.

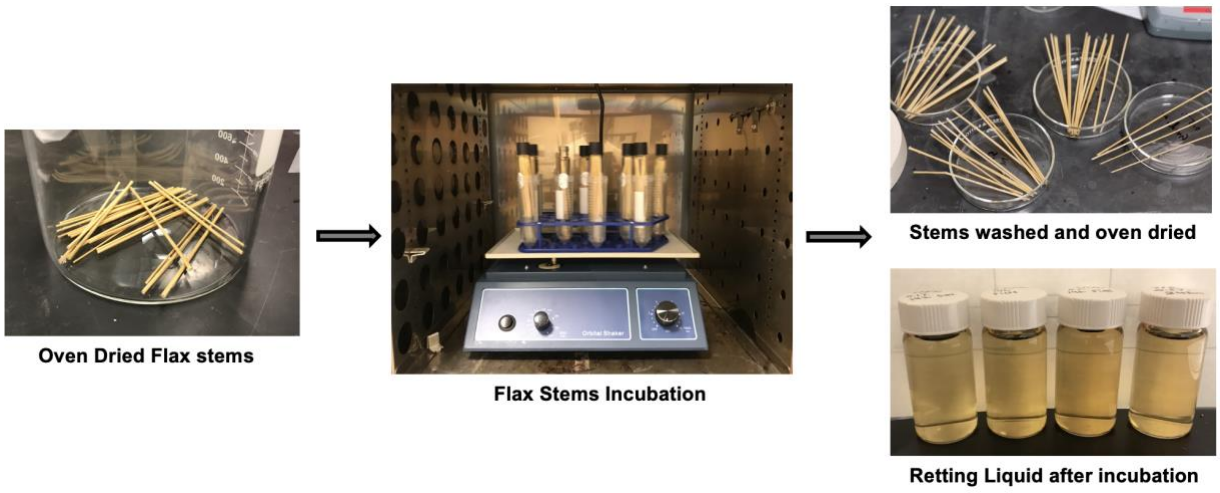

Figure 2.3 Lab scale enzymatic retting of flax stems

For natural fiber studies at different retting levels, it is essential to eliminate the defects and damage by later mechanical extraction. **Figure 2.4** shows the steps during careful hand

extraction of fibers from dew and enzyme retted stems. Each flax stem was first crushed (35 % ideal compression from Chapter 3) through a rolling mill to uniformly flatten the cylindrical structure. Then the bast layer strips were hand peeled from both sides of the flattened stems and a pin frog (9 pins/cm^2) was used for hackling to divide the bast strip bundles at weak interphases (weak link theory [24]) into fine technical fibers. Depending on the retting degree, fibers obtained from a single stem circumference after hackling varied from 15-28 in number.

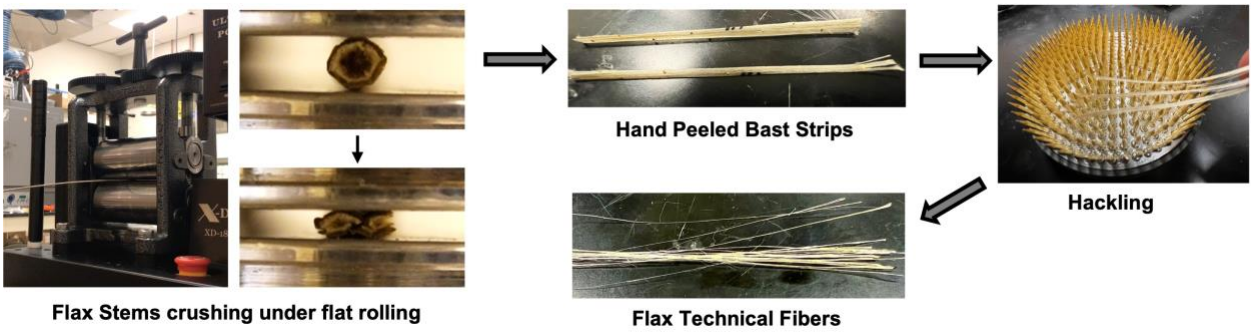

Figure 2.4 Hand extraction of flax fibers

2.4 Retting Efficiency Measures

As discussed earlier in Chapter 1, retting degree has an impact on the ease of separation of bast fibers from rest of the stem as well as the size and quality of technical fibers. Existing methods for retting degree characterization are based on qualitative measures such as morphology investigation or user defined ranking system prone to biases such as popularly used fried test, where retted stems are placed in boiling water test tube and vortexed for a certain amount of time. Later based on number of fibers separated the user ranks the stems on a scale of usually 0-5 to define the degree of retting. These tests lack in quantitatively characterizing the cohesive bond between the fibers and stems after retting. In the current study, peel test (mechanical) and reducing

sugar analysis (chemical) was performed on retted stems as more quantitative measures for retting degree and the correlation between the two is studied later in this chapter.

2.4.1 Peel test

Mechanical peel tests are generally used to characterize and study bond strength in adhesive tapes. Retting weakens the pectin bond between the bast fiber-woody core interphase and as in adhesive tape case, a peel test can be used to characterize this bond strength at different degrees of retting to find the optimal condition for later mechanical extraction [62]. Peel Test configuration depends on the angle formed by peeling arm of flexible adherent (bast fiber layer) with the rigid adherent (woody core) and it is important that this angle is maintained for the entire peeling distance.

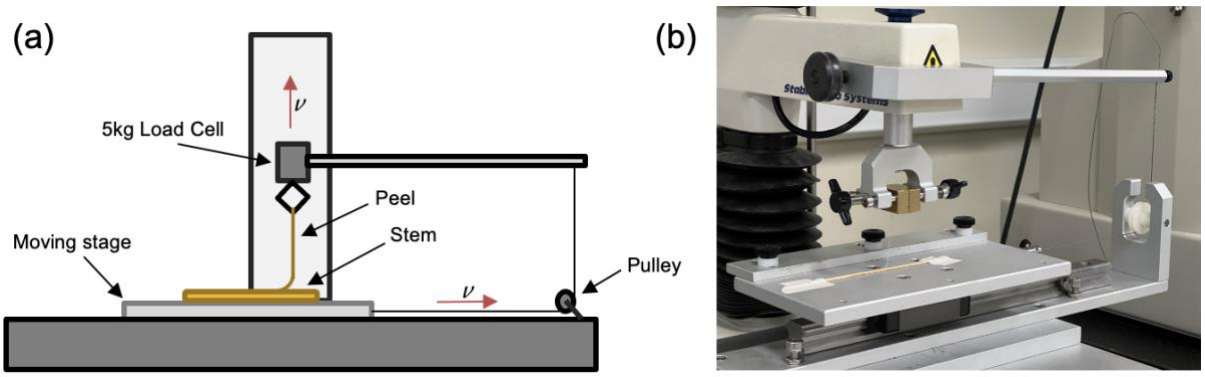

Figure 2.5 (a) Schematic and (b) actual set up for 90° peel testing of bast layer from woody core

In current study, 90° peel tests were carried out on flax stems using a Texture Analyzer from Texture Technologies Corp. with a 5 kg (~50 N) load cell, suitable for measuring strength of the weak pectin bond between the bast-woody core interphase. **Figure 2.5** shows the schematic and working principle of this set-up. Here, stems were attached to horizontal moving stage and 0.5 mm wide bast strip cut with parallel blades was peeled and clamped to the top grips, making an

angle of 90° with the stem. A trigger force of 30 g (~0.3 N) and a test speed of 0.5 mm/sec was applied to the top clamp moving upwards while pulling the stage in horizontal direction with same speed through pulley action, thereby always maintaining the 90° angle between bast strip and the stem.

Peel tests were carried out on dew retted and control stems (S_0) samples as well as those listed in **Table 2.1**. Peel force per unit bast width (N/m) is plotted against peeling distance (mm) and average peel force (N/m) was calculated upon force stabilization between 5-25 mm peeling distance from this curve. This calculated average peel force/bast strip width (N/m) can be expressed in terms of peeling energy required per unit surface area of peeled bast strip (J/m^2) and used to express peel test results in this study. It should be noted that this peel energy is the qualitative metric and not the true quantitative assessment of actual peel energy. Three stems from each retting condition were tested twice (6 peel trials per condition) and statistical analysis were performed on resultant peel energy values. It is worth noting that the part of the stem, where leaves were present, the peel energy rises significantly and was rejected in the measurements in this study.

2.4.2 Reducing sugar analysis of enzyme retting liquid samples

Sugar compounds capable of acting as reducing agents are considered as reducing sugars. They form free aldehyde or ketone groups in alkaline medium, capable of acting as reducing agent when treated with compounds like Benedict's reagent, Tollen's reagent, etc., thereby, converting into carboxylic acid during the reaction [94]. Glucose, galactose, glyceraldehyde, fructose, ribose are some examples of reducing sugars.

Effectiveness of enzymatic retting through characterizing the reducing sugar amount released in retting liquid has been explored in prior literature [94]. Dinitro Salicylic Acid or DNS method (Miller, 1959) is generally used for reducing sugar analysis in biochemistry where in

alkaline solution 3,5-dinitrosalicylic acid (DNS) is reduced to 3-amino-5-nitrosalicylic acid by reducing sugars and is used here to characterize the retting effectiveness during enzymatic retting experiments. In this method, 100 ml of 1 mg/ml dextrose (Sigma Aldrich) stock solution was prepared. Then 0.2 ml, 0.4 ml, 0.6 ml, 0.8 ml, and 1 ml of this solution used to make 2 ml standard solutions of known concentration and a blank solution having 2 ml distilled water. Similar to standard solutions, 1 ml of unknown samples was diluted with 1ml distilled water to make up the total volume to 2 ml. Then, 1 ml DNS reagent (prepared according to Miller protocol) was added to the above solutions followed by heating in a water bath at 100°C for 5 minutes and then cooling in ice bath to stop the reaction. The solutions were then diluted by adding 7 ml distilled water to make up the volume to 10 ml in all test tubes. The solution color changes during the reaction due to 3,5-dinitrosalicylic acid conversion to 3-amino-5-nitrosalicylic acid and the absorbance of these solutions were measured using Varian- Cary 50 Bio UV-Visible Spectrometer (blank solution used for baseline correction) at 540 nm, the excitation wavelength for 3-amino-5-nitrosalicylic acid molecule. Absorbance data obtained from standard solutions was used to find the characteristic equation between absorbance and reducing sugar concentration. Then the unknown amount of reducing sugars in retting liquid collected from different experiments in this study was calculated using this characteristic equation.

In this chapter, retting liquid samples collected from 3 repeated trials of different enzymatic retting conditions were analyzed for total reducing sugars content released during retting process using this DNS method and the total reducing sugar content was reported as average of these three trials in mg/ml of retting liquid for each retting condition.

2.5 Scanning Electron Microscopy (SEM) of flax stems

Cross sections of flax stems resulting from varying retting conditions were also visualized for the respective bast fiber bundle division using JEOL IT500 scanning electron microscope (SEM) with 5-10 kV accelerating voltage. The flax stems were mounted in epoxy, polished, and coated with 30 nm thick layer of gold-palladium. Average bast thickness was determined using Image J software for preliminary dew vs enzyme retting study.

2.6 Single Fiber Tensile Testing for Fiber Property Evaluation

To study the retting condition and degree effects on fiber properties, single technical fibers were tested using ASTM C1557 – 14 standard used for synthetic fibers as guidance. **Figure 2.6** shows the steps involved during single fiber tensile testing and modifications during these steps are further discussed in this section to improve the reliability of mechanical testing data. Additionally, a MATLAB code was written for automating the data analysis of large datasets in tensile analysis.

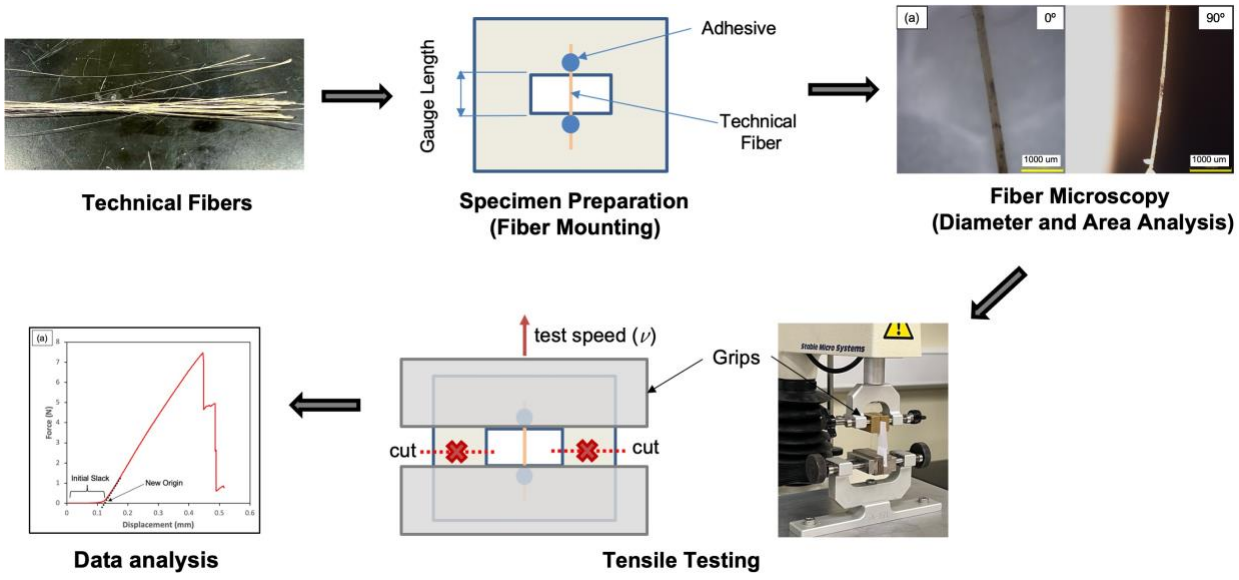

Figure 2.6 Steps involved in single fiber tensile testing

2.6.1 Specimen preparation and gauge length considerations

Selected technical fibers from both dew and enzyme retting conditions were glued to paper frame tabs using cyanoacrylate adhesive at desired gauge length according to ASTM C1557 – 14 standard (**Figure 2.7**). The specimens prepared were then conditioned at 50% relative humidity at 23°C in a humidity chamber for 24 hours prior to tensile testing.

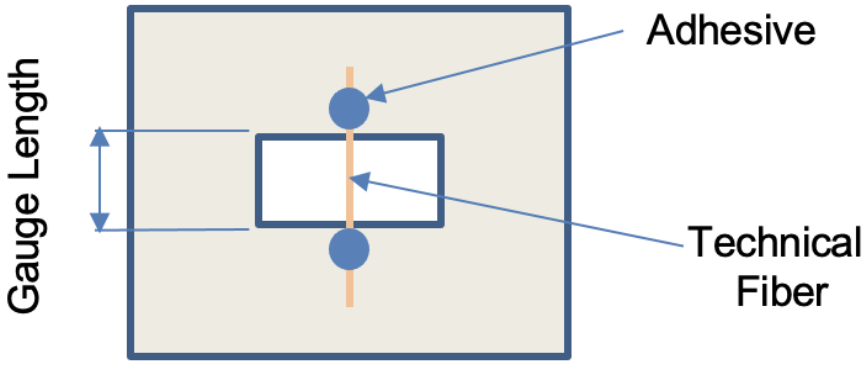

Figure 2.7 Single fiber mounting on paper tab for tensile testing

Two different gauge lengths were considered to visualize the effect of retting conditions and resulting cross sectional area of fibers on tensile properties. Here, 10 mm gauge length was chosen for assessing the technical fiber failure primarily through elementary fibers (around 20 mm in length) and 30 mm gauge length was considered for incorporating the fiber failure through middle lamella pectin interphase between the elementary fibers as shown in **Figure 2.8**, also explored by in previous mechanical studies of technical fibers [14,89]. In single stem studies, the two separate gauge lengths were used to compare properties of different retting condition groups

within the particular gauge length, and not with one another as stems used for two different gauge length were different (**Figure 2.2)**.

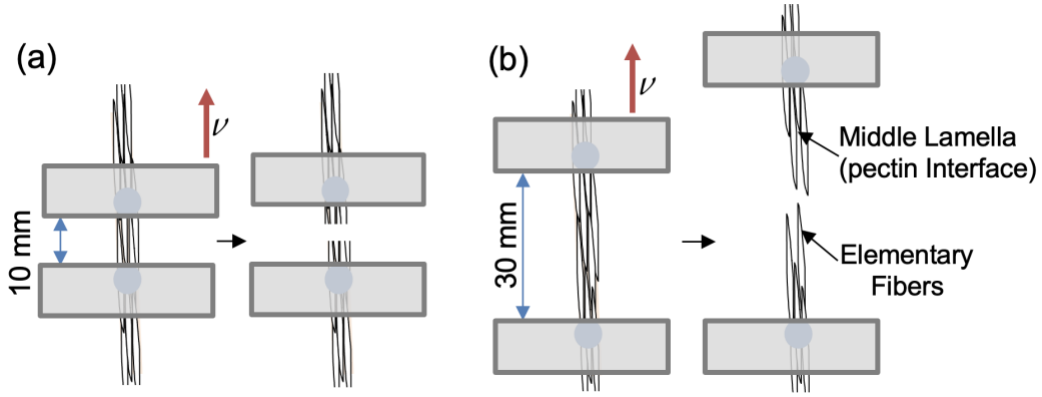

Figure 2.8 Schematic representation of role of elementary fiber interfaces during tensile test failure under (a) gauge length of 10 mm and (b) gauge length of 30 mm

2.6.2 Fiber microscopy

An Olympus DSX510 digital microscope was used for optical microscopy on randomly selected technical fibers under polarized light (PO) mode. To study the varying diameter, images were taken in two directions for each technical fiber, first at 0 degree and then rotating the fiber 90 degree. ImageJ software was used diameter analysis and 8 measurements were taken for calculating mean diameters in both directions along 1 cm gauge length of the technical fiber. The number of measurements were scaled up accordingly for increased gauge length testing cases here. The mean diameters for two directions were denoted as D1 and D2 respectively, where D1 is the longer dimension and D2 being shorter dimension.

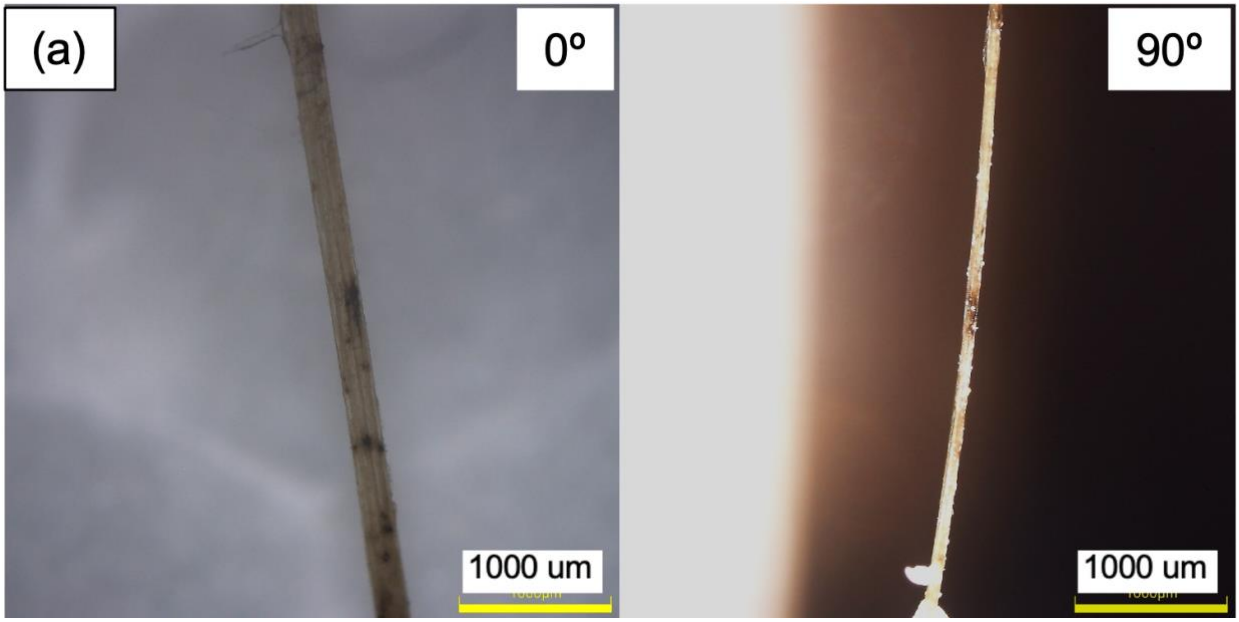

Figure 2.9 Light Microscopy images for 0° and 90° rotation of a dew retted fiber

As an example, **Figure 2.9** here shows the polarized light microscopy images for 0- and 90-degree rotation of a dew retted fiber. From the observation we can see the dimension of these fibers vary a lot in the two directions. In this case, the mean diameters for 0° (D1) and 90° rotation (D2) for dew retted fiber were 219 um and 76 um, with 10 um and 12 um as standard deviation respectively along the 10 mm gauge length.

2.6.3 Fiber cross-sectional area estimation

The ASTM C1557 – 14 standard suggests for circular assumption of fibers and measuring diameter only in one direction. Correct area estimation is necessary to estimate the tensile modulus and strength. Indirect diameter measurement methods using density have also been used before in literature [76]. In this study, an ellipse approximation was considered using the diameter values obtained with direct measurement of diameter in two directions to better estimate the tensile properties. To validate the accuracy of this estimation, 20 technical fibers diameter were analyzed

in two dimensions with the method as described in previous section using Olympus DSX510 digital microscope. Then these fibers were mounted into epoxy, grinded and polished for cross section observation under same microscope. The area obtained from using D1, D2 for ellipse approximation was compared with actual area measured after mounting and cross section imaging using ImageJ software.

Figure 2.10(a) shows the area evaluated using ellipse approximation using D1 and D2 diameters measured with light microscopy compared with the actual cross section area in **Figure 2.10(b).** The ellipse approximation on 20 fiber samples gives over or under-estimating the area by maximum 5%. Hence, ellipse approximation is considered better over a circular approximation to correctly estimate tensile properties of technical fibers.

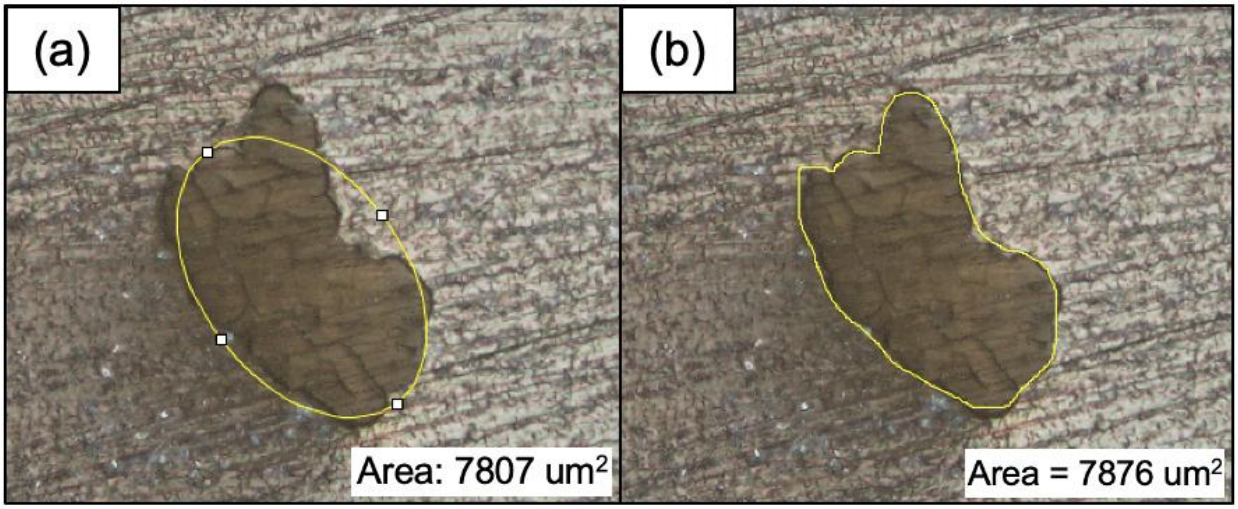

Figure 2.10 ImageJ comparison for (a) area using ellipse approximation and (b) actual area

2.6.4 Fiber testing apparatus

Tensile tests were performed in accordance with ASTM C1557 – 14 standard on conditioned fiber specimens by using a Texture Analyzer from Texture Technologies Corp. with

a 5 kg (~50 N) load cell. The specimens were mounted under the tensile grips to maintain the desired gauge length and the paper mount was cut on either side before the test started as shown in **Figure 2.11**. Trigger force of 3 g (~0.03 N) and a crosshead speed of 0.01 mm/sec was chosen for the tensile test.

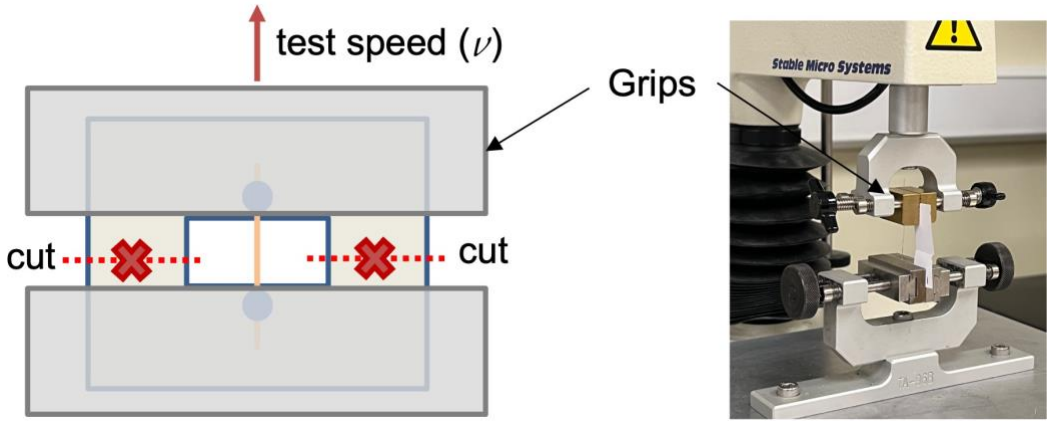

Figure 2.11 Schematic and apparatus for single fiber tensile testing

2.6.5 System compliance and elongation correction in data analysis

The system compliance correction is performed to remove additional deformations such as machine frame, grips, fastening etc. from the measured crosshead displacement data. This correction is necessary for correct estimation of modulus and elongation. In cases where an external extensometer can't be used due to size limitations of specimen (technical fibers here), digital image correlation (DIC) can provide the correct estimation for elongation [76]. Performing DIC on each fiber in a large dataset can be tedious and indirect methods are generally used to calculate machine compliance. In this study, the indirect compliance calculation was done using the method described in ASTM C1557 – 14 standard and compared with the results obtained from conventional compliance correction method where a stiff (non-deformable) material is used between the grips for the given force range.

According to ASTM C1557 – 14 standard, the compliance is calculated from the equation (2.1), where compliance is the intercept of the plot of (ΔL/F) which is inverse of slope of force-crosshead displacement curves, versus (l_o/A) for various specimens.

$$\frac{\Delta L}{F} = \frac{l_o}{EA} + C_s \tag{2.1}$$

Where, ΔL= recorded cross head movement

F= recorded force value, N

l_o = gauge length of the specimen, mm

A = area of the specimen (technical fiber here), mm^2

C_s = system compliance, mm/N

E = fiber Young's modulus, N/mm^2

For conventional system compliance measurement, a steel specimen of varying width from 1-5 mm were used between the grips and tensile test was run at similar conditions as single technical fiber testing. Since the stiff steel specimens exhibit a negligible displacement under 50 N load, the compliance was measured by averaging the inverse of slope of force-displacement curve.

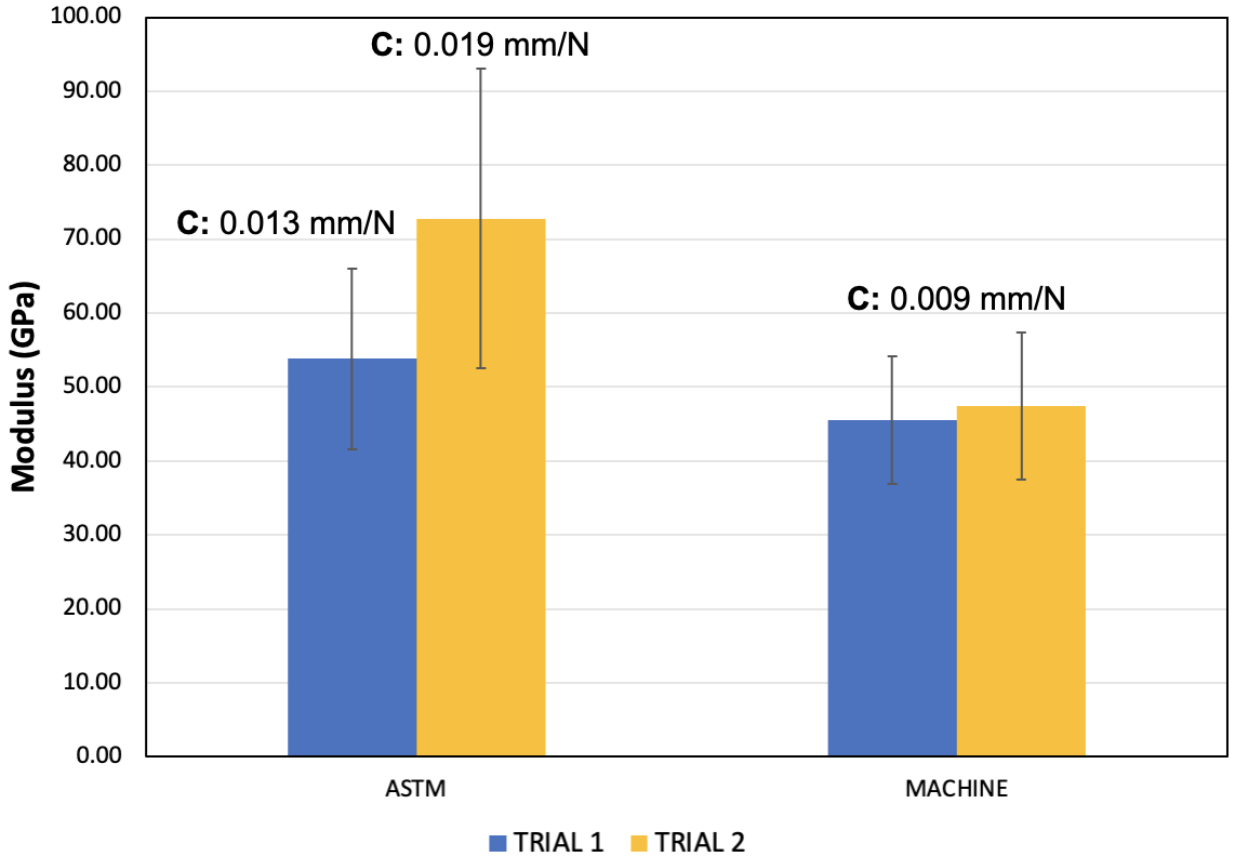

Figure 2.12 Enzyme retted technical fibers modulus comparation after ASTM C1557 – 14 standard and machine compliance correction between 2 trials

Figure 2.12 shows the difference in modulus obtained after compliance correction using ASTM C1557 – 14 standard and machine compliance for two different trials for same batch of ER technical fibers. The machine compliance after using steel specimen between the tensile grips was calculated to be 0.09 mm/N. On the other hand, during two trials the system compliance using the ASTM C1557 – 14 standard gives different values of 0.013 mm/N and 0.019 mm/N respectively. This variation occurs due to variation in gauge length (l_o) and technical fiber area (A) of different tensile specimens, leading to inconsistency in estimating the mean modulus of these fibers as compared to consistent mean modulus values obtained using machine compliance correction

between the two trials. Hence, in this study, machine compliance correction is used to compare the dew and enzyme retted technical fiber properties.

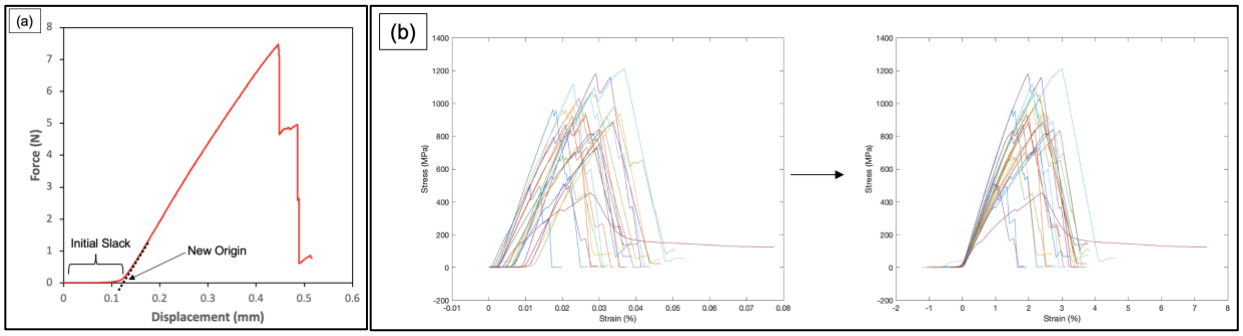

Figure 2.13 Initial slack removal by (a) correcting initial linear region and (b) bringing start position to zero

Different technical fiber tensile specimens also show differing amount of initial slack, caused by varying tautness of the fiber between the grips and needs to be corrected in addition to the compliance correction. In this study, the linear region of the force-displacement profile was extended to displacement-axis as shown in **Figure 2.13(a)** and then bringing this starting position to zero as seen in **Figure 2.13(b)** where all the curves in a sample group were corrected for initial slack after compliance correction. Hence the actual elongation (Δl) in this study is calculated by equation (2.2):

$$\Delta l = \Delta L - C_s F - initial\ slack \qquad (2.2)$$

2.7 Statistical Analysis

All statistical analysis in this chapter was performed using R Studio software and results were expressed as "calculated average ± standard deviation (SD)". For enzyme retted groups of samples (S_{L6}-S_{H24}), Analysis of Variance (ANOVA) method was used to assess the statistical significance of the effect of two studied factors (concentration (Conc) and time of enzymatic

retting) and their interaction (Conc : Time) on the resultant properties including, average peel energy, total reducing sugar released, fiber cross-sectional area, modulus, and tensile strength. For every property, two-way ANOVA with interaction model were created. The ANOVA results of each variable's F-statistic (F-value) and significance p-value associated with it (Prob > F) were summarized.

To further assess ANOVA results, multiple pairwise mean significance comparisons were done as well between different retting condition groups. Here, paired T-Test (parametric) or Mann-Whitney-Wilcoxon (non-parametric) test was used based on normality check using Shapiro-wilk test. Analysis of average peel energy, total reducing sugar released and composite's tensile properties was done using Paired T-Test due to normal condition. In case of single fiber properties, such as cross-sectional area, modulus, and tensile strength, Mann-Whitney-Wilcoxon was used for pairwise mean comparisons due to sample size being small, unequal, or fails to follow normal distribution among one or more retting groups. Hanana et al. also used this statistical method for analyzing mechanical properties of single alfa fibers in a prior enzyme retting study [44]. We take the rule of p-value < 0.05 to reject the null hypothesis at the significance level 5%. Letter notation was used for significance labeling where, variables with the same letter labels (e.g., a, b, c, etc.) are statistically not different at 5% significance level.

2.8 Results and Discussion

2.8.1 Dew vs Enzymatic: Effect of Retting Type on Fiber Bundle Separation and Properties

Scanning electron micrograph of the cross section of a non-retted flax stem is shown in **Figure 2.14**, where we can see the bast fiber bundles around the circumference of flax stem. The dimension of the final technical fiber obtained after extraction process depends upon the division of these bast fiber bundles. Here, these bundles are divided along the circumferential direction with

a length dimension (C) much larger than the radial direction dimension or bast width (W). From ImageJ analysis of the given flax stem, the bast width (W) ranges from 50-100 um and length (C) ranges from 70-350 um.

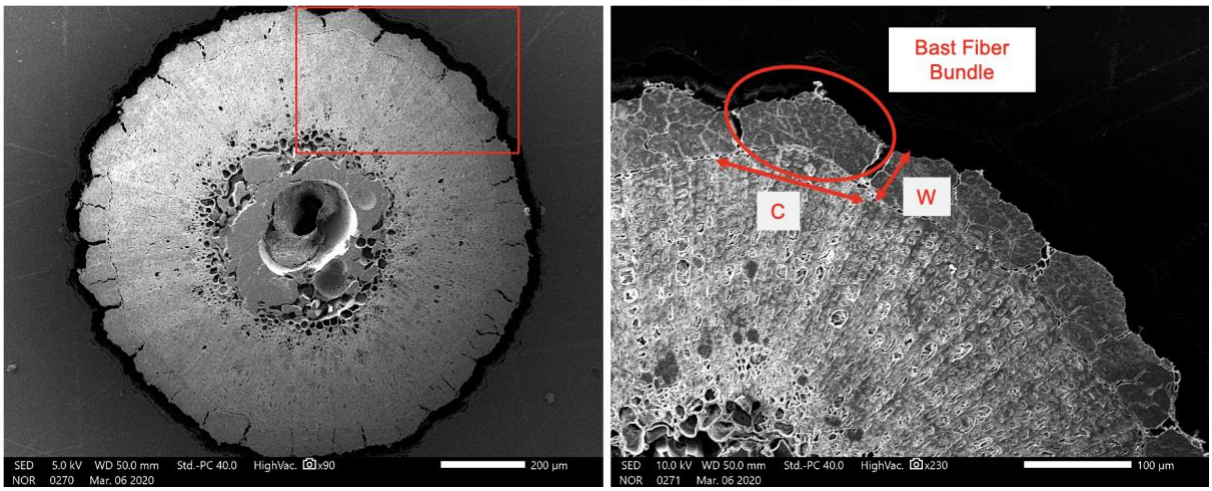

Figure 2.14 Scanning electron micrograph of a non-retted flax stem

Figure 2.15 shows a comparison between fibers extracted from enzyme retted (a) and dew retted (b) stems when observed under optical microscope. Technical fibers from enzymatic retted stems had finer and uniform cross-section when compared to fibers from dew retted stem, in which fibrillations were observed at certain regions. **Figure 2.16** shows a comparison between loop test between fibers extracted from enzyme retted (a) and dew retted (b) stems. Here, a smooth loop for similar radius of curvature shows fiber from enzyme retted stem performed better in loop test when compared to fibers from dew retted stems. As reported previously by Bos et al. [20,37], the sharp bends seen here in a fiber loop formed from dew retted stem indicates presence or increased tendency of occurrence of higher micro-compressive defects or kink bands in these fibers.

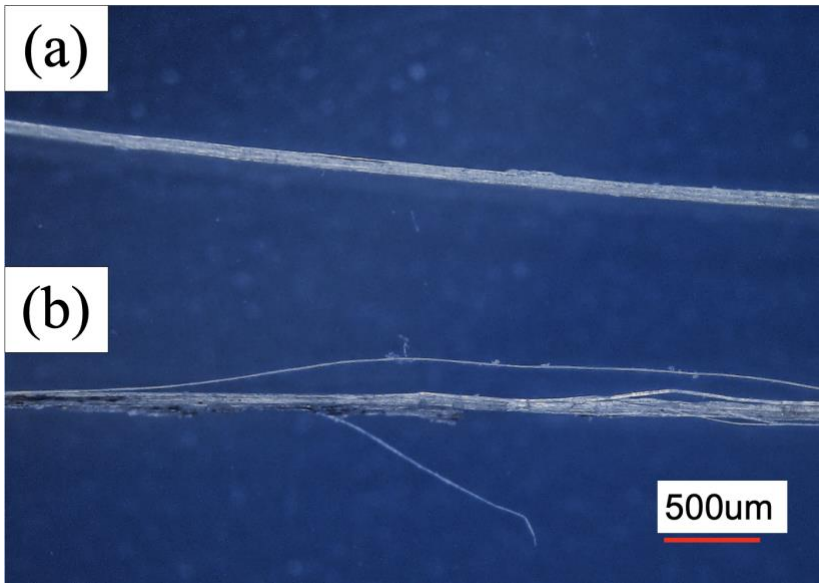

Figure 2.15 Optical microscopy for (a) lab scale enzyme retted stem fibers (b) dew retted stem fibers

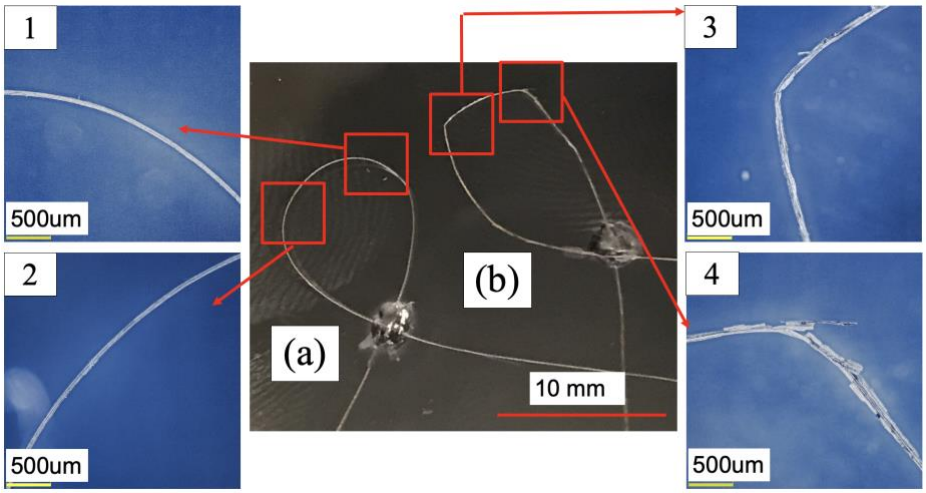

Figure 2.16 Loop test comparison for single fiber extracted from (a) lab scale enzymatic retting (b) Field (dew) retting

Table 2.2 shows the diameter measurements from optical microscopy for 40 technical fibers extracted from dew retted and enzyme retted stems. The standard deviations are reported in parenthesis and percentage in standard deviation error as S.D. %. Enzyme retted technical fibers are significantly smaller in D1 ($p < 0.01$) and have a lower S.D.% in both D1 and D2 than dew

retted fibers. There was no statistical difference found in means of D2 for the fibers in two groups ($p > 0.1$). Also, D2 for both dew and enzyme retted fibers lies in the range of bast width (W) as seen in SEM of a non-retted stem previously (**Figure 2.14**). This suggests that the bast fiber bundles are more probable to divide along circumferential direction than across the bast width during the extraction process.

Table 2.2 Diameter for dew and enzyme retted fibers

Diameter	**Dew Retted**	**Enzyme Retted**
D1 [um]	193 ± 107^{a}	110 ± 41^{b}
S.D. %	56 %	37 %
D2 [um]	86 ± 16^{a}	78 ± 14^{a}
S.D. %	19 %	18 %

results expressed as "average ± SD"
Values within a column followed by the same letter are not significantly different ($p > 0.05$) by paired T-Test

To understand the bast fiber bundle division during extraction further, ratio of D1/D2 was plotted against D1 for dew and enzyme retted fibers (**Figure 2.17**). Here we see that that both dew and enzyme retted fibers show a linear trend with D1/D2 increasing as D1 is increasing. This insight signifies that the fibers with higher D1 have higher D1/D2 ratio or the variation in diameter is due to D1 dimension than D2 dimension. The scatter is low in case of enzyme retted fibers indicating that controlled enzyme retting divides the bast fiber layer into finer and uniform technical fibers than dew retted fibers case.

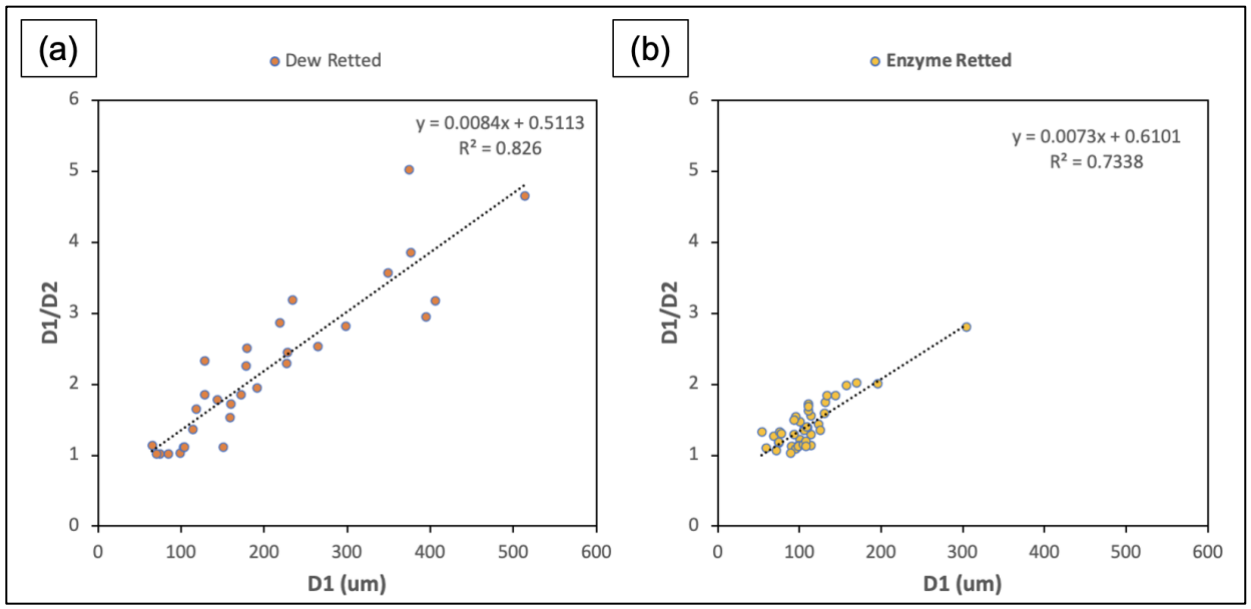

Figure 2.17 D1/D2 vs D1 for (a) dew and (b) enzyme retted fibers

The tensile properties of dew and enzyme retted technical fibers after correcting for compliance and initial slack are reported in **Table 2.3**. Here, enzyme retted fibers show significantly higher modulus ($p < 0.001$) and tensile strength ($p < 0.001$) values with lower standard deviation than dew retted fibers. Enzyme retted fibers also fail at higher forces and have higher elongation than dew retted fibers.

Table 2.3 Tensile properties of dew and enzyme retted fibers

Properties	**Dew Retted**	**Enzyme Retted**
Modulus [GPa]	34 ± 11^{a}	46 ± 9^{b}
S.D. %	33 %	19 %
Tensile strength [MPa]	545 ± 249^{a}	884 ± 227^{b}
S.D. %	46 %	26 %
Elongation [%]	1.8 ± 0.6)	2.2 ± 0.5
S.D. %	34 %	23 %

results expressed as "average ± SD"
Values within a column followed by the same letter are not significantly different ($p > 0.05$) by paired T-Test

The improvement in tensile properties of enzyme retted fibers over dew retting is attributed to the microorganisms degrading the structural component cellulose in addition to the pectin glue [41,95]. Another reason for improved mechanical performance hypothesized is the diameter effect which states that as the diameter reduces, the number of inherent defects in these technical fibers also reduces, giving rise to higher mechanical performance [65,66,96]. This can be visualized from a graph between tensile property with respect to area as seen in **Figure 2.18 (a, b).** However, such a graph is highly scattered and to better interpretation, average tensile strength and modulus are plotted for area intervals of 5000 um^2 in **Figure 2.18 (b, d).** Both tensile strength and modulus shows a decreasing trend as the area of these technical fibers increases. Also, the area spread is reduced and shifted to lower area values, showing higher tensile values in case of enzyme retted technical fibers. However, a highly scattered area distribution with more fibers lying towards higher area distribution region is one of the reason for reduced mechanical properties in case of dew retting. Also, in the same area interval of 5000-1000 um^2, enzyme retted fibers have higher tensile properties compared to dew retted fiber, showing the degradation of cellulose in dew retted.

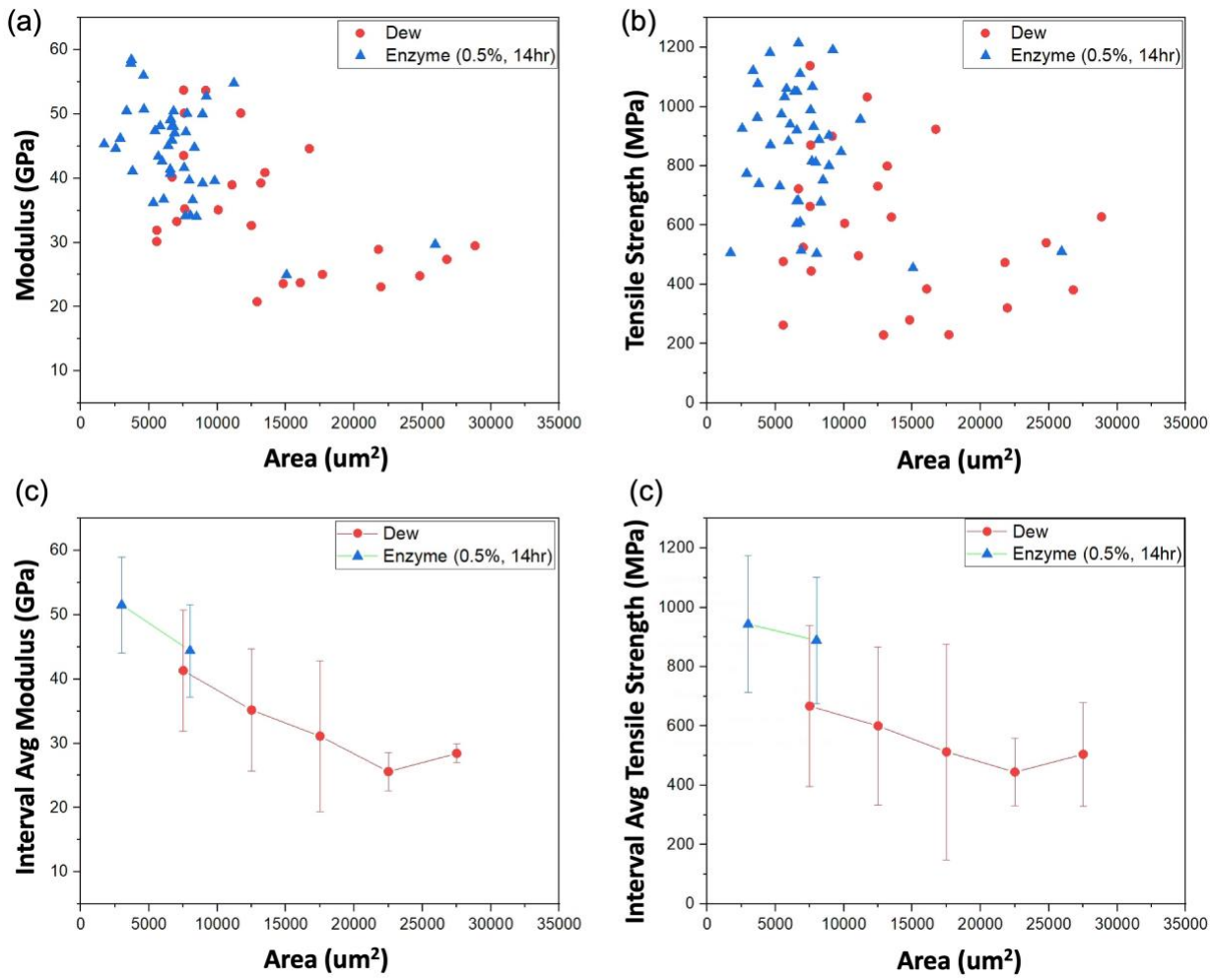

Figure 2.18 (a, b) Tensile strength and modulus against fiber area; (c, d) Alternate representation as Interval average tensile strength and modulus with respect to area intervals (5000um^2) for dew retted and enzyme retted fibers

2.8.2 Enzymatic retting condition effect on peel energy for bast separation from woody core

The behavior of peeling force required to separate the bast from woody core of samples resulting from different retting conditions in the study over the peeling distance of 25 mm is shown in **Figure 2.19**. Here, we see an oscillation pattern, where the crack initiates upon reaching a critical load followed by a drop in force while propagating over a short distance before reaching

to a point for the crack to reach the critical load again. Similar behavior was observed previously in case of dew retting of hemp stems [62].

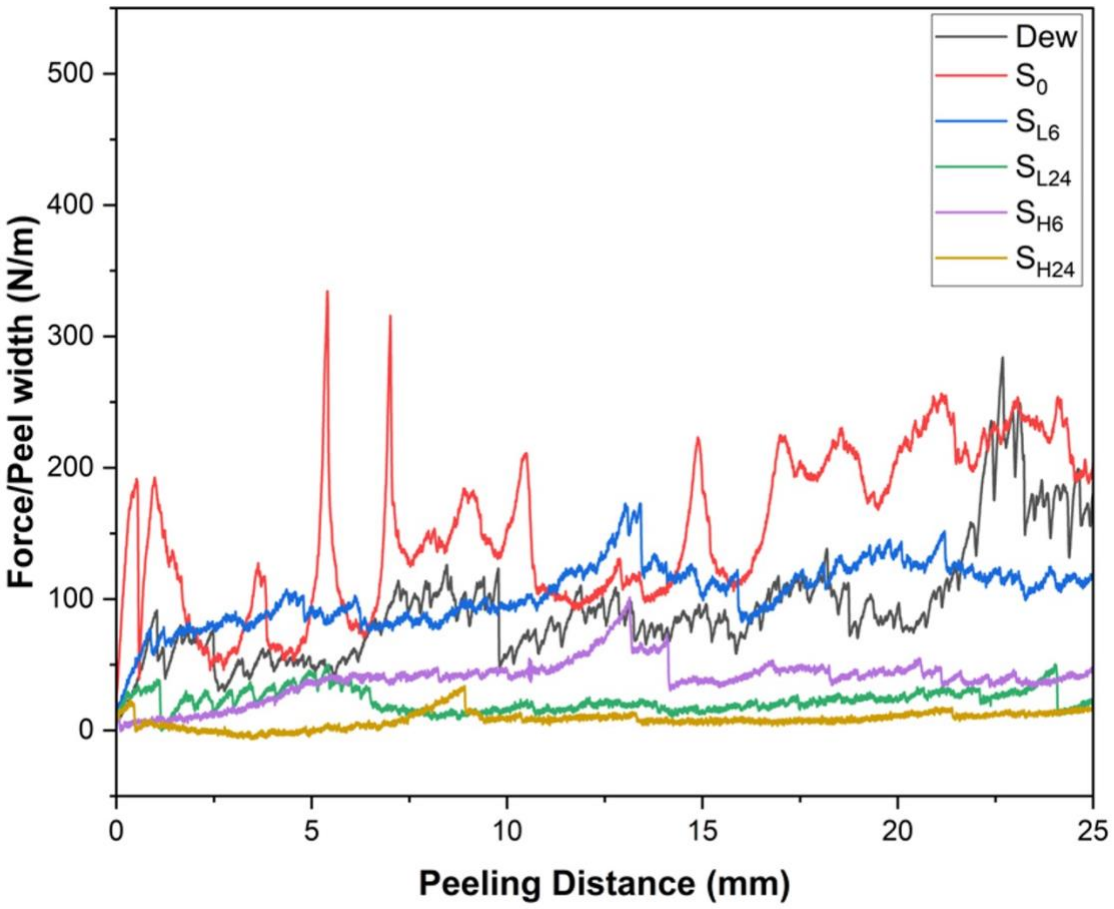

Figure 2.19 Observed peeling force/width behavior for samples from different retting conditions in the study

The average force/peel width (N/m) and the variation (standard deviation) due to oscillations over peel distance of 5-25 mm are summarized in **Table 2.4** for the sample in **Figure 2.19**. S_0 sample showed the highest peeling force as expected. As the bast-wood interphase is degraded with increasing degree of retting, the average peeling force is also reduced along with the standard deviation. Enzymatic retting is observed to play a significant role in consistent retting of flax stems, as seen in case of S_{L24}, S_{H6} and S_{H24}, where the critical load required each time for

crack to propagate or variation in peel force/width reduces. Here, a high enzyme concentration in case S_{H6} seems to effectively reduce the peeling force as compared to S_{L6} for same incubation time of retting (6 hours). Additionally, in case of dew and S_{L6}, significant fluctuation of average force is seen over the longer peeling distance due to inconsistent retting. Hence, the peel energy/bast area (J/m^2) is calculated over longer peel distance of 5-25 mm, which was 5-15 mm in previous studies [62,97]. However, the average peel force calculated here for S_0 sample is close to the values measured by Réquilé et al. in case of non-retted hemp at low speed (140 ±18 N/m) [62].

Table 2.4 Peeling Force (N/m) for a single case of peeling of samples in the study

Sample	**Retting Condition**	**Peeling Force [N/m]**
Dew	Field Retted, 10 weeks	104 ± 42
S_0	Buffer, 24 h	167 ± 52
S_{L6}	0.5 % Enzyme-Buffer (v/v), 6 h	117 ± 13
S_{L24}	0.5 % Enzyme-Buffer (v/v), 24 h	22 ± 8
S_{H6}	2 % Enzyme-Buffer (v/v), 6 h	45 ± 10
S_{H24}	2 % Enzyme-Buffer (v/v), 24 h	10 ± 5

results expressed as "average ± SD"

To consider the random sample induced variation, we conducted the repetitive tests for different samples under the same retting condition. **Figure 2.20** shows the results of average peel force (N/m) or peel energy (J/m^2) (as the height of bar) for 6 different trials under the same retting condition of S_{L6}. These peel energy values were used for statistical analysis of peel energy among different retting condition groups.

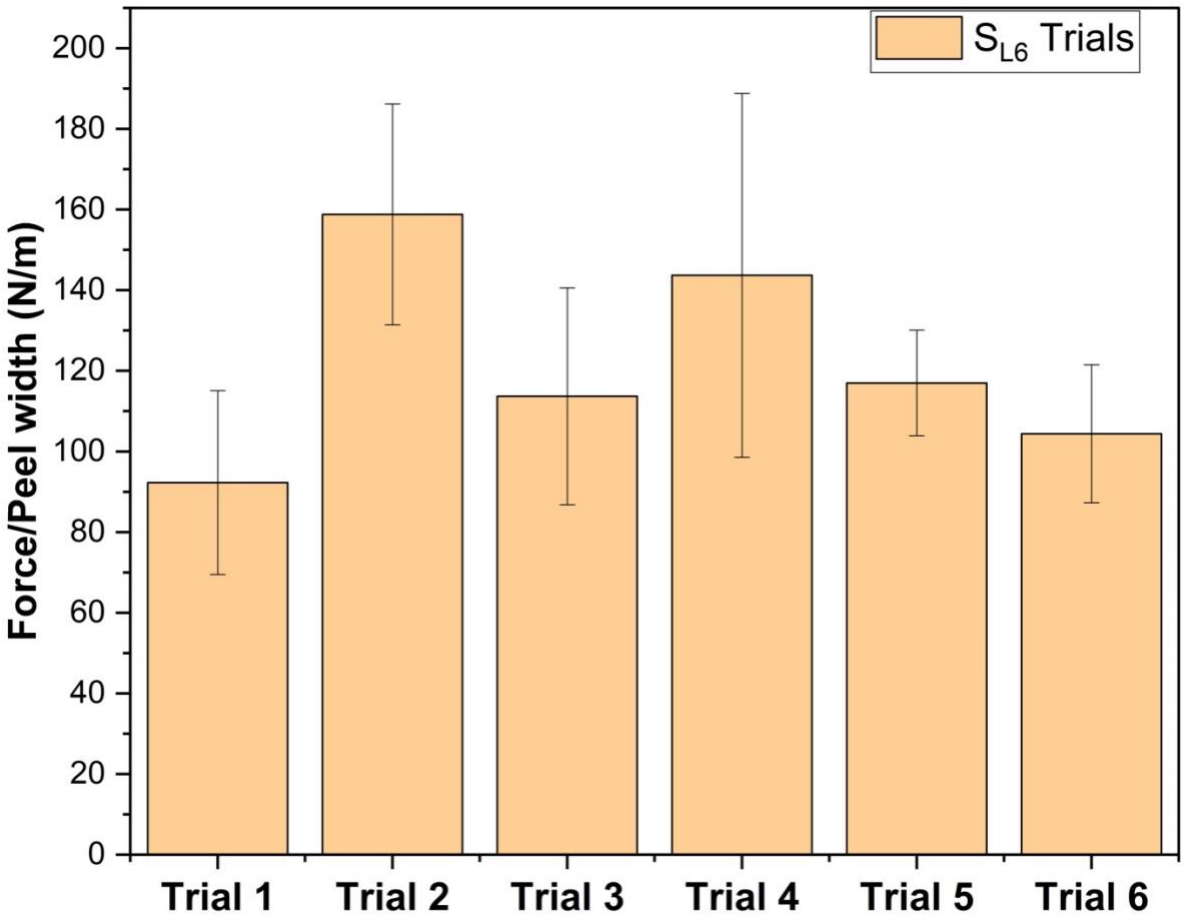

Figure 2.20 Peeling force (N/m) for six trials of retting condition S_{L6} (0.5 %, 6 h)

Figure 2.21 shows the average and variation (S.D.) of peel energy values from the six peel test trials in each retting condition group. Here, the same letter labels shown indicate the mean of peeling forces under those cases are not statistically different under the significance level 5% by statistical paired T-Test. The sample average of peel energy of S_{L6} (122 ± 25 J/m^2, $p = 0.07$) is not significantly different from that of S_0 (165 ± 45 J/m^2) due to insufficient retting of $S_{L6,}$ but dew retting case (80 ± 23 J/m^2, $p < 0.05$) is significantly different from S_0. **Table 2.5** shows the summary of ANOVA results of F-statistics (F_c, F_T, F_i) and the corresponding significance levels (p-value). Because all resultant p-values satisfy $p < 0.05$, it concludes the retting concentration and

time along with their interactions significantly affect peel energy. This observation is consistent with **Figure 2.21**, where significant effect of retting time is shown by the significantly decreased peeling energy upon increasing retting time from S_{L6} (122 ± 25 J/m^2) to S_{L24} (34 ± 11 J/m^2, $p < 0.01$) and from S_{H6} (56 ± 17 J/m^2) to S_{H24} (17 ± 9 J/m^2, $p < 0.01$), under fixed enzyme concentration. Similarly, the significant effect of concentration is shown by the significant decrease in peeling energy when increasing enzyme concentration under the fixed time, i.e., from S_{L6} to S_{H6} ($p < 0.01$) and from S_{L24} to S_{H24} ($p < 0.01$). In addition, the significant interaction between concentration and time is shown by the different sensitivities of time (or concentration) effect under different concentration (or time) levels. Specifically, under the high concentration level, the decreased average peeling energy between S_{H6} and S_{H24} (56 – 17 = 39 J/m^2), is smaller than between S_{L6} and S_{L24} (122 - 34 = 88 J/m^2). This indicates that peeling energy is more sensitively affected by the retting time under the low concentration level of 0.5% than 2%. Similarly, peeling energy is also more sensitively affected by the concentration level under the short retting time of 6 h than 24 h. It is also interesting to note that peel energy in S_{H6} is comparable to the case of Dew ($p = 0.07$).

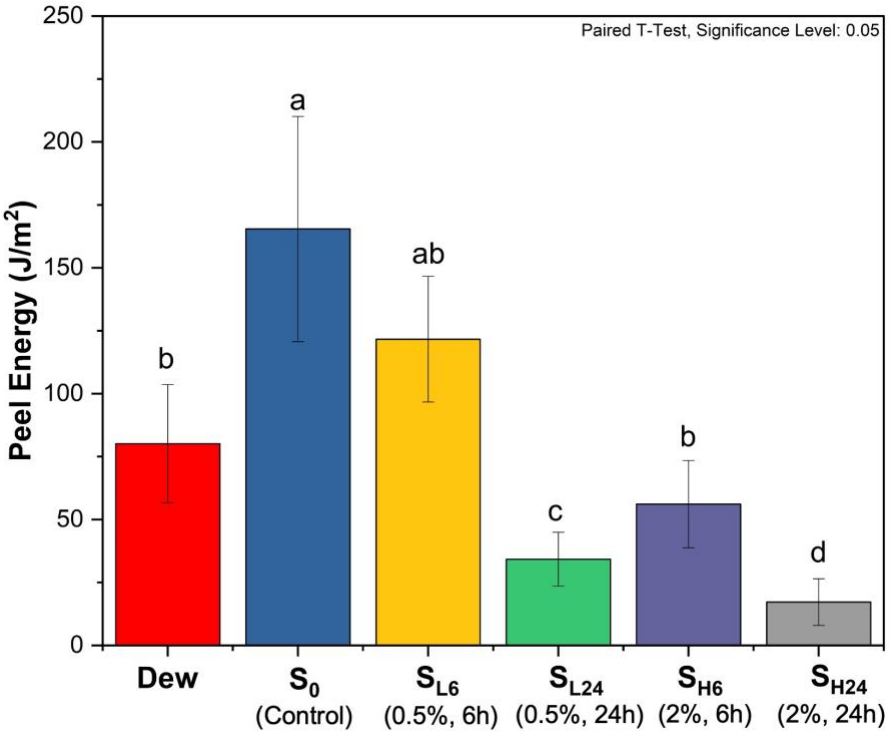

Figure 2.21 Average Peel energy for different retting condition groups in the study

Table 2.5 Summary of ANOVA results for peel energy

	F_c (Conc)	F_t (Time)	F_i (Conc : Time)
Peel Energy [J/m²]	36.37 (6.8e-6)***	85.16 (1.2e-8)***	12.53 (0.002)**

results expressed as "F-value (Prob > F)"
Significance codes: *p > 0.05* : not significant, **p < 0.05, **p < 0.01, ***p < 0.001*

2.8.3 Reducing sugar analysis on retting liquid and correlation with peel energy

For calculating the amount of reducing sugars, first the calibration curve is created (**Figure 2.22**) using standard glucose solutions of known concentration and respective absorbance values is measured using UV-Visible Spectrometer at 540 nm. Here, the curve comes out to be a straight line with a r^2 value of 0.9973 and the characteristic equation as C (mg of sugar/ml) = 4.4224*A (absorbance). This equation is used to evaluate concentration or amount of reducing sugars

released into the retting liquid from the absorbance values measured for three retting trials in each retting condition group as shown in **Table 2.6**.

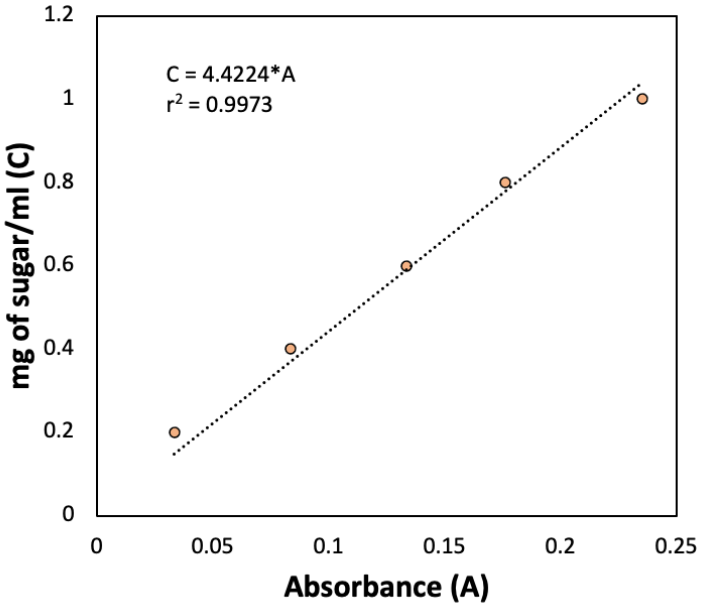

Figure 2.22 Calibration curve for evaluating reducing sugar content

Table 2.6 Absorbance values from UV- Visible spectroscopy for evaluation of unknown reducing sugar content

		Absorbance	**Concentration (mg/ml)**
Control	Trial 1	0.4511	1.9952
	Trail 2	0.3202	1.4159
	Trial 3	0.4151	1.8358
0.5%, 6h	Trial 1	0.8202	3.6271
	Trail 2	0.6733	2.9777
	Trial 3	0.7962	3.5211
0.5%, 24h	Trial 1	1.6368	7.2386
	Trail 2	1.5317	6.7739
	Trial 3	1.2822	5.6703
2%, 6h	Trial 1	1.2616	5.5791
	Trail 2	1.2009	5.3107
	Trial 3	1.1086	4.9026
2%, 24h	Trial 1	2.0502	9.0670
	Trail 2	2.2581	9.9861
	Trial 3	1.9159	8.4730

Further, the average and standard deviation (S.D.) of total amount of reducing sugars released into the retting liquid from the three retting trials in each retting condition group is shown in **Figure 2.23**. A higher amount of reducing sugar indicates higher effectiveness of enzyme in dissolving the middle lamella pectin interphases [44,87]. The amount of sugar released significantly increased from 1.7 ± 0.29 mg/ml in S_0 to 3.4 ± 0.35 mg/ml in S_{L6} ($p < 0.01$) as a result of enzyme retting. From ANOVA results summary in **Table 2.7**, it shows that retting concentration and time significantly affect the amount of reducing sugars liberated during the enzymatic retting. This observation is further seen from **Figure 2.23,** where significant effect of retting time is shown by the significantly increased amount of sugars released upon increasing retting time from S_{L6} (3.4 ± 0.35 mg/ml) to S_{L24} (6.6 ± 0.8 mg/ml, $p < 0.01$) and from S_{H6} (5.3 ± 0.34 mg/ml) to S_{H24} (9 ± 0.76 mg/ml, $p < 0.01$), under fixed enzyme concentration. Similarly, the significant effect of concentration is shown by the significant increase in liberating sugar amount when increasing enzyme concentration under the fixed time, i.e., from S_{L6} to S_{H6} ($p < 0.01$) and from S_{L24} to S_{H24} ($p < 0.01$). The sugar amount released in S_{L24} and S_{H6} was found not significantly different ($p = 0.09$). Moreover, a similar value of reducing sugar content (6.6 mg/ml) in retting liquid under the same enzyme (Pectinex® Ultra SPL) was seen to be reported by Majumdar et al. for the case of enzymatic retting of jute ribbons [87].

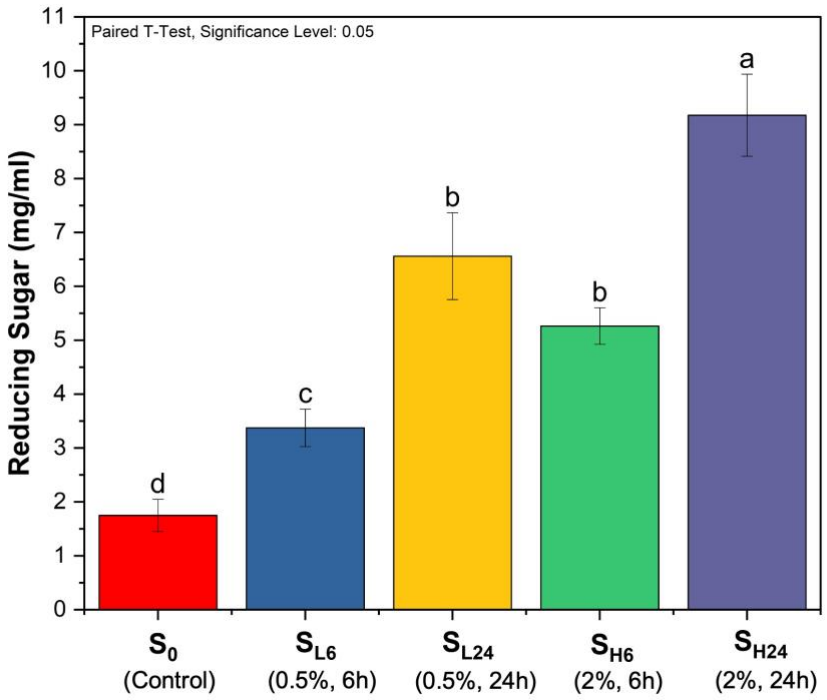

Figure 2.23 Total reducing sugar amount released in retting liquid for enzyme effectiveness

Table 2.7 Summary of ANOVA results for reducing sugar content

	F_c (Conc)	F_t (Time)	F_i (Conc : Time)
Sugar [mg/ml]	41.11 (1.2e-4)***	102.10 (3.3e-6)***	1.08 (0.33), ns

results expressed as "F-value (Prob > F)"
Significance codes: $p > 0.05$ ns: not significant, $*p < 0.05$, $**p < 0.01$, $***p < 0.001$

Moreover, the peel energy is plotted against reducing sugar released for various conditions of enzymatic retting in **Figure 2.24** to further understand the effect of reducing sugar released on peel energy. Here, as released reducing sugar content increases, the peel energy decreases. This shows that the one of sugars getting released inside the retting liquid was coming from degradation of the pectin rich layer holding the bast fiber bundles to the woody core. Detailed analysis of retting liquid by Majumdar et al. showed that the galacturonic acid to be one of the predominant sugars in the total sugar content [87], which is the primary sugar formed by hydrolysis of pectin and responsible for the reduction of peel energy during separation of bast from woody core. Earlier in

this study, it was shown statistically that both the enzyme concentration and duration of incubation time have a significantly impact on liberating reducing sugars and peel energy, hence the degree of retting. Moreover, as the retting degree progresses, the variation (SD) in peel energy reduces while increasing in case of reducing sugar released. The initial linearity in relationship between peel energy and reducing sugar also begins to asymptote as enzyme concentration and incubation time increases from S_{L6} to S_{H24}, where the rate of release of reducing sugars is faster than the decrease in peel energy. We hypothesize that this is due to the degradation of the pectin bond around the bast-wood interphase while the reducing sugars is still being liberating from other parts of the flax stem.

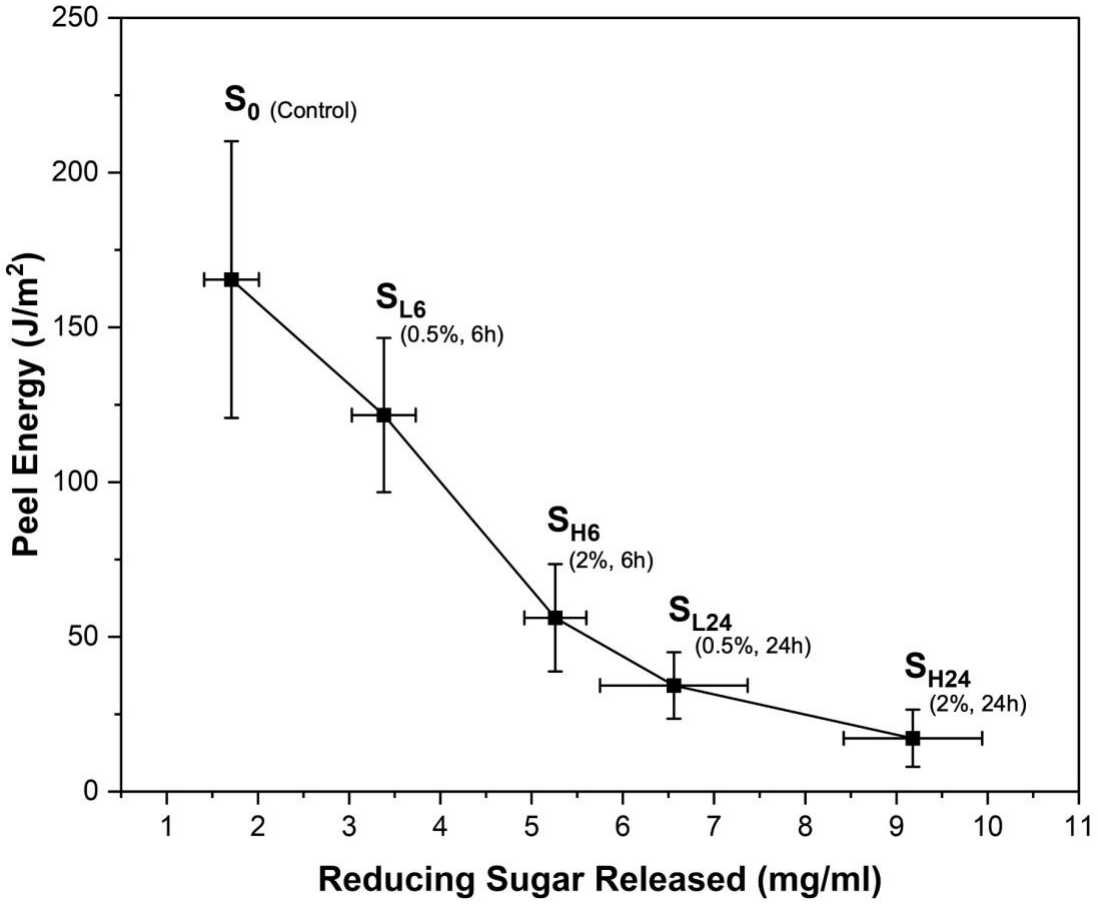

Figure 2.24 Peel energy vs reducing sugar released for different enzyme retted samples

2.8.4 Enzymatic retting condition effect on bast differentiation and comparison with peel energy

To understand the effect of retting condition on the bast fiber bundle differentiation or fiber fineness, the cross-sectional area of resulting technical fibers under different retting conditions are shown in **Figure 2.25**, where the two boxes correspond to the gauge length of 10 mm and 30 mm, respectively. Here, a right skewed distribution among different retting groups is observed, particularly in for gauge length of 10 mm, where the mean marked as "¤" is above the median value marked as "—" within the box plot. The similar skewed distribution pattern for the technical fibers' diameters and areas has also been reported by other studies in literature [42,43,78]. **Figure 2.25** also shows that the average of fiber areas is not significantly different between the gauge length of 10 mm and 30mm for all retting condition groups ($p > 0.1$). However, the spread of the area measurement distribution (SD) and skewness is smaller in the case of gauge length of 30 mm than that of 10 mm. This is due to increase in number of measurement for estimating the mean diameters over longer length of the technical fiber used for area calculation in case of gauge length of 30 mm.

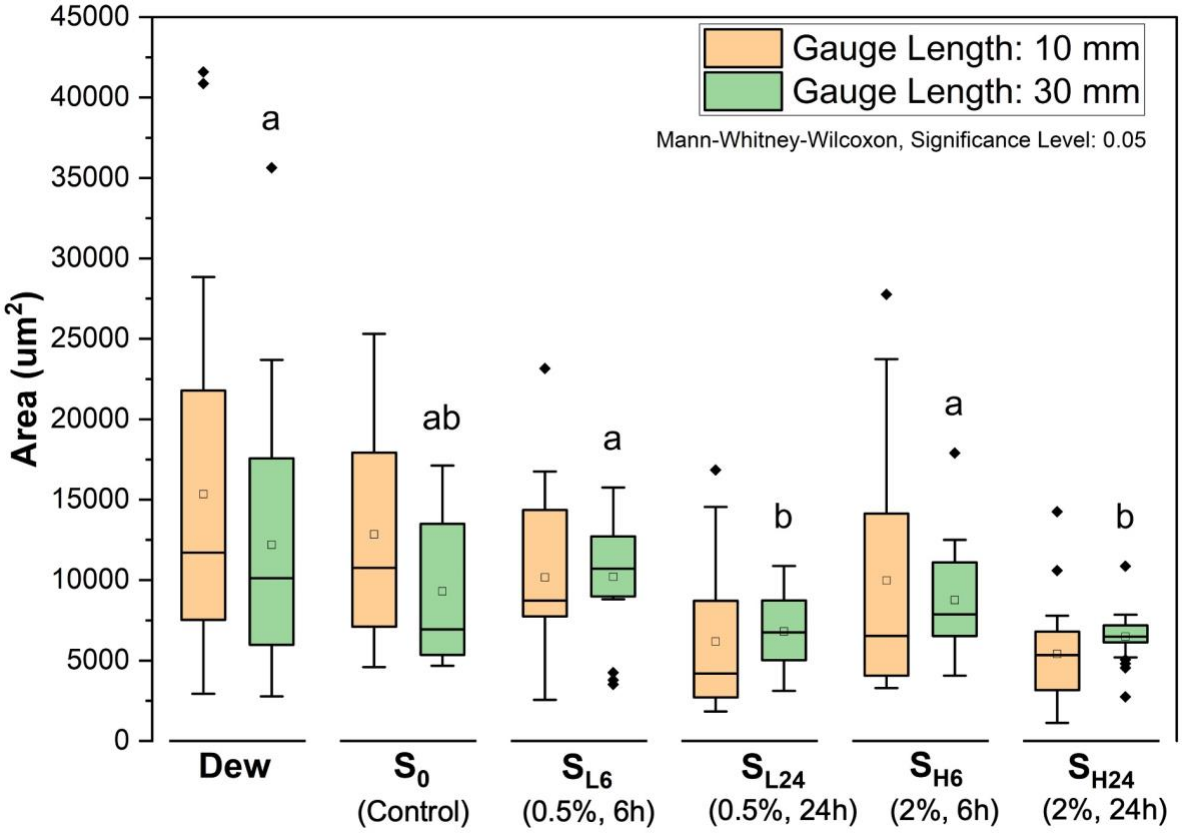

Figure 2.25 Cross-sectional area distribution for technical fibers from different retting conditions and gauge length in current study (significance markings are with respect to groups from gauge length 30 mm)

Furthermore, ANOVA summary in **Table 2.8** shows that only retting time significantly affects the technical fiber cross-sectional area or bast bundle differentiation during enzymatic retting ($p < 0.001$). This can be further seen from **Figure 2.25**, where significant effect of retting time is shown by the significant decrease in fiber cross-sectional area upon increasing retting time from S_{L6} to S_{L24} ($p < 0.01$) and from S_{H6} to S_{H24} ($p < 0.01$), while keeping enzyme concentration fixed in both gauge length cases. However, the significant effect of concentration is not shown upon increasing enzyme concentration keeping time fixed, i.e., from S_{L6} to S_{H6} ($p > 0.1$) and from S_{L24} to S_{H24} ($p > 0.1$) in both gauge length cases. Furthermore, there is no significant differences

among the areas of Dew, S_0, S_{L6} ($p > 0.1$) due to insufficient retting and high variation. And the areas from S_{L24} were found to be statistically different significantly from S_{H6} in gauge length of 30 mm ($p < 0.05$), which is not the case for gauge length of 10 mm ($p = 0.06$). Although, the mean and median for S_{H6} is higher than S_{L24} in both gauge length cases, it is difficult to conclude the statistical difference in areas here due to the high variation in S_{L24} & S_{H6} and p - values being close to threshold of rejecting the null hypothesis.

Table 2.8 Summary of ANOVA results for areas from gauge length (GL) of 10 mm and 30 mm

	F_c (Conc)	**F_t (Time)**	**F_i (Conc : Time)**
Area [um^2] (GL: 10)	0.28 (0.59), ns	13.96 (3.6e-4)***	0.06 (0.8), ns
Area [um^2] (GL: 30)	1.31 (0.25), ns	19.04 (4.0e-5)***	0.80 (0.37), ns

results expressed as "F-value (Prob > F)", GL: gauge length in mm
Significance codes: *p > 0.05* ns: not significant, **p < 0.05, **p < 0.01, ***p < 0.001*

To further visualize the bast bundle differentiation, in addition to extracted technical fiber cross section measurements, scanning electron microscopy (SEM) was done on the stem cross sections resulting under different retting conditions as shown in **Figure 2.26**. Here, the inter-bast or bast bundle divisions are marked by red arrow heads and the fractures or intra-bast bundle divisions are marked by golden arrow heads. Similar morphology of retted flax stems was visualized in literature for dew and enzymatic retting [64,81,89,98]. From **Figure 2.26**, S_0 sample here shows the largest bast bundle size with minimum differentiation. Compared to S_0, bast bundles are more divided in dew retting with some intra-bast cracks. Further with enzyme retting, slightly smaller bast bundles are observed in the case of S_{L6} compared to S_0, with no further intra-bast fractures. But, higher intra-bast fractures were observed upon increasing incubation time from S_{L6} to S_{L24} and from S_{H6} to S_{H24}, when enzyme concentration kept same. Moreover, similar morphology of cross section is seen upon increasing enzyme concentration upon keeping retting

time same from S_{L6} to S_{H6} and from S_{L24} to S_{H24}, indicating lower effect of enzyme concentration on bast bundle differentiation.

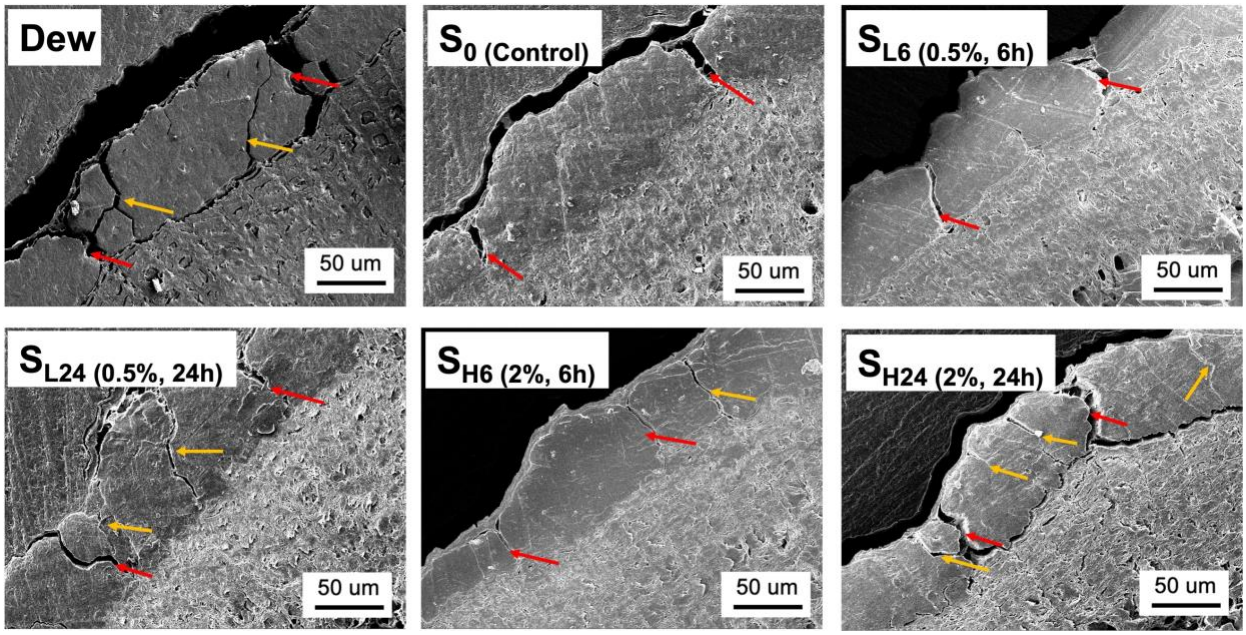

Figure 2.26 Scanning electron micrograph (SEM) of stem cross section from different retting conditions (red arrows for bast bundle divisions, golden arrows for fractures within bast bundles)

From both technical fiber area measurements from optical microscopy and scanning electron microscopy of flax stems, we observe that the time has significant effect over bast bundle differentiation. The longer the incubation time of enzyme retting, the more the differentiation of the bast bundle into finer technical fibers. However, in case of peel energy or bond strength of bast-woody core interphase, both time and concentration have significant effect. This is due to the fact the bast fiber region consists of thick cellulosic walls and lignin [62], in contrast to surrounding area which is made up of thin cell walls with low lignin content, hence, it is easier for the enzyme to degrade the pectin rich middle lamella of thin cell walls and other components in this region . This is also shown by some biological studies in case of dew retting, where the occurrence of

bacteria and enzyme activities are higher in the surrounding bast region [62,89]. With the increase of incubation time of enzyme retting, the enzyme is able to penetrate and degrade the middle lamella within bast bundles, resulting in finer technical fibers in case of S_{L24} and S_{H24}.

2.8.5 Retting condition effect on single technical fibers tensile properties

The tensile modulus and strength for both gauge length cases of technical fibers testing under different retting conditions are summarized in **Figure 2.27** and **Figure 2.28** respectively. Their corresponding ANOVA results are summarized in **Table 2.9**. Non-parametric statistical testing method of Mann-Whitney-Wilcoxon is used to compare the mean of different groups. Depending on the method of experimental tests and the area estimation, the tensile property values reported in literature varies. But the tensile values found in this study falls within the range reported in literature [26,60,79,89]. Also, the tensile properties at gauge length 30 mm if compared to 10 mm are higher here, which is contradicting to the usual declining trend in tensile properties with increasing gauge length [24,99], but, it is to be noted that stem used for testing these two gauge lengths are different and the intent of current single stem study is to evaluate the retting conditions effect within respective gauge lengths only.

Table 2.9 Summary of ANOVA results for single fiber tensile properties

	F_c (Conc)	F_t (Time)	F_i (Conc : Time)
M (GL: 10)	0.20 (0.66), ns	3.93 (0.051), ns	0.72 (0.4), ns
TS (GL: 10)	0.33 (0.57), ns	0.96 (0.33), ns	0.07 (0.8), ns
M (GL: 30)	1.63 (0.2), ns	5.89 (0.02)*	8.6 (0.004)**
TS (GL: 30)	0.33 (0.57), ns	0.52 (0.47), ns	15.67 (0.0002)***

results expressed as "F-value (Prob > F)", M: Modulus in GPa, TS: Tensile Strength in MPa, GL: gauge length in mm

Significance codes: $p > 0.05$ ns: not significant, $*p < 0.05$, $**p < 0.01$, $***p < 0.001$

Technical fiber modulus depends on the property of elementary fibers and their ability to transfer load across the middle lamella interphases [26,34,100,101]. Due to the inconsistent or low retting degree in the case of Dew and S_0, a significantly lower modulus ($p < 0.01$) compared to enzyme retted fibers (except the case of gauge length 10 mm where S_{H6} was comparable to Dew ($p > 0.1$)). We hypothesize that the hackling is unable to break the fiber bundles at weak interphases or fails to remove unwanted epidermis tissues from fiber, which do not contribute effectively to transferring load, thus resulting in a lower modulus [82,101]. The ANOVA results in **Table 2.9** showed no statistically significant effect of incubation time and enzyme concentration on the modulus at gauge length of 10 mm ($p > 0.05$). This is consistent from **Figure 2.27**, where all four groups (S_{L6}-S_{H24}) were found statistically comparable ($p > 0.05$) in later pairwise comparisons. This also shows that the structural component of cellulose within elementary fibers is not affected by different conditions of enzyme retting as compared to Dew retting where microorganisms degrade the structural component cellulose in addition to middle lamella interphase, that degrades the tensile properties [26,43].

However, in the case of gauge length of 30 mm, the ANOVA results in **Table 2.9** show that the incubation time ($p < 0.05$). and the interaction between time & concentration have a significant effect on technical fiber modulus ($p < 0.01$). This is consistent with **Figure 2.27**, which shows a significant increase in technical fiber modulus from 6 hours in S_{L6} to 24 hours in S_{L24} ($p < 0.05$). In contrast, at the high concentration case of S_{H6} and S_{H24}, the effect of incubation time is not significant, which shows the interaction between concentration and time is significant ($p < 0.05$). It was hypothesized here that the variation during manual hackling of sample S_{L6} was unable to remove the weak links within the bast bundles.

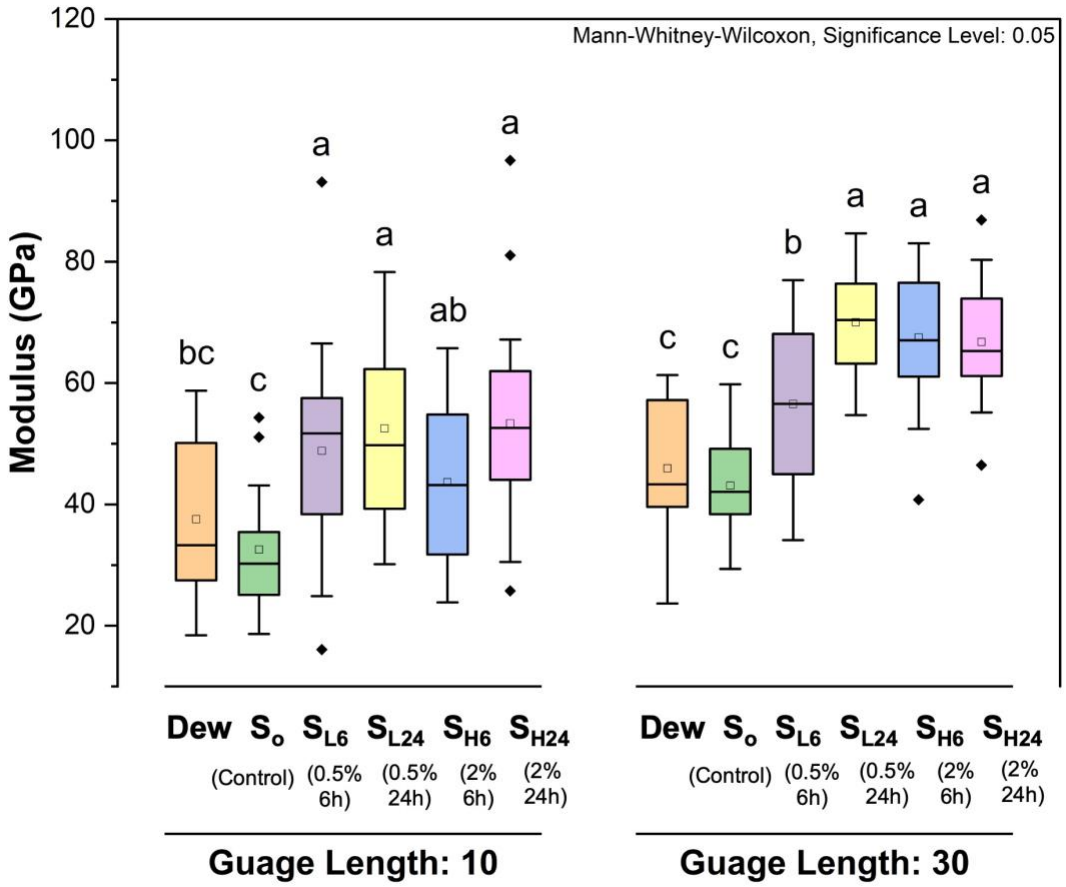

Figure 2.27 Modulus of technical fibers from different retting conditions and gauge length in current study

Tensile strength of technical fibers depends upon the strength of both elementary fibers and the interphase between them. The ANOVA results in **Table 2.9** showed no significant effect of incubation time and enzyme concentration on the tensile strength at gauge length of 10 mm ($p > 0.05$). This is consistent from **Figure 2.28**, where all four enzyme retted groups (S_{L6}-S_{H24}) along with S_0 were found statistically comparable in later pairwise comparison ($p > 0.05$). Again, here it shows that the elementary fibers were unaffected by enzyme retting conditions. Dew retted fibers were significantly weaker ($p < 0.05$) compared to other groups in the study, except S_{L6} ($p > 0.05$) where the variability was high as well.

Further, the gauge length case of 30 mm ANOVA studies (**Table 2.9**) also didn't show a significant effect of concentration or time over tensile strength. However, similar to the modulus case, the interaction between time and concentration has a significant effect ($p < 0.05$). This is further observed from **Figure 2.28**, where S_{L6} and S_0 showed high variability and significant lower tensile strength values than S_{H6} ($p < 0.5$), whereas the strength was comparable for S_{L24} and S_{H6} ($p > 0.05$). Inconsistent, poor retting with inability to remove the unwanted material such as waxes and epidermis during hackling were found responsible for lower strength here [24,26,101]. The tensile strength of S_{L6} was not found significantly different than S_{L24}, however, the sample S_{H24} here showed significantly lower tensile strength when compared to S_{H6} ($p < 0.05$), which shows the interaction between concentration and time is significant ($p < 0.001$). Further, this shows that increasing enzyme concentration with time to the level of very high degree of retting (S_{H24}) can significantly degrade fiber quality by making the interphases weak within the technical fiber, an affect not seen at gauge length of 10 mm, hence indicating over-retting. Dew retted samples also show significantly lower tensile strength when compared to S_{L24} and S_{H6} ($p < 0.05$) but was comparable to S_{H24} ($p > 0.05$) due to inconsistent retting and cellulose degradation [26,43].

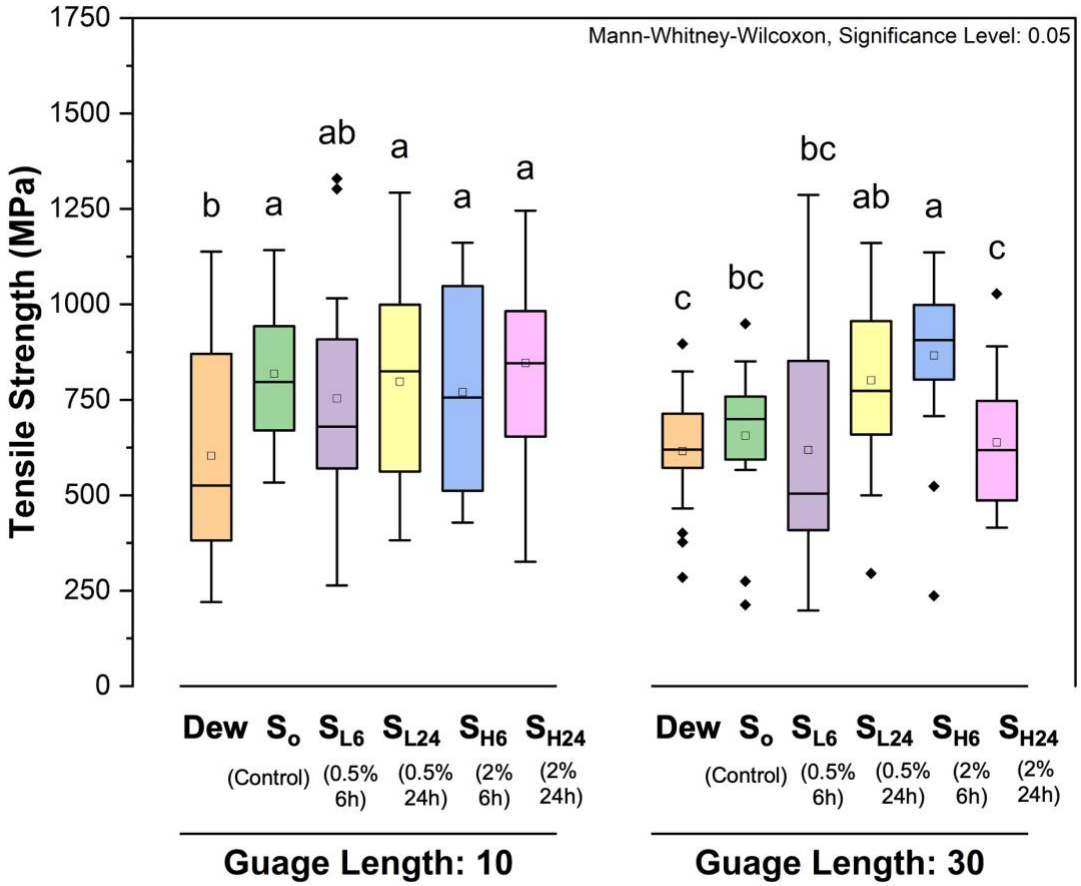

Figure 2.28 Tensile Strength of technical fibers from different retting conditions and gauge length in current study

2.8.6 Effect of resulting fiber cross-sectional area on tensile properties

As previously discussed in Chapter 1, a graph between tensile properties and fiber diameter or cross-sectional area is highly scattered and difficult to interpret if multiple groups are involved [26,66,78]. In this section, to better study the effect of cross-sectional area resulting from various retting conditions over tensile properties, the area is categorized into intervals of 5000 um^2 (a 5000 um^2 area corresponds to about 40 um in diameter) and average tensile values are plotted for different groups within those intervals.

Figure 2.29 (a & b) shows variation of modulus for different retting conditions in the respective area intervals. A decrease in mean modulus is observed for all groups as the interval progresses to a larger area in the case of gauge length 10 mm, which is not clearly shown in the case of 30 mm when the elementary fiber interphases play an important role. Moreover, this modulus decline is higher at the larger area region than at the smaller area region where the variation is very high. Modulus values of Dew and S_0 observed to lie towards the lower values compared to other groups in respective intervals (for both gauge lengths) and also distributed into larger area intervals (also can be seen from **Figure 2.25**), a reason for statistically significantly lower modulus as seen in previous section for these cases. S_{L6} has the highest variation among other enzyme retted groups in the area intervals and scattered towards higher area intervals. S_{L24}, S_{H6} and S_{H24} are distributed towards the lower interval area and have a higher modulus values, meaning enzymatic retting being efficient in removing the weak interphases.

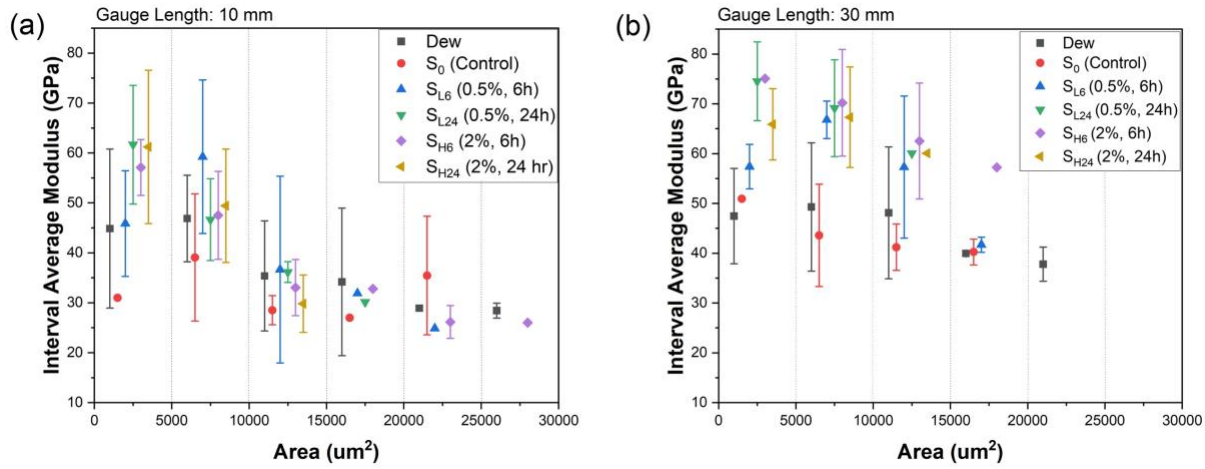

Figure 2.29 Area Interval average modulus for (a) gauge length of 10 mm and (b) gauge length of 30 mm

Figure 2.30 (a & b) shows variation of tensile strength for different retting conditions in the respective area intervals. Similar to modulus, a very prominent decline in tensile strength is

observed for all groups as the interval progresses to a larger area in case of 10 mm gauge length. Role of interphase strength resulting from varying retting conditions comes into play with cross-sectional defects at 30 mm gauge length and a sharp declining trend in tensile strength isn't observed here. Moreover, similar to modulus the variation in tensile properties is higher within smaller area intervals and it is difficult to estimate the negative relationship with good correlation. Dew retted fibers show lower strength values than other groups at gauge length of 10 mm within same area intervals, indicating the cellulosic degradation in elementary fibers due to microorganisms' activity. Tensile strength of groups S_0 and S_{L6}-S_{H24} are comparable at 10 mm gauge length. Further over longer gauge length of 30 mm, differences between the retted groups becomes more noticeable. Technical fibers from Dew, S_0 and S_{L6} having high variation and distributed around large area intervals shows significantly low tensile strength. S_{H6} shows higher strength values at smaller area intervals than other groups, showing the effect of high enzyme concentration and low incubation time in effectively removing the weak links and unwanted tissues with preserving the strength of interphase within the technical fiber bundle. Lastly, where a high enzyme concentration and incubation time result in finest fibers with narrow area distribution in case of S_{H24}, these fibers show lower strength values in their respective smaller area intervals at 30 mm gauge length, indicating the weakening of interphases between the elementary fibers along the length due to over retting.

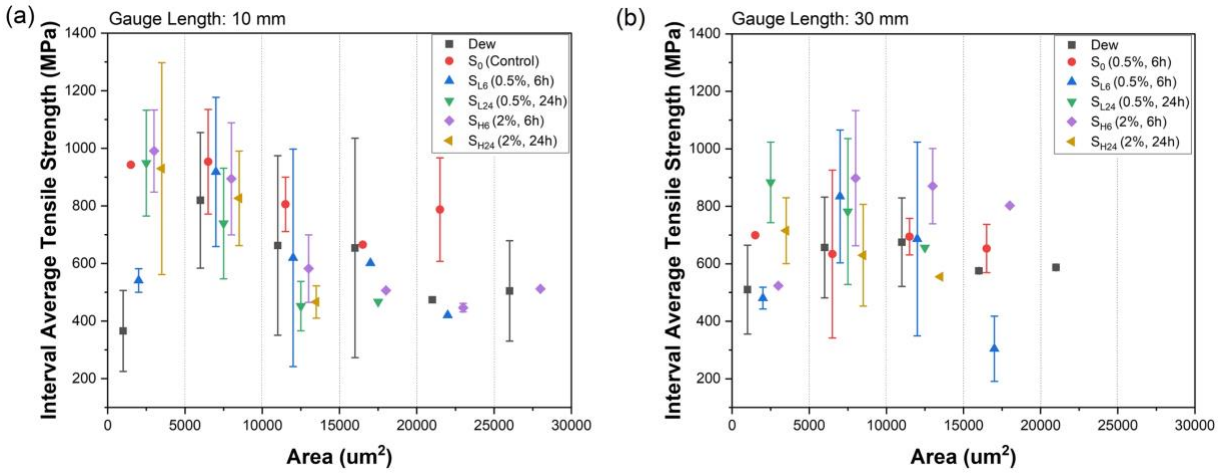

Figure 2.30 Area Interval average modulus for (a) gauge length of 10 mm and (b) gauge length of 30 mm

2.9 Conclusions

In this chapter, first improvements in the measurement of the fiber tensile properties are discussed, where an ellipse approximation is used over circular cross- section approximation and proved to be better with actual area evaluation of technical fibers. Also, using machine compliance over system compliance calculated using ASTM C1557 – 14 standard showed more reliability and reproducibility of tensile results. Initial slack correction was also implemented for accurate measurement of mean elongation %. Non-retted flax stems were observed under SEM and the bast layer bundle dimensions here were compared to the optical microscope measured dimensions of technical fibers obtained with dew and enzyme retted process. It was observed that the extraction process divides these fiber bundles across circumferential direction rather than dividing across the bast width. The mean circumference dimension for enzyme retted fibers were found to be lower with less standard deviation than dew retted fibers. Fibers extracted with controlled enzyme retting shows significantly improved modulus and tensile strength over fibers extracted from dew retted stems during preliminary studies of effect of retting type.

Furthermore, specimens from a single stem were treated with different enzyme retting conditions, and the effect of enzyme concentration and incubation time (duration of retting) over bast separation efficiency, resulting technical fiber dimensions and tensile properties was investigated. Bast fiber layer-woody core interphase strength was measured through 90° peel test and expressed as peel energy in J/m^2. Peel energy measured from 90° peel test and analysis of reducing sugar liberated in retting solution were established as measures for quantitative evaluation of retting efficiency or degree of retting. Statistical analysis through ANOVA showed that both concentration of enzyme and retting duration has significant effect on peel energy and reducing sugar content. Peel energy values were inversely correlated with reducing sugar content from different retting conditions. In addition to bast separation, bast differentiation into technical fibers resulting from different retting conditions were evaluated through fiber and stem cross-sectional measurements using optical microscopy and scanning electron microscopy (SEM) respectively. Through visual and statistical analysis here, it was seen that only retting duration plays significant role in bast differentiation than enzyme concentration as no significant decrease in fiber area is observed upon increasing enzyme concentration from S_{L6} to S_{H6} keeping incubation time constant, although S_{H6} sample showed significant decrease in peel energy when compared to S_{L6}. Hence, it is possible to design an enzymatic retting process with smaller duration of incubation time to achieve desired degree of retting for later mechanical extraction steps.

Single technical fiber tensile properties were evaluated at 10 mm gauge length and 30 mm gauge length for various retting conditions in single stem study and correlated with fiber cross-sectional area as interval averages. Two interesting cases of enzyme retting were discussed, one with higher incubation time but low enzyme concentration (S_{L24}) and another high enzyme concentration but low incubation time (S_{H6}), and both showed the highest tensile properties of

fibers but different fiber fineness. Importance of gauge length in tensile testing is seen when fine fibers from high enzyme concentration and incubation time (S_{H24}) showed tensile properties comparable to other groups at 10 mm gauge length but significantly low properties at 30 mm gauge length when role of elementary fiber interphase comes into play, indicating degradation of technical fiber performance at high degree of enzyme retting. *Lastly, 0.5 % enzyme concentration and 24 hours incubation time (sample S_{L24}) is chosen as enzyme retting condition for further improved extraction studies in later chapters of this dissertation.*

Chapter 3
Mechanical Stem Breaking Process Improvement

3.1 Introduction

After retting, the next step in the process of fiber extraction is mechanical breaking, where the retted stems are passed between the gear teeth or flute profile of rotating rollers, to break and separate the inside brittle woody core from the bast fiber layer [24,26]. The equipment used here is termed as a fiber decorticator or stem breaker. Studies shows that during mechanical extraction steps, fibers generate kink bands caused by the bending and compression induced during the process, that significantly degrades mechanical properties of flax fibers [67,68,102].

The research in this chapter aims to evaluate the fiber damage occurring at the single stem level during mechanical breaking and develop insights for high quality natural fiber extraction. The stems are retted using the enzymatic retting conditions from chapter 2. Then, fracturing of retted stems under compression and bending are studied using compression and 3-point bending tests, along with real time observation of fracturing events through recording high quality video. The force-compression data obtained from compression tests are used to generate the constitutive material model for the woody core of flax stems. Analysis of stem bending under a wide range of tool geometries is done using finite element modelling (FEM) and an improved breaking process with an improved roller profile is developed. Finally, the impact of this improved stem breaking process on extracted fiber properties is evaluated.

3.2 Experimental

3.2.1 Flax stems

Raw flax stems of Agatha variety used in this study were grown under uniform conditions at Orgon State University research farm in 2019 spring and provided by Fibrevolution™. Also, for greater uniformity in sampling through experiments, the middle 25 cm long section of these stems with diameter 1.5 ± 0.15 mm was chosen for enzyme retting [38,91,92].

3.2.2 Enzymatic retting and fiber extraction

Pectinex® Ultra SPL (procured from Sigma Aldrich) with enzyme activity equal or greater than 3,800 units/mL according to product data sheet was used for lab scale retting of raw flax stems. Enzyme-buffer solution of 0.5% (v/v) was prepared with sodium acetate buffer (0.05 M, 4.5 pH) and flax stems taken in 1:25 ratio (gm:ml) with this enzyme solution in a test tube at room temperature, following by incubation at 40 °C for a duration of 24 hours while shaking horizontally at 100 rpm. Flax stems were gently washed after retting five times with distilled water and dried at 100 °C for 24hr before any mechanical testing or fiber extraction.

Technical fiber bast strips were carefully extracted manually or through breaking stems under rolling depending on different experiments in this study. These bast strips were then hackled into finer technical fibers using a pin frog (9 pins/cm^2) and kept at 50% relative humidity at 23 °C in a humidity chamber for conditioning prior tensile testing.

3.2.3 Single technical fiber microscopy and tensile testing

As discussed in chapter 2, improved ASTM C1557 – 14 standard was used in chapter for sample preparation and testing single technical fibers. Here, 15 randomly selected fibers were

mounted on paper frame tabs using cyanoacrylate adhesive at 10 mm gauge length to reduce the elementary fiber interphase contribution [14]. Optical microscopy was done on mounted fibers using Olympus DSX510 digital microscope in polarized light (PO) mode, first front view and later rotating the fiber 90 degrees for side view. Average of 8 measurements along each direction was used to estimate the respective diameters and ellipse approximation was used to calculate the cross-sectional area of technical fibers here, used in prior studies for better evaluating the tensile properties of fibers [68,103]. Later, tensile tests on conditioned extracted fibers were performed by using a Texture Analyzer from Texture Technologies Corp. with a 50 N load cell capacity. The paper mount was cut after mounting the fibers in the tensile grips and crosshead speed of 0.01 mm/sec was chosen with trigger force of 0.03 N for the tensile test. The tensile data was corrected for initial slack in elongation and system compliance (calculated using a stiff specimen under tensile testing with same parameters as fiber test) for better estimation of modulus.

3.2.4 Stem fracture analysis under compression and bending tests

Compression tests on 1.25 cm long retted stem samples were done using a Texture Analyzer from Texture Technologies Corp. with a 300 N load cell and the fracture events were monitored through video recording. Initial diameter at the start of compression is determined at the trigger force of 0.3 N and stems were compressed under parallel plates (25 mm in diameter) to a maximum force of 80 N with test speed (ν) of 0.05 mm/sec maintained during the complete compression-decompression cycle. Moreover, compression cycling was done with 25µm increments in displacement at test speed of 0.01 mm/sec to determine the elastic-plastic deformation transition within the linear region of force-compression curve. Further, to study the impact of sample non-uniformity, the effect of leaf bumps (parts on stem where leaves were present) on woody core samples in compression curve profile was evaluated. For better

visualization of leaf bump here, Olympus DSX510 digital microscope was used for generating a 3D profile scan of the woody core. Also, repeatability within a single stem was evaluated by performing compression tests on multiple woody core samples from a single stem.

Further, to compare the compression of stems under parallel plates with the compression under rolling between flat rollers (65 mm roller diameter) of a rolling mill, rotating at 0.55 rpm (ϖ) as shown in **Figure 3.1**, two samples were taken adjacent to each other from a single retted stem. In prior studies, this approach was shown to deliver repeatable mechanical test results [91]. The samples were crushed by exposing to an equal amount of compression (ideal compression limit determined during compression tests) through both the processes. The crushed stem samples were then compression tested using the Texture Analyzer to observe the subsequent force-compression curves. In addition, fibers manually extracted from as-retted and the crushed stem specimens, each taken from the middle section of a single retted stem, were tensile tested.

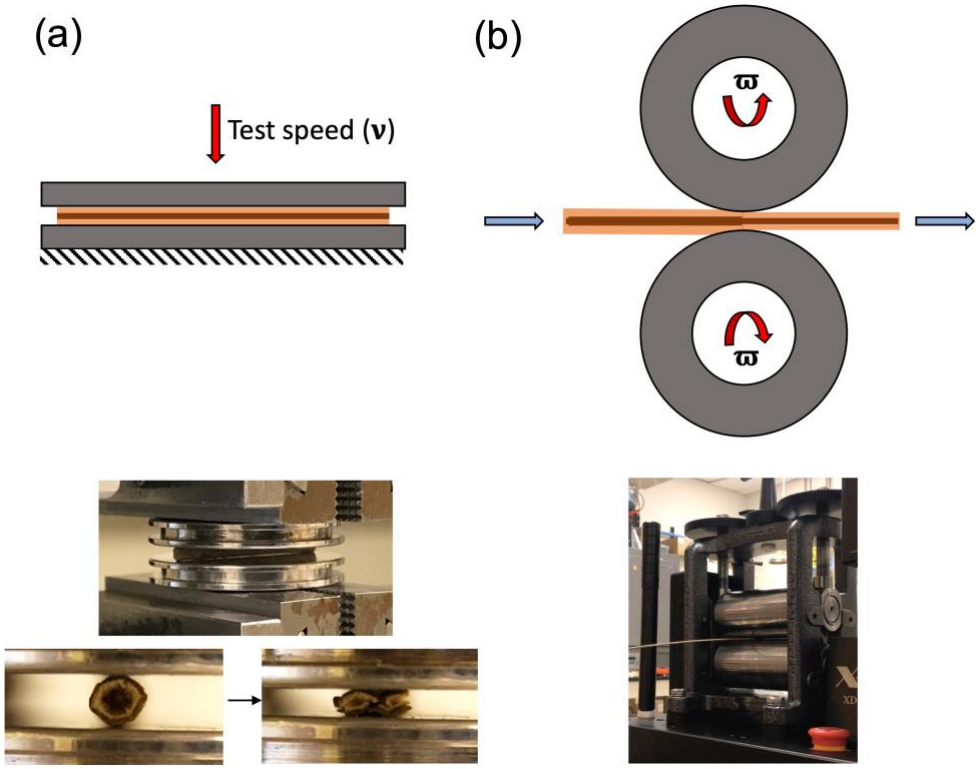

Figure 3.1 Stem compression under (a) parallel plate (b) rolling

Retted stems were also subjected to 3-point bending test using a Dynamic Mechanical Analyzer or DMA (RSA-3 by TA Instruments) having 34 N load cell capacity. Span lengths of 25 mm and 40 mm were chosen according to ASTM D 790, having high enough span length to stem diameter ratio to avoid shear effects [38]. Tool geometry consists of chisel tip with a 0.1 mm tip diameter. Stem lengths were taken about 20-25 % longer than of support span length. The deflection of load tool was set at 0.05 mm/sec and 0.01 N was taken as trigger force for test start. The estimation of bending radius for both span length case at max force can be done from **Figure 3.2**, using simple geometric calculations as shown in equation (3.1), also previously used in literature for beam bending studies by Ouaar et al. [104]. And the maximum tensile strain (ε_t) here is given by equation (3.2).

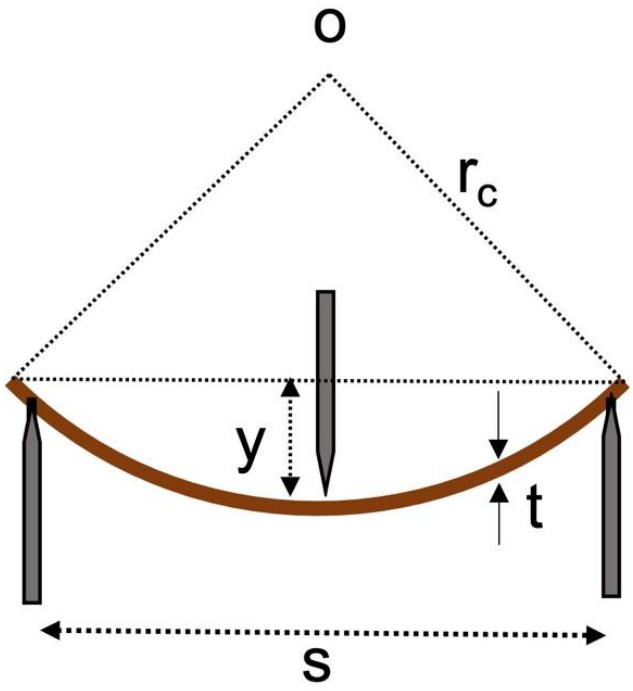

Figure 3.2 Radius of curvature during bending

$$r_c = \frac{s^2 + 4y^2}{8y} + \frac{t}{2} \tag{3.1}$$

$$\varepsilon_t = \frac{t}{2r_c} \tag{3.2}$$

where, r_c = radius of curvature during bending, s = span length and, y = tool deflection, t = stem thickness or diameter.

Moreover, from prior studies by Baley et. al., considering stem or woody core as beams with hollow circular cross-section, the bending stiffness at lower strains is proportional to the slope of force-deflection curve by equation (3.3) [38].

$$Bending\ Stiffness\ (EI) = \frac{dF}{dy}\frac{s^3}{48} \tag{3.3}$$

where, E = apparent bending modulus, I = area moment of inertia and, F = recorded force value.

3.2.5 Finite element modelling (FEM) of flax stems and predictions

The purpose of finite element model (FEM) studies here is to guide the design of breaking roller profile for minimizing the damage of fibers during extraction. To develop a finite element model for flax stems under various tool geometries for breaking, constitutive material properties need to be evaluated for the flax plant stem. Simplified constitutive material properties for the woody core were determined from the experimental force-displacement profile data obtained from the radial and axial compression tests. The results were correlated with a finite element model (FEM) of the woody core, modeled as an orthotropic elastic-perfect plastic material before fracture using ABAQUS/standard. The stresses predicted from finite element analysis (FEA) were

correlated with the visual observations during compression testing in order to predict the occurrence of initial fracture and verification of the simplified FE model. Further, to evaluate the capability of this material model, the obtained constitutive material properties were used to predict the force-displacement curve of another woody core sample from the same stem with twice the length and compared with the experimentally obtained force-displacement curve from the compression of same woody core sample.

The developed material model was used to study the bending of stems under a wide range of tool geometries through static finite element modeling (FEM) of 3-point bending in ABAQUS/standard. A hollow tube of length 60 mm with outside and inside diameter of 1.32 mm and 0.84 mm respectively was used for simplified model of woody core. These dimensions were calculated as the average from 5 cross-section diameter measurements of the woody core under optical microscope. The aim of this simplified mechanical model is to provide guidance in studying effects such as strain behavior from varying tool configurations during bending. The woody core was meshed using linear hexahedral elements of C3D8R type. The number of elements were varied along thickness from 5 to 12 elements and length from 100 to 400 for mesh sensitivity analysis. Final mesh has 60 elements along circumferential direction, 10 elements along thickness direction and 363 elements along length with 217,800 in total elements after sensitivity analysis. Analytical rigid body shell was used for modelling different tool profiles in FEM and general contact interaction property with 0.1 frictional coefficient (μ), tangential & normal behavior was used between tool - woody core interphase. Amplitude time step of 1 mm deflection is applied as load on top tool. Out of the wide range of bending tool geometries modelled with FEM, particularly 3-point bending with wider tool geometry is discussed here. In addition, the bending tool geometries

studied under FEM were also experimentally studied by creating similar tool profiles using 3D-printing with PLA for stem bending tests using DMA.

3.2.6 Improved stem breaking and extracted fiber characterization

Based on the bending studies, an improved stem breaking process with improved flute profile of roller was designed for fiber extraction. The impact of the improved tool geometry was first studied in DMA bending tests to determine the ideal roller gap. Since breaking rollers with a circular flute channel profile are commonly used for stem breaking [63,73] they were also tested as the baseline roller geometry. 3D-printing using PLA was used for prototyping the roller and tool geometry in DMA tests. Further, for fiber extraction studies from improved and baseline roller profile, two 5 cm stem samples were taken from the middle section of a single retted stem, each passed three times through the respective pair of fluted rollers rotating at 0.55 rpm, to break and separate the woody core from the bast layer. Then, manual shaking of these bast strips was done to remove any remaining attached woody core material followed by hackling into finer technical fibers.

For characterization, single fiber tensile tests were carried out on extracted fibers from the baseline and improved breaking roller profiles. Additionally, scanning electron microscopy (SEM) was done on the extracted fibers. The extracted fibers were first mounted on flat metal stubs with adhesive carbon tape and sputter coated with 30 nm thick layer of gold-palladium. JEOL IT500 scanning electron microscope was used to visualize the morphology of fibers at 10 kV accelerating voltage under high vacuum.

3.2.7 Statistical analysis

For multiple pairwise mean significance comparisons in this study, two-sample T-Test was done using R Studio software. Significance threshold was taken as 95% confidence interval, where a p-value < 0.05 indicates the rejection of null hypothesis and the mean differences to be statistically significant. For expressing results significance labeling was done using letter notation, where means having same letter (a, b, etc.) were statistically not significantly different.

3.3 Results and Discussion

3.3.1 Stem breaking studies under flat platen compression

The force - compression curve for a single compression-decompression cycle of an as-retted flax stem sample (S1) and its woody core (X1, after manually peeling the bast layer) is shown in **Figure 3.3(a)** and corresponding visual images of the marked events occurring real time are shown in **Figure 3.3(b)**. Within region 1 of the force-compression profile, both stem and woody core samples follow a similar elastic behavior, with the full stem exhibiting higher stiffness and breaking force than its woody core as expected. The flax stem shows an initial linear elastic behavior followed by non-linear behavior with top & bottom fracturing of the inside woody core occurring due to local buckling at events 2 and 3 in region I. Further compression in region II, shows the sideway splitting of both bast layer and woody core at event 4.

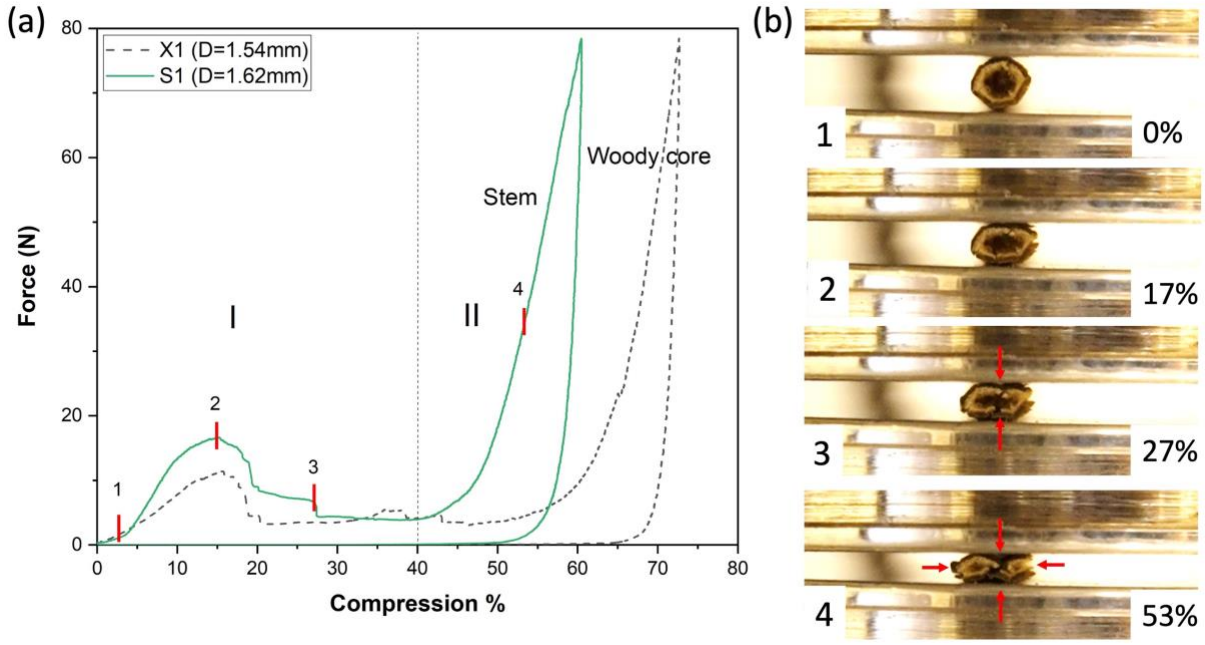

Figure 3.3 (a) Force-compression curve for an as-retted flax stem (S1) compared to its woody core (X1) and (b) visual observation of events occurring at various points during compression

It can be concluded that approximately 35% compression is required to obtain fracturing of woody core while avoiding damage to stems and bast fibers by over compression. Further, during compression cycling done within 5% compression (75um plate displacement). the flax stem exhibits perfectly elastic behavior (**Figure 3.4**). After 6% compression (100um plate displacement), a deviation from elastic to plastic behavior is observed.

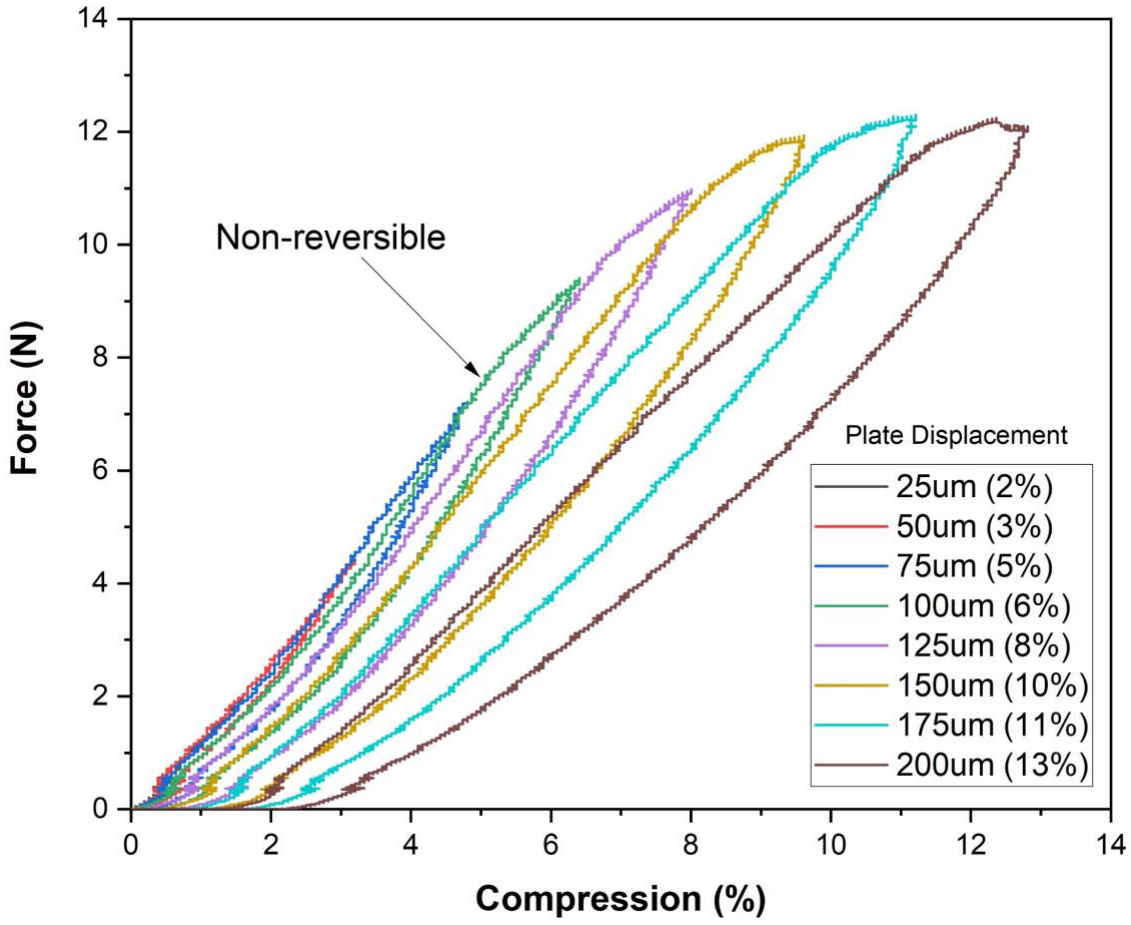

Figure 3.4 Flax stem compression cycling for determination of elastic to plastic transition

3.3.2 Improvement in reliability and repeatability of compression tests

One of the major challenges during compression testing of flax stems is that at the start of the tests, not all the surface of stem is in contact with the compression plates. Stems can vary in shape and non-uniformity may arise due to factors such as change in diameter due to growth variation and due to the presence of leaves as shown in **Figure 3.5(a)**, where presence of leaf left a bump in the middle of stem, leaving a gap between the platens as compared to a specimen without a leaf bump (**Figure 3.5(c)**). This leaf bump can be better visualized in **Figure 3.5(b)** that shows the 3D profile scan of woody core sample with leaf bump.

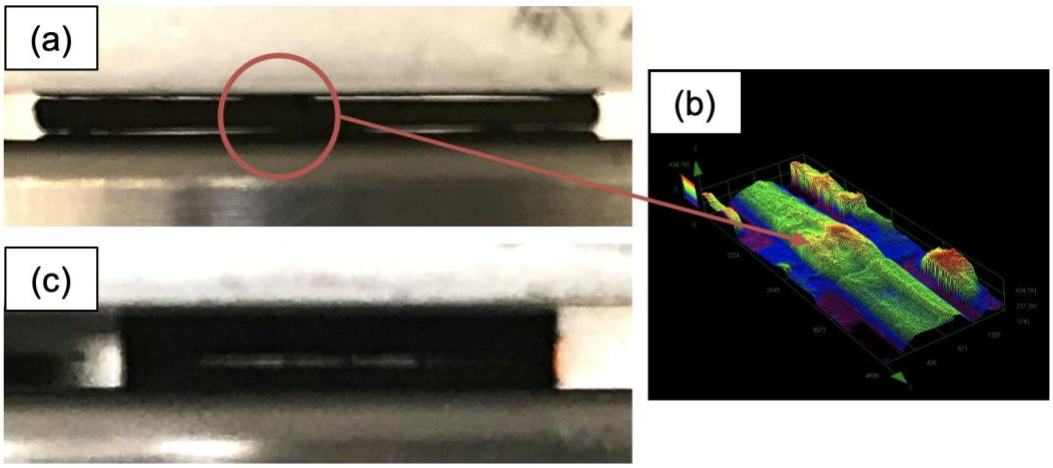

Figure 3.5 (a) Woody core with Leaf bump in middle (b) 3D profile scan of woody core sample with leaf bump in middle (c) Woody core with no Leaf bumps (flat sample)

Figure 3.6 compares the force-compression profile for a stem containing a leaf bump and a flat sample where no-leaf bumps were present. In the leaf bump sample, the slope of the linear region is initially lower until the complete surface is in contact with compression plates. After full contact, the slope is similar to the sample where no leaf bumps were present. Hence, this initial change in slope of the linear region can be explained as being caused by geometric non-uniformity of plant stems.

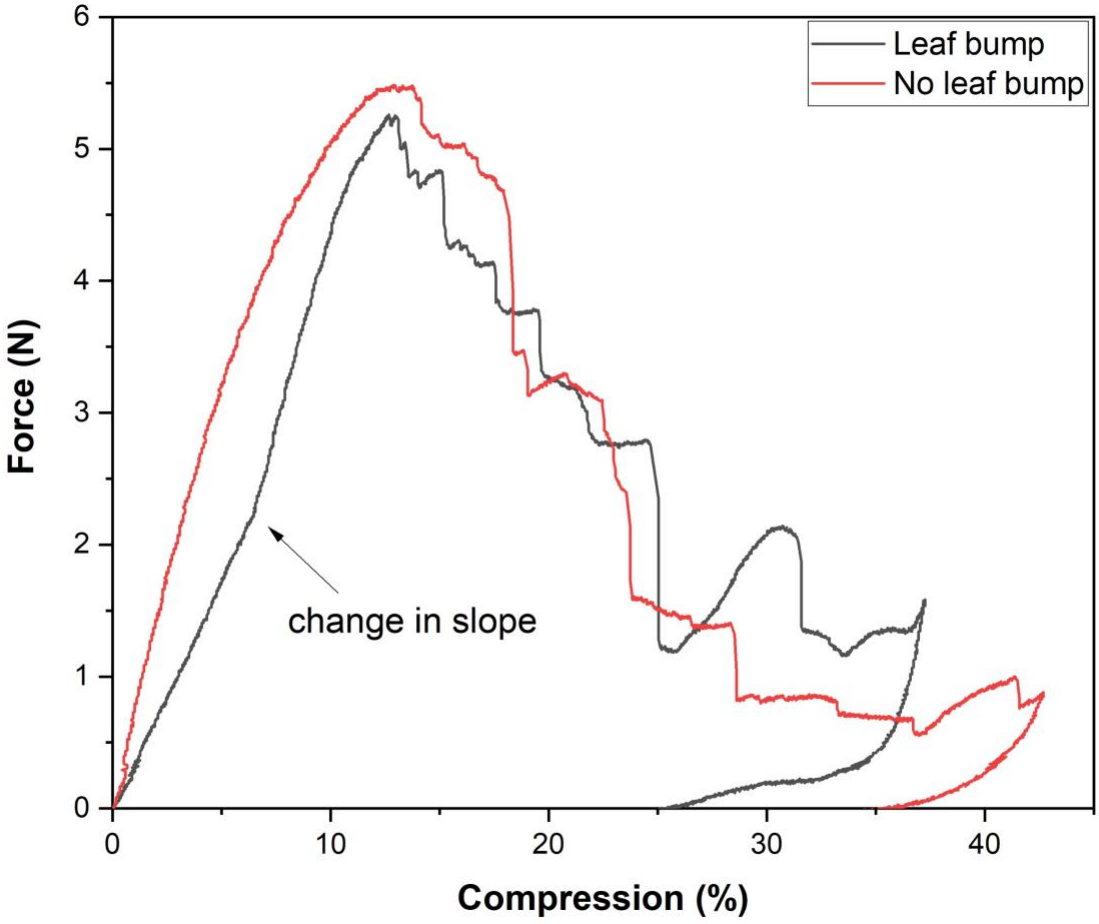

Figure 3.6 Force-compression profile comparison for a non-uniform (Leaf) sample and uniform sample (No Leaf)

Another major challenge during compression testing is the repeatability of compression curves between different plant stem samples. Flax stems vary in diameter and composition from bottom to top along length within a single stem as well as between different stems. In this study, woody core samples taken from middle section of a single stem, show repeatability in compression profile in the initial linear and elastic region (**Figure 3.7**). After the linear region, differences are seen in the fracturing events, however the overall curves were able to trace a similar overall path in the force-compression profile.

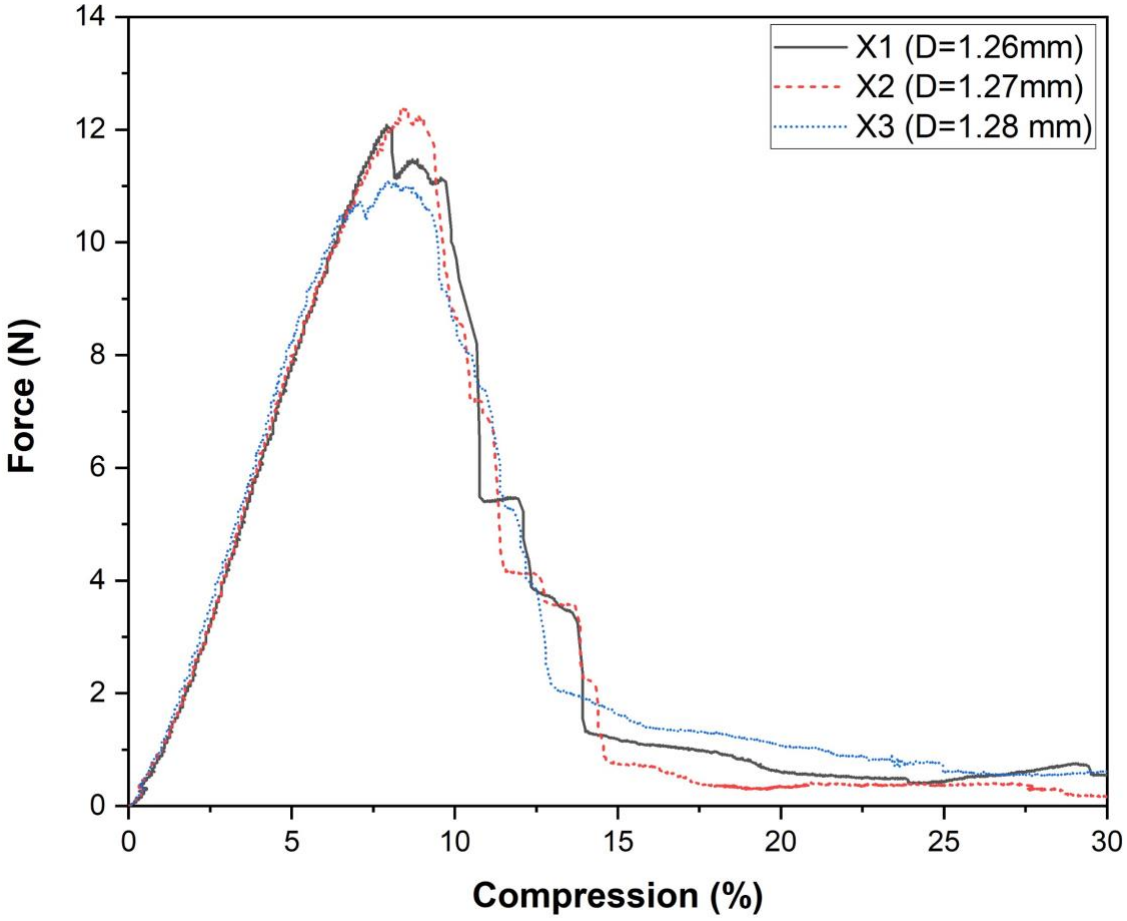

Figure 3.7 Force- Compression profile comparison for three woody core samples (X1, X2, X3) from a single stem

Therefore, for maintaining reliability in mechanical testing throughout this thesis, leaf bumps are avoided during sample preparation. Also, for studying various effects and maintain repeatability in experiments, sampling is restricted to a single stem as seen in Chapter 2 single stem studies and further will be used in this chapter as well.

3.3.3 Flat platen and rolling compression comparison

In industrial scale production, at times the breaking is initiated with crushing the stems under rolling with flat rollers [46,63]. To compare the crushing of stems under parallel plate and rolling compression, the force-compression curve of the two adjacent samples from a single retted

flax stem, each crushed to 35 % compression limit of previously shown region I with the respective method of compression, are compared in **Figure 3.8**. Here, the force-compression curve of these two samples correlated well with each other, hence, parallel plate compression can give a good estimate of stem fracturing under rolling compression.

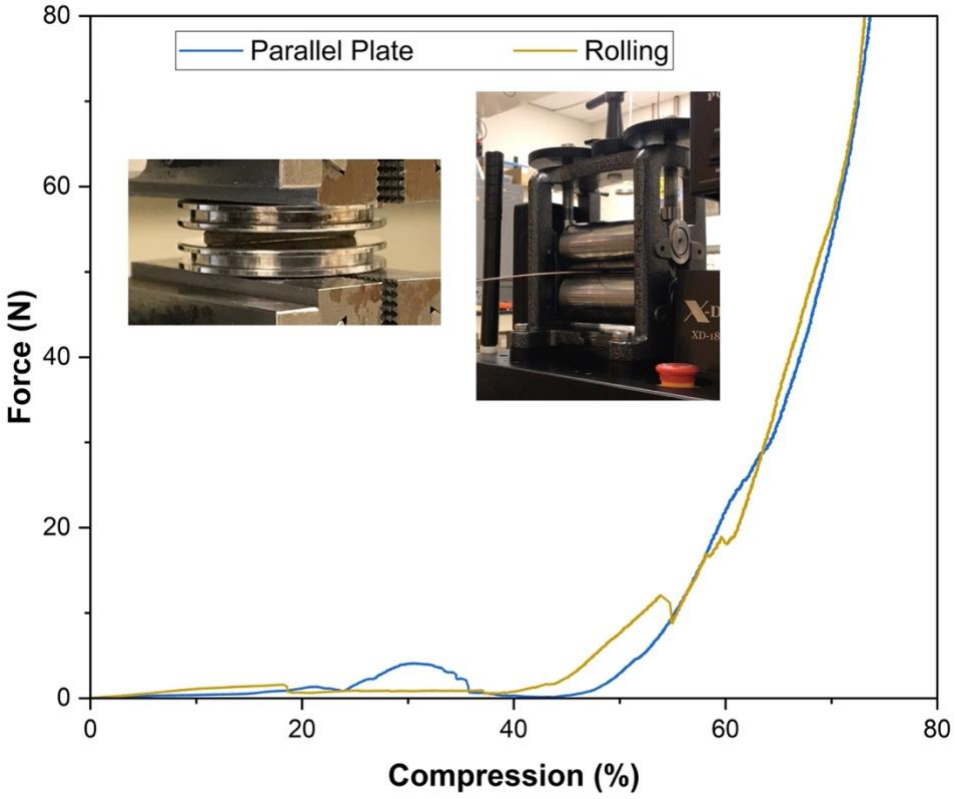

Figure 3.8 Force-compression curve for crushed (35 % compression) stems under parallel plate and rolling

Further, the tensile properties of the technical fibers extracted from as-retted and crushed (35 % compression of retted stem under rolling) stem specimens are shown in **Table 3.1**. The cross-sectional area, modulus, and tensile strength of technical fibers from both groups were found statistically comparable ($p > 0.1$), which indicates that the fiber properties remain unaffected under 35% compression limit of region I shown in **Figure 3.3(a)**. Also, reduction in variation or relative

standard deviation (SD) in % is observed in case of fiber properties from crushed stems, indicating reduced variation in manual peeling of bast strips from the as-retted stem case.

Table 3.1 Tensile properties of manually extracted fibers from as-retted and crushed flax stems

Sample	Area [um^2]	Modulus [GPa]	Tensile Strength [MPa]
As-retted	8030 ± 59 % [a]	47.7 ± 20 % [a]	889 ± 28 % [a]
Crushed (35 %)	6134 ± 43 % [a]	43.6 ± 17% [a]	880 ± 24 % [a]

results expressed as "average ± SD %"
Values within a column followed by the same letter are not significantly different ($p > 0.05$)

3.3.4 Stem breaking studies under bending

The force- deflection curve of as-retted stems under 3-point bending for 40 mm and 25 mm spans is shown in **Figure 3.9(a)**. An initial linear elastic region is seen in bending with loss in initial linearity due to higher displacement of central point before breaking in both the cases. This loss in linearity was also observed in previous studies by Baley et al. [38]. Also as expected, higher bending stiffness in case of 25 mm span is observed with a rapid force drop after point of maximum force, thus leading to a more rapid failure. While bending stiffness increases by lowering the span, the deflection of the tool needed to reach fracture also reduces. Therefore, it is more appropriate to plot the data as maximum tensile strain (ε_t) determined from radius of curvature, rather than deflection as shown in **Figure 3.9(b)**. Similar linear curve profile and strain values are observed for both the span cases at the time of initial failure here. Also, for same amount of deflection, higher tensile strain is observed in case of 25 mm span. This evaluation of changing bending stiffness with spans guides in estimating optimal tool deflection or roller gap for stem fracturing under bending, especially in case of small diameter rollers where the pitch of flutes (support span) is small and tight roller gap (high deflection) can cause high bending strains due to high bending stiffness, leading to defects such as kinks in bast layer fibers.

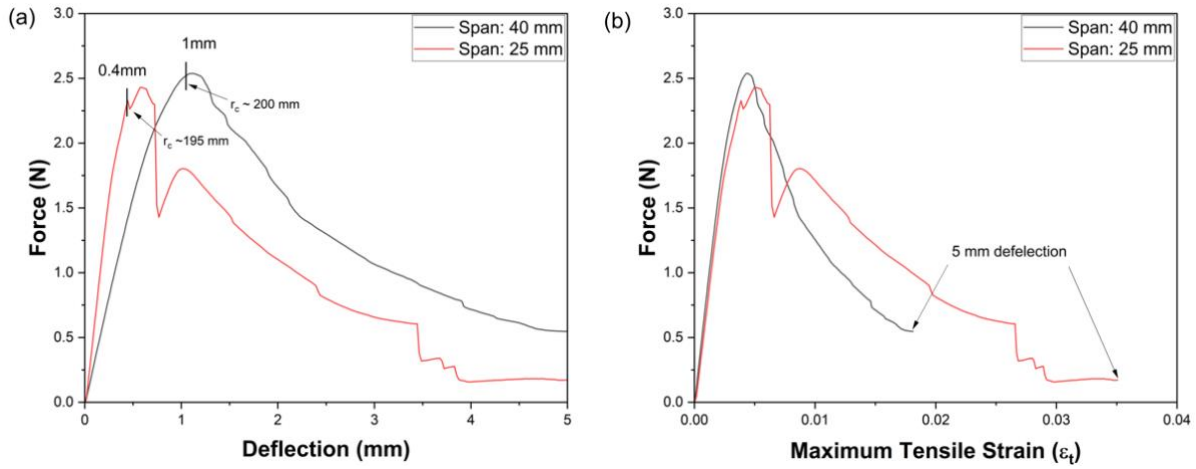

Figure 3.9 (a) Force-deflection and (b) force- strain curve for 3-point bending of retted flax stems under 40 mm and 25 mm spans

3.3.5 FEA modelling of stem compression and constitutive material properties

Since the woody core acts as a horizontally isotropic material under compression, the material model can be simplified as transversely isotropic from orthotropic elastic material. The elastic parameters obtained from correlating the finite element model for woody core under compression and the experimentally generated force-compression data are summarized in **Table 3.2**. Here, the transverse modulus (E1=E2) has the most impact on the results as compared to the axial elastic modulus (E3). For simplification, the woody core is modelled as an elastic-perfectly plastic material and the yield stress obtained from correlation is 2 MPa.

Table 3.2 Elastic properties of flax stem woody core

E_1=E_2 [MPa]	**E_3 [MPa]**	**N_{12}**	**N_{23}=N_{13}**	**G_{12} (f(E_1)) [MPa]**	**G_{13}=G_{23} [MPa]**
100	670	0.56	0.04	32	116

E= Modulus; N= poison's ratio; G= shear modulus; directions: 1, 2, 3 ~ axis: x, y, z

The FE model for compression of woody core shows stress concentration areas indicating the origin for initial fracture (**Figure 3.10(b)**), which correlated well with the experimental observations from compression tests as shown in **Figure 3.10(a)**.

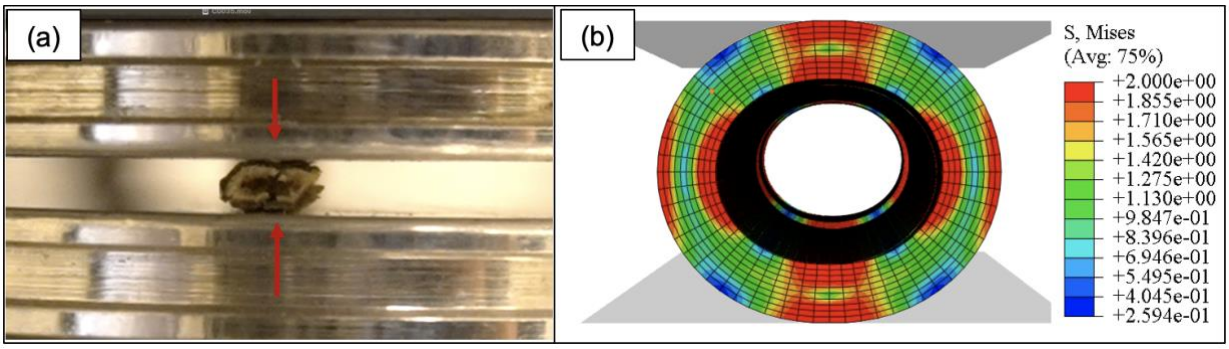

Figure 3.10 (a) Experimental observation for initial fracture vs (b) high stress- concentration areas in the FEM of woody core under compression

The obtained material parameters were used to model another woody core sample from same stem but with twice the length. The force-displacement profile obtained from FEM correlated well with the experimentally obtained compression curve for the longer core sample (**Figure 3.11**). This indicates that the simplified material model can be used to model stems during breaking process for estimating optimal roller profile.

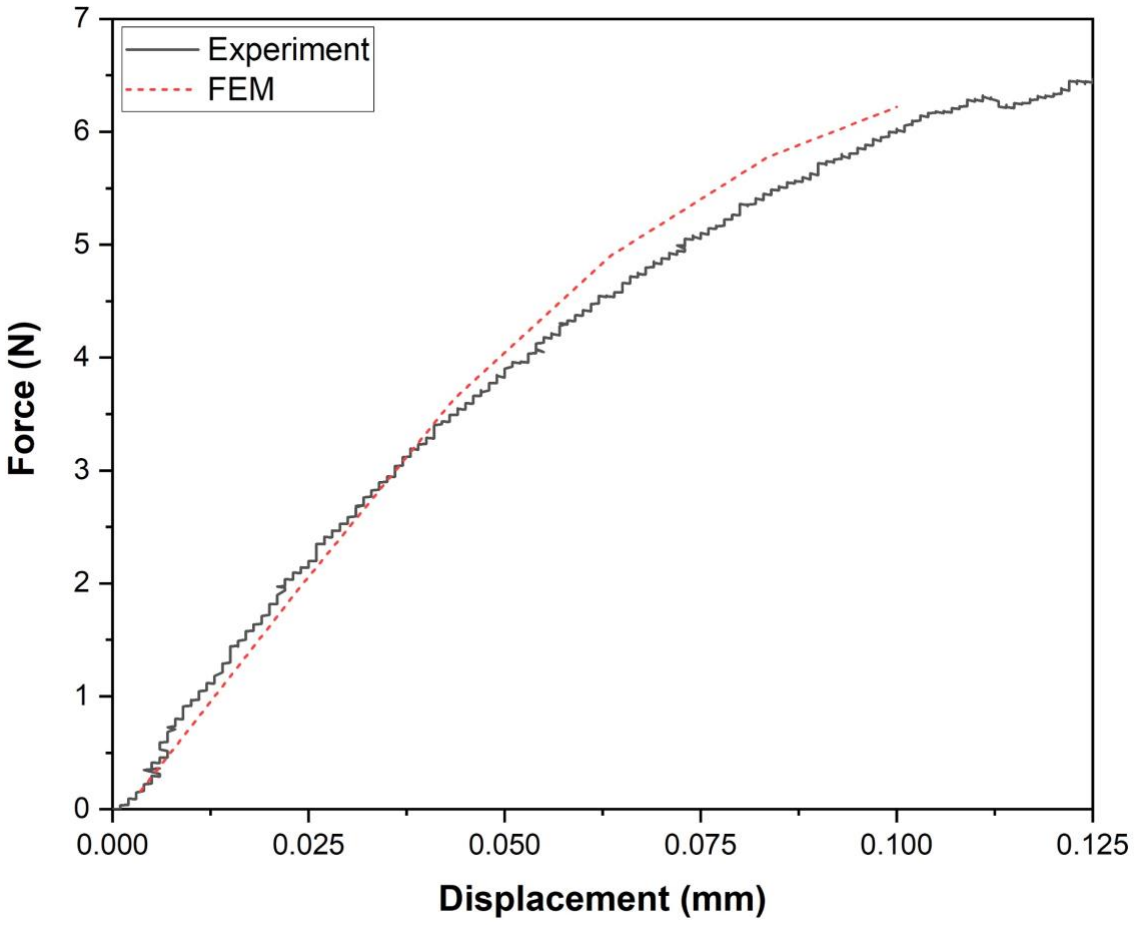

Figure 3.11 Comparison of Force-Displacement profile for 1-inch woody core sample obtained from compression test experimentally and Finite Element Modelling (FEM)

3.3.6 FEA modeling of stem bending under various tool geometries

Industrial rollers have gear geometries with flute widths much larger than the stem diameter. And the schematic of this wide tool geometry under a 3-point bending test with respect to commonly used chisel tip geometry is shown here in **Figure 3.12**.

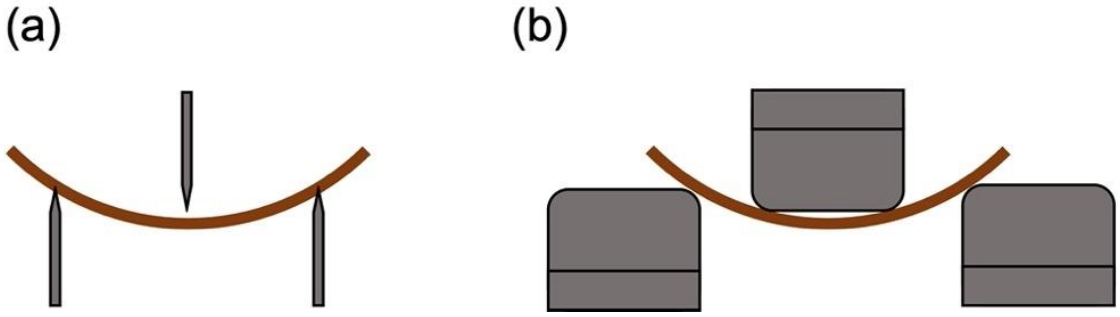

Figure 3.12 Three-point bending test configuration with (a) commonly used chisel and (b) a wide tool geometry

To visualize the effect of bending under 3-point geometry with a wider tool, finite element model (FEM) for the stem woody core is created using ABAQUS as shown in **Figure 3.13(a)**. A 20 mm wide geometry with corner fillet radius of 2.5 mm and large radius of curvature is chosen for top load tool. Hence, the width of the load span is ~ 15 mm. Further, 45 mm support span is chosen, where each support tool is 5 mm wide with 5 mm radius of curvature. Moreover, an equivalent 4- point bend model with similar support span and top load span of 45 mm and 15 mm respectively is created (as shown in **Figure 3.13(b)**), having all tool dimensions being 5 mm in width with 5 mm radius of curvature. Derived constitutive material parameters summarized in **Table 3.2** are used to model the woody core as orthotropic elastic material. Here, both the models show similar elastic strain (EE) throughout the woody core along with two high strain regions at the tool contact points.

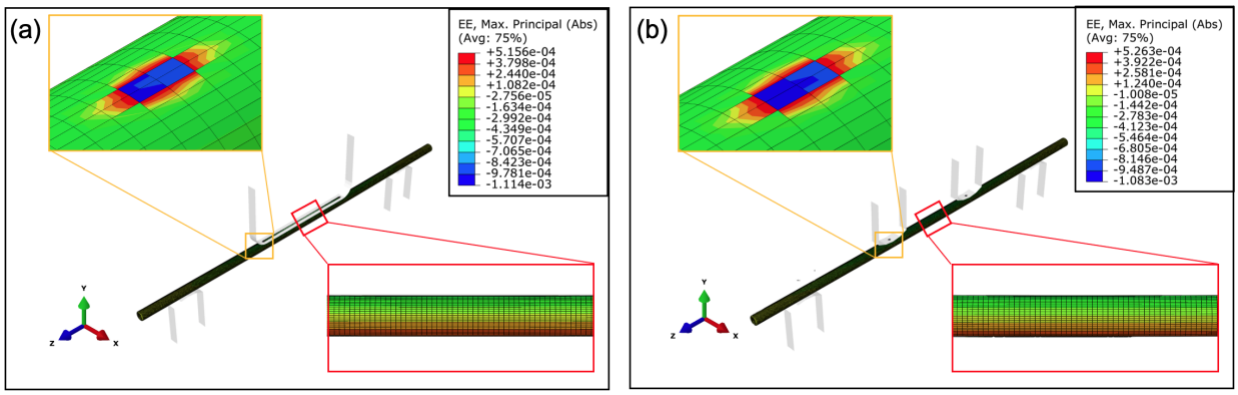

Figure 3.13 Finite element model (FEM) for (a) 3-point bending with wide tool geometry and (b) equivalent 4-point geometry

The maximum principal elastic strain (EE) along the linear nodal path at top middle section of woody core is taken as output from ABAQUS for 0.1 mm top tool deflection from both the models and compared in **Figure 3.14**. Here, both the models show similar compressive strain curve for top part of woody core, where the strain increases from support to load span followed by a constant strain region along the width of wider load tool or between the load span tools in case of 4-point bending. Also, the curve shows two high strain regions as spikes in both the models at the tool contact points. This shows that the 3-point bending of stems under wider tool is essentially similar to the bending under 4 - point geometry, where the load span between top two tools is equivalent to the width of the 3-point load tool.

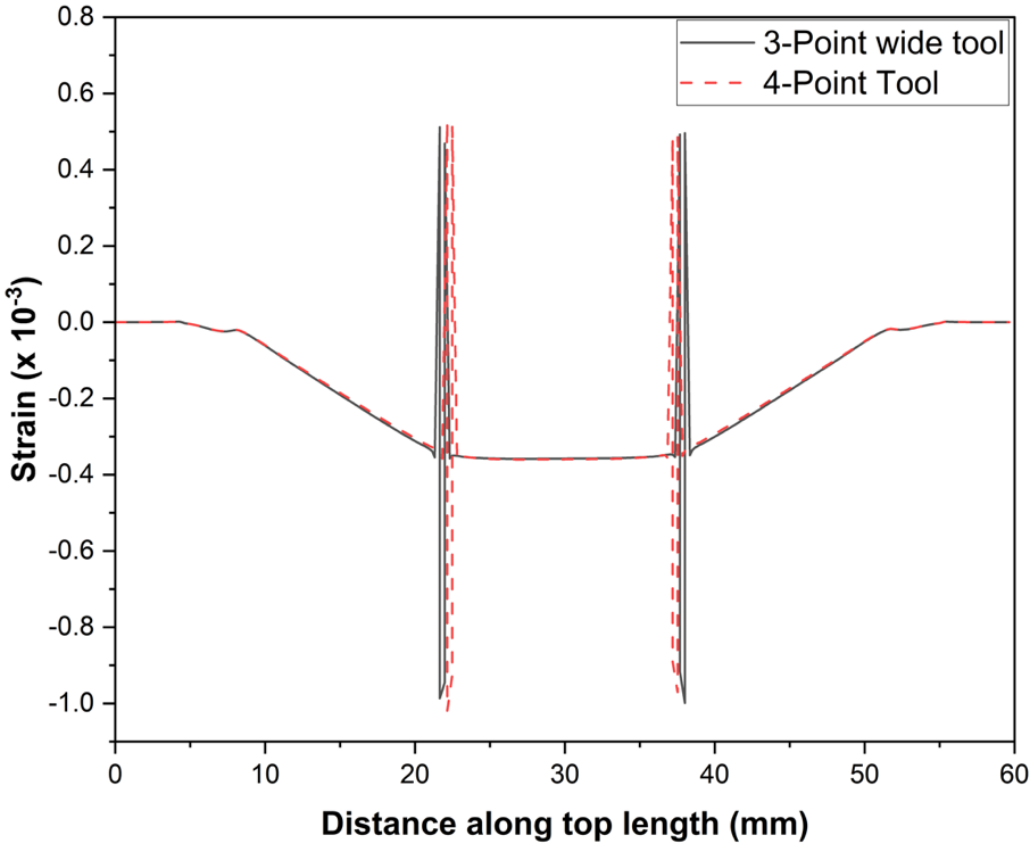

Figure 3.14 Compressive strain output on top suface of woody core for 3-point bending with wide tool geometry and equivalent 4-point geometry

Furthermore, for experimental studies, similar load and support tools configuration discussed in above two cases are created for bending of stem samples (taken from a single flax stem) using DMA and the force- deflection curves are summarized in **Figure 3.15**. Here, initial linear elastic region of force-deflection curve from 3-point wide tool geometry correlated well with the 4-point tool bending curve and the major fracturing event in both the cases seen around 1.5 mm of tool deflection. However, a 4-point geometry here, allows more displacement of center point, causing higher non-linearity and gradual forces drop leading to a less rapid failure than a 3-point wide tool geometry. We hypothesis that this is due the middle gap between top tools allowing for the bast layer to buckle, while giving space to inside woody core to fracture gradually.

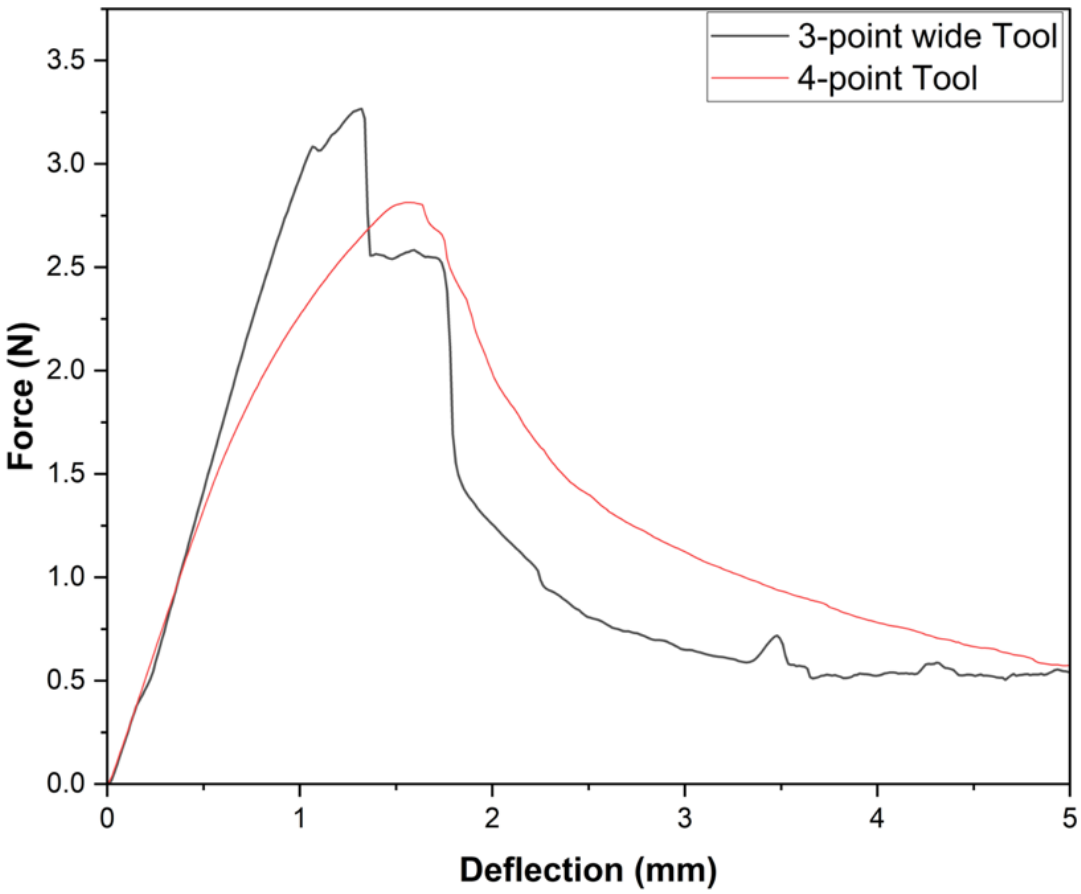

Figure 3.15 Force- deflection curve from experimental bending of retted flax stems under 3-point bending with wide tool geometry and equivalent 4-point geometry

3.3.7 Improved roller profile and effect of compression on stems prior bending

Taking guidance from the FEA studies, a 4-point bend geometry was selected for the improved flute profile for breaker rollers. **Figure 3.16** shows the baseline and improved roller profiles along with corresponding meshing of flutes during rolling operation. The various geometric parameters for both roller profiles are summarized in **Table 3.3**. Circular flute channel geometry, taken here as baseline roller profile had a narrow clearance between the tools during closing and induces high bending strains when compared to the improved roller profile for same deflection of tool.

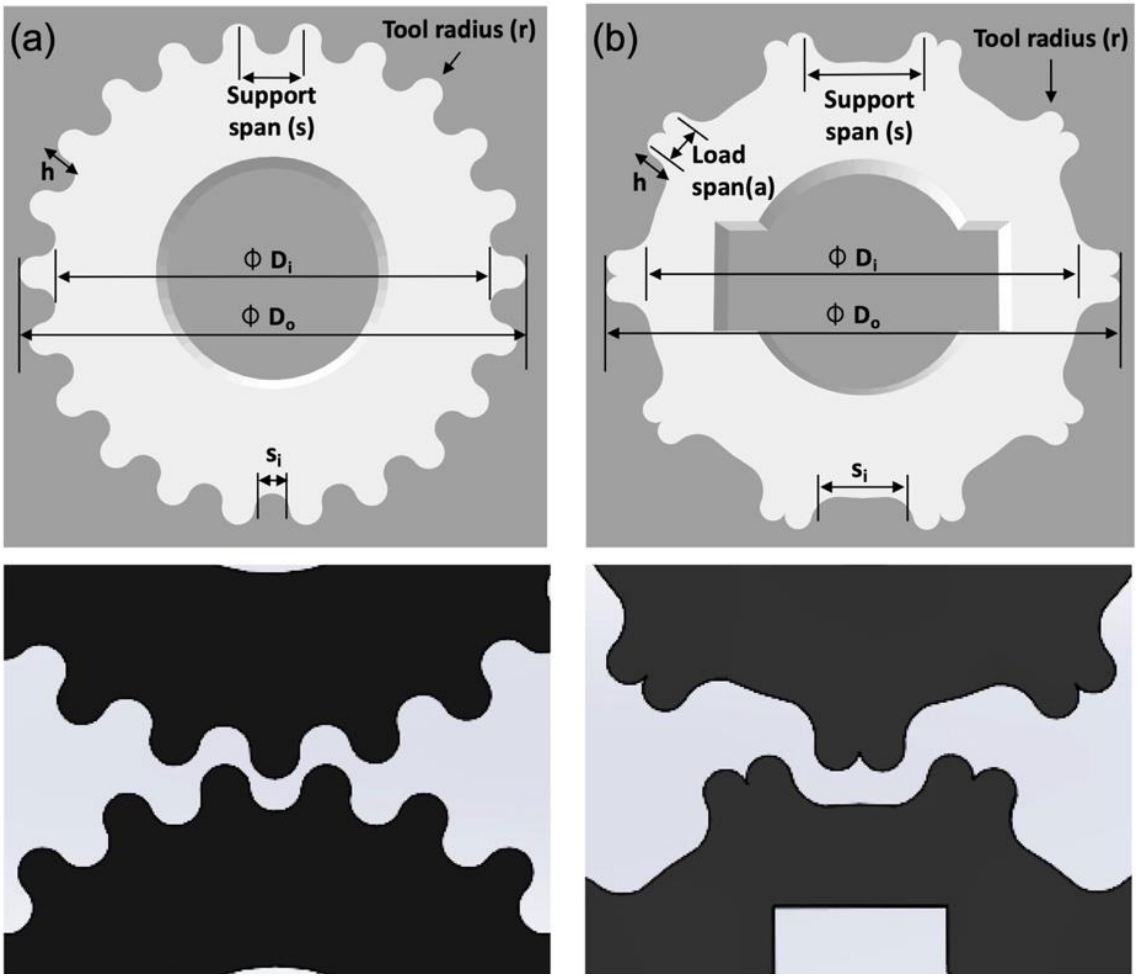

Figure 3.16 (a) Baseline and (b) improved profile of rollers along with respective view of flute meshing during rolling operation

Table 3.3 Roller's profile geometric parameters summary

	Baseline Profile	**Improved Profile**
Outside diameter (D_o)	69.6 mm	69.5 mm
Inside diameter (D_i)	60.4 mm	58.1 mm
No of Flutes (#)	22	10
Tool radius (r)	2.3 mm	2 mm
Tool width (w)	4.5 mm (~2r)	8 mm (~4r)
Tool Height (h)	4.6 mm ((D_o-Di)/2)	5.7 mm
Load span (a)	-	4 mm (~2r)
Support span (s)	9.4 mm (~4r)	16 mm
Inner span width (s_i)	4.8 mm	12 mm
Ratio s:a	-	4:1
Closing tool clearance (c)	0.15 mm ((s_i – w)/2)	2 mm

Figure 3.17 shows the DMA 4-point bending experiment using the improved roller profile and the resulting force-deflection curve. Here, the bending behavior of as-retted stem sample was compared with the crushed stem sample (35 % compression under rolling), each taken from middle section of a single enzyme retted stem. The slope of initial linear region in case of crushed stem is much lower than that of as-retted stem, indicating significant reduction in bending stiffness. The reduction observed is greater than expected based solely on stem thickness reduction. Also, the fracture occurs at much higher force in case of as-retted stem along with significant reduction in force afterwards indicating a more rapid failure than crushed stem fracture which is gradual. Hence, it is a better practice to crush the stems under flat rolling with optimal roller gap (estimated earlier around 35 %) before subjecting to bending or breaking. Moreover, the major fracturing of both as-retted and crushed stems levels out around 3 mm deflection, hence, the optimal roller gap/opening is maintained for 3 mm deflection during breaking operation with improved roller profile, to prevent excessive bending stains and damage to bast layer.

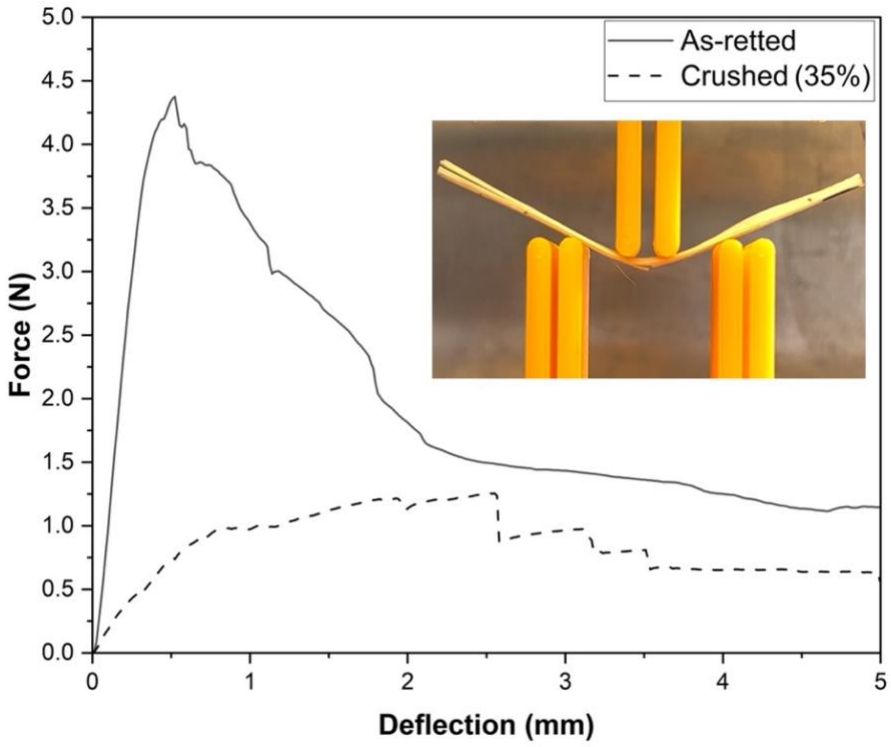

Figure 3.17 Four-point bending of enzyme retted stems using DMA to mimic rolling operation with improved roller profile

3.3.8 Fiber extraction through improved mechanical breaking and property evaluation

The following steps are recommended for improving the breaking process:

a. Crushing of retted stems to 35 % compression using flat rollers to initiate fracture of woody core.

b. To break and separate the woody core from bast utilize rollers with an improved profile. The roller gap is kept such as to maintain 3 mm maximum tool deflection during stem bending.

c. Shaking and hackling of extracted bast layers to finer technical fibers.

The tensile test results for fibers extracted from both the baseline and the improved roller profile are summarized in **Table 3.4**. Note that the cross-sectional area of the fibers was comparable for the two different roller profiles ($p > 0.5$), as it depends upon initial retting condition which was same. However, both tensile modulus and strength were significantly higher ($p < 0.001$) for fibers extracted using the improved roller profile. Further, reduction of variability or relative standard deviation in % in modulus and area is observed in case of extraction from baseline roller profile, an effect observed in prior studies as well where excessive mechanical beating of fibers during mechanical extraction reduces the strength and variability when compared to carefully hand extracted fibers [57].

Table 3.4 Tensile property comparison for technical fibers extracted from breaking process with baseline and improved roller profile

	Area [um^2]	**Modulus [GPa]**	**Tensile Strength [MPa]**
Baseline Roller	6563 ± 30 % [a]	37.6 ± 17 % [a]	350 ± 51 % [a]
Improved Roller	6841 ± 44 % [a]	52.5 ± 22 % [b]	1032 ± 22 % [b]

results expressed as "average ± SD %"
Values within a column followed by the same letter are not significantly different ($p > 0.05$)

Figure 3.18 shows scanning electron micrographs (SEM) of extracted fibers from the two cases of roller profile. Permanent deformation under excessive bending is observed in fibers extracted using the baseline roller profile (**Figure 3.18(a, b)**), compared to fibers extracted from the improved roller profile which were mostly aligned straight (**Figure 3.18(c)**). Kink bands and splitting of technical fibers is observed as in fibers extracted from the baseline roller profile, indicating the weakening of elementary fiber cells interphases within technical fiber bundle under high mechanical bending strains, thus affecting the overall integrity of the technical fiber and hence reduction in tensile strength and modulus.

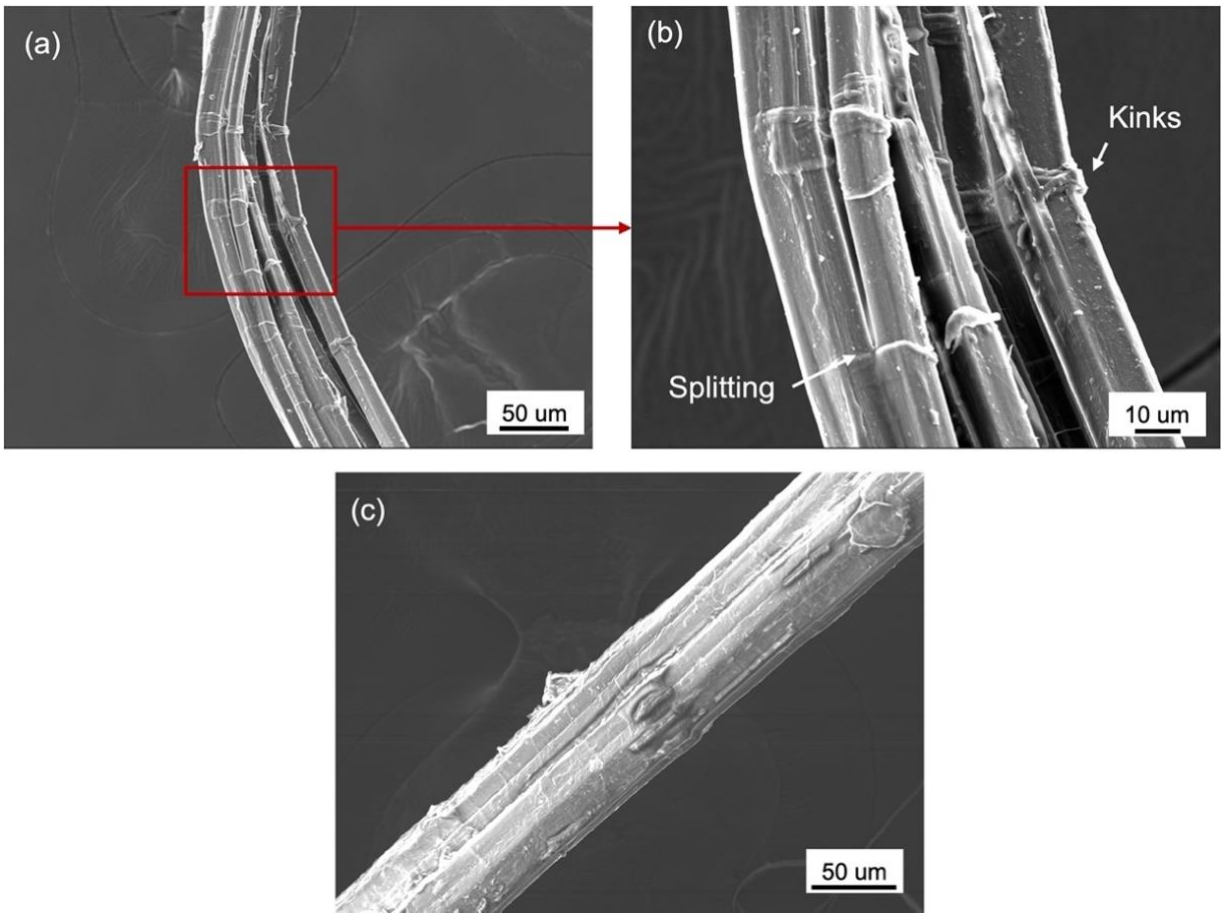

Figure 3.18 Scanning electron micrographs (SEM) for extracted fibers from (a, b) baseline and (c) improved roller profile

3.4 Conclusions

Fracture occurring within a retted flax stem during the mechanical extraction step called breaking was studied by testing retted stem samples under compression and bending. Correlating fracture events in the force-compression curve during compression with visual fracture observation gave insights into the ideal compression limit (~ 35 %) needed to optimally fracture the inside woody core and avoid damage from over compression. Compression under parallel plate was found to have similar force-compression curves with compression under rolling, and compression

within the optimal limit showed to have no significant effect on tensile properties of extracted enzyme retted fibers. The data from compression tests of woody core were used to evaluate the constitutive material properties for woody core and the preliminary finite element model for compression of woody core shows stress concentration areas matching the visual observation for the initial fracturing event.

The effect of changing the length of support spans was studied during 3-point bending tests of retted stems, where the bending radius of curvature and maximum tensile strain leading to fracture was found to be similar between different spans. The 3-point bending with wide tool geometry was studied through finite element analysis (FEA) along with experiments and found to be equivalent to a 4-point bending geometry. An improved roller profile with 4-point bending geometry was designed for breaker rollers and the importance of crushing stems prior breaking was studied. For baseline comparison, a roller profile was created to subject stems under high bending strains and fibers extracted from both breaking rollers were characterized for tensile properties. Baseline breaking roller profile significantly degrade the fiber modulus and tensile strength. Further, microscopic observation under scanning electron microscope (SEM) showed permanent bending deformations in fibers extracted from baseline roller profile. Here along with kink band defects and splitting of technical fibers was seen, indicating damage to inside elementary fiber cell interphases under high bending strains. Lastly, we believe that taking the guidance from single stem fracture studies here, it possible to design the extraction process on large scale for future studies to extract fibers from stem bundles with minimal damage for green structural composites.

Chapter 4
Improved Fiber Extraction and Composite Fabrication

4.1 Introduction

In structural applications, the composites reinforced with unidirectional (UD) or continuous fibers are preferred as they show high strength and modulus than chopped fibers [24,105]. Hence, the initial aim of this chapter is to extract long fibers from multiple stems in contrast to single stems studies previously seen in Chapter 2 & 3 using different retting conditions and improved mechanical extraction. Here, the fiber yield is evaluated at each step in the extraction process and compared with literature. Further, this chapter explores evaluating fiber performance in lab scale fabricated small unidirectional fiber composites, using fibers belonging to different retting conditions. Fiber properties were back calculated using composite's rule of mixtures and compared with fiber properties from single fiber tests. A similar trend of fiber properties between the two methods was observed and improvements were suggested on improving reliability of testing and decreasing variability in composite properties.

4.2 Experimental

4.2.1 Improved lab scale fiber extraction

Taking guidance from the Chapter 2 and 3, the following steps were considered for extracting fibers from multiple stems in different retting condition groups and also shown in **Figure 4.1**:

a. Bulk stems of length 10 cm each were retted for different retting using enzymatic retting procedure described in Chapter 2.

b. Each retted stem was compressed to 35 % under rolling operation between flat rollers to reduce the stiffness of woody core as described in Chapter 3. Here, multiple stems were laid side by side throughout the length of the flat roller.

c. Compressed stems were passed under bending side-by side along length of improved profile roller described in Chapter 3, to break and separate the woody core from bast. This process was repeated four times, with each time flipping the broken stem to reverse the points under compression to tension and vice-versa. The roller gap was kept as such to maintain 3 mm maximum tool deflection during stem bending as seen during Chapter 3 studies.

d. The received stems were given a manual shaking, allowing the shives to fall off. Then hackling of extracted bast layers were done using the pin frog as described in chapter 2. Here, bast strips obtained from 3 stems were hackled a time to receive fine technical fibers.

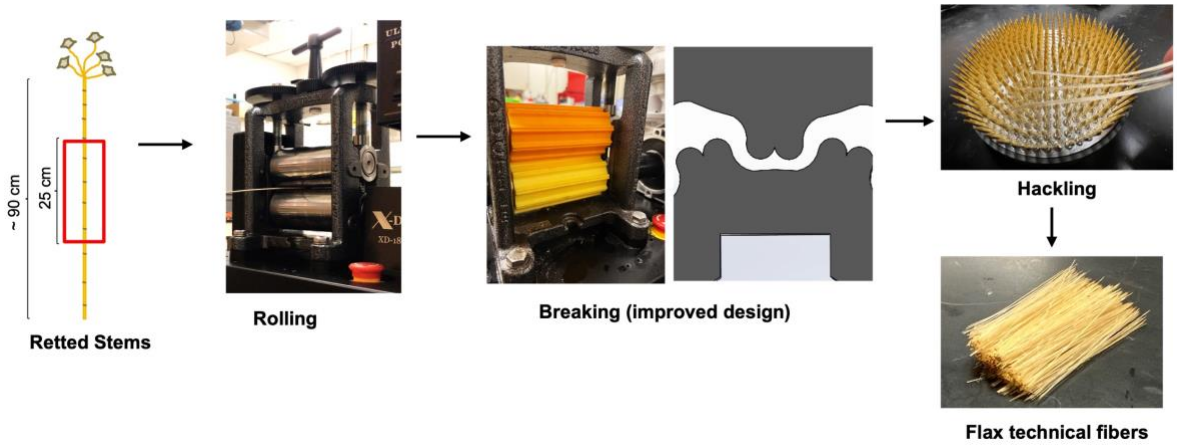

Figure 4.1 Improved fiber extraction process

4.2.2 Fiber yield analysis from extraction process

To determine yield from initial retting process, the oven dried stems at 60 °C were weighed before and after the retting, to calculate % decrease in stem weight. Then, fiber quantity after breaking and hackling step was measured as percentage of this biomass at the start of mechanical extraction. Fiber yield analysis was done on dew retted stems and enzyme retted stems from conditions S_{L24} (0.5%, 24h), S_{H6} (2%, 6h)and S_{H24} (2%, 24h). In addition, effect on fiber yield with varying stem diameter was also investigated by hand extraction of bast strips.

4.2.3 Unidirectional composite fabrication

Unidirectional composites in this study are fabricated from modifications of ISO 10618 standard and Impregnated Fiber Bundle Test methodology (IFBT) used by authors to determine the natural fiber properties in composites [43,106]. Due to limitation of fiber amount extracted from a single stem, enzymatic retting was done on multiple randomly selected flax stems for different retting conditions in similar way as described for single stem enzyme retting. Three composite samples were fabricated, each for fibers obtained from industry extracted Dew (Fibrevolution^{TM}), and lab scale improved mechanical extraction of Dew, S_{L24}, S_{H6} and S_{H24} retting conditions. S_{L6} and S_0 samples were not used in composite fabrication due to low retting degree for being extracted from the lab scale mechanical extraction.

Table 4.1 Fiber amount needed per composite sample

Vol of mold (V_c)	**Fiber Volume (V_f: 25%*V_c)**	**Fiber weight (w_f) @density (ρ_f): 1.45[g/cc]**
0.14 cc	0.035 cc	0.05 g (~145 fibers of 35mm length*)

*assuming per stem perimeter ~20 fibers extracted

Steps in the composite fabrication process are shown in **Figure 4.2**. Silicon molds of dimension 35 mm x 2 mm x 2 mm (V_c) were used for composite dog bone sample fabrication here. As shown in **Table 4.1**, to achieve 25 % fiber volution fraction assuming fiber density of 1.45 g/cc for the given mold dimension of composite, 0.05 gm hackled technical fibers ($w_f = V_c * V_f * \rho_f$) is required. The fibers were cut and formed into straight bundles with ends lightly glued with cyanoacrylate adhesive to hold them together. The bundles were conditioned for 24 hour at 60 °C prior to incorporate into matrix for composite fabrication. A low viscosity epoxy resin (670 cps) was chosen as composite matrix for efficient fiber bundle impregnation. Composite Envisions epoxy resin (1159), commonly used for vacuum RTM molding process was mixed with Composite Envisions hardener (1161) in 3:1 ratio followed by vacuum degassing for 10 minutes to removes air bubbles. The neat Epoxy has modulus of 2 GPa, tensile strength of 69 MPa and % elongation at break as 4 % according to product data sheet. High elongation of matrix is required for fibers to fail first during tensile testing [106]. The pre-conditioned technical fiber bundles were then impregnated into the epoxy mixture and vacuum degassing again for 10 minutes. The impregnated fiber bundles were then placed to take the shape of the mold and compressed with a flat top plate to distribute the excess resin uniformly across the mold. After curing for 24 hours at 60 °C, the composite samples were sanded to remove the excess cured epoxy material and achieve a top flat surface.

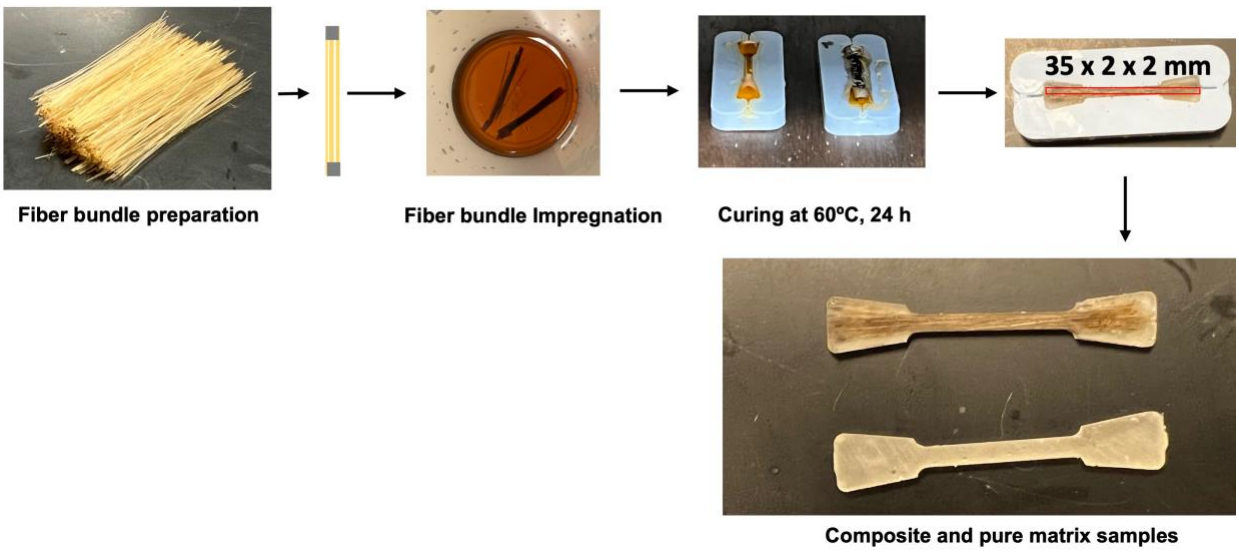

Figure 4.2 Composite Fabrication Process

4.2.4 Composite tensile testing

Longitudinal tensile tests on composite samples were performed in accordance with ASTM D 3039 by using Instron 3345 universal testing machine (UTM), with a 5 kN load cell. The specimens (preconditioned at 60 °C for 24 hours) were mounted at 20 mm gauge length and a crosshead speed of 0.01 mm/sec with 1000 g (~10 N) preload was chosen for the tensile test. Tensile tests were video recorded with a high-resolution camera and image analysis was done using ImageJ for actual crosshead movement to estimate the system compliance. Correction in respective strain measurement was applied from measured system compliance to better evaluate the young's modulus between 0.2 % and 0.5 % strain. Cross-sectional area was measured at composite failure site for each sample to closely estimate the modulus and tensile strength of composites in this study. Additionally, fiber tensile properties were back calculated from composite properties using simple rule of mixtures (equation 4.1 and 4.2) and compared with the single fiber test results, as seen in previous literature [106].

$$M_f = \frac{M_c - M_m(1 - V_f)}{V_f} \tag{4.1}$$

$$TS_f = \frac{TS_c - TS_m(1 - V_f)}{V_f} \tag{4.2}$$

Where, M = Modulus; TS= Tensile Strength; Subscripts: f = fiber, c = composite, m = matrix

4.2.5 Statistical Analysis

Multiple pairwise mean significance comparisons were done in this study using two-sample T-Test in R Studio software with a 95 % confidence interval (p-value < 0.5 for the mean differences to be statistically significant). Letter notation was used for expressing results, where means having same letter (a, b, etc.) were statistically not significantly different.

4.3 Results and Discussion

4.3.1 Fiber yield from lab scale fiber extraction

For preliminary evaluation of stem fiber content, fibers from dew retted stems of varying width/diameter were hand extracted as described in Chapter 2 and the extracted fiber percentage based on initial stem weight is summarized in **Table 4.2**. We observe that the thicker stems have increased fiber amount, but the percentage of fiber amount within stem remains around 50 %, also consistent with previous literature studies [53].

Table 4.2 Effect of stem width (diameter) on fiber content

Stem width [mm]	Stem weight [g]	Fiber weight [g]	Fiber amount [%]
1.30	0.127	0.060	47
1.59	0.177	0.079	45
2.02	0.290	0.153	52

Further, the stem weight reduction after enzymatic retting and average fiber yield after the breaking and hackling steps of mechanical extraction from three stem trials are summarized in **Table 4.3**. Here, the differences in the stem weight loss from different enzyme retting conditions followed the general trend, where the retting condition of high enzyme concentration of 2 % and retting duration of 24 hours (S_{H24}) resulted in highest weight loss. Moreover, the average fiber yield of 47% is observed after breaking among different retting groups, except S_{H6}, where the insufficient retting leads to fiber loss during breaking operation. Also, the final fiber yield after hackling ranges between 26-30%, except S_{H6} due to higher fiber loss. These values remain consistent from previous literature, where 25 % fiber yield observed in lab scale extraction and 15 % from industry scale extraction [53]. Lastly, a high degree of retting in case of S_{H24} leads to high fiber yield of 30 % with minimum fiber losses in between mechanical extraction steps.

Table 4.3 Yield at different steps in extraction process

Retting conditions	Stem weight reduction after retting [%]	Fiber yield after breaking [%] [a]	Fiber yield after hackling [%] [a]
Dew	-	47 %	26 %
S_{L24} (0.5%, 24h)	12 %	47 %	27 %
S_{H6} (2%, 6h)	11 %	43 %	21 %
S_{H24} (2%, 24h)	13 %	48 %	30 %

[a] results are average of 3 stem trials

4.3.2 Retting condition effect on unidirectional fiber composite performance

The goal is to establish a rapid evaluation of composite and back calculated fiber tensile properties with the limited amount of fiber material available for lab scale trials. In addition, the study is done to elucidate the limitations of this method. **Figure 4.3** shows modulus and tensile strength of the prepared composites. Pairwise T-Test is used for significance comparisons in this section. Similar dog bone sample trials made from neat epoxy gives the modulus of 2.08 ± 0.07 GPa and the tensile strength of 60 ± 4 MPa. For comparison, the composites reinforced with industry extracted dew retted fibers showed a significantly lower modulus of 6.9 ± 0.6 GPa when compared to composites with lab extracted dew retted fibers having modulus of 8.6 ± 0.9 GPa ($p < 0.05$). Also, lab extracted dew fibers in composites showed significantly lower modulus to the composites from enzyme retted fibers ($p < 0.05$). Modulus of composites within enzyme groups (S_{L24} : 12.3 ± 1.7 GPa; S_{H6} : 11.9 ± 2.2 GPa; S_{H24} : 11.74 ± 1.53 GPa) were found statistically comparable ($p > 0.5$). This trend is similar to what observed in single fiber testing at 10 mm & 30 mm gauge lengths in chapter 2. Within the enzyme retted groups, S_{H24} and S_{L24} showed a lower variation, due to the better individualization of bast into finer technical fibers that leads to the improvement in dispersion in the polymer matrix. This effect is consistent with the previous studies as well [43,89].

Figure 4.3 (b) shows the tensile strength of composites in the study. Here, composites reinforced with industry extracted dew retted fibers again showed significantly low tensile strength of 111 ± 10 MPa than composites with lab extracted dew fibers having strength of 160 ± 22 MPa ($p < 0.05$). The composites under the enzyme retted condition S_{L24} results in highest tensile strength of 209 ± 38 MPa, followed by S_{H6} (189 ± 22 MPa) and S_{H24} (161 ± 5 MPa), respectively. Despite of the observed trend in average tensile values here, due to the high variation no statistical

differences were found in the tensile strength of composites from the lab extracted dew and enzyme retted fibers ($p > 0.05$). A similar observation was also found in the composites from manual hand extracted enzyme and dew retted fibers by Jana et al. [43]. Moreover, the tensile properties of composites are sensitive to manufacturing parameters such as volume fraction or porosity, under which high variations of tensile strength are expected as compared to modulus [43,106].

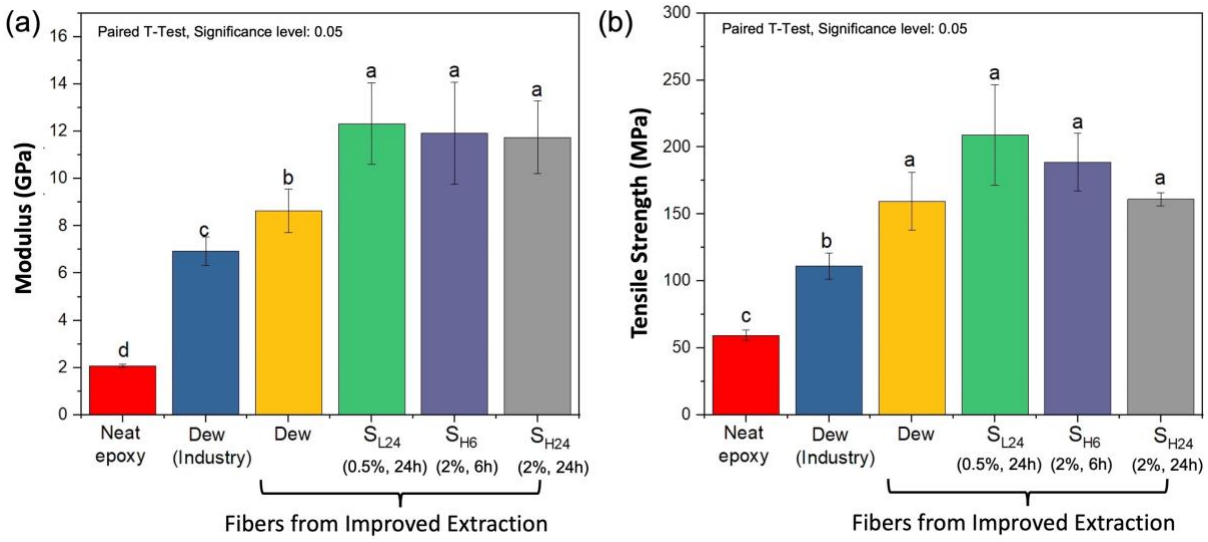

Figure 4.3 Effect of retting conditions on composite performance. (a) Young's Modulus (b) Tensile Strength (Neat: measured pure epoxy properties from 11 trials)

4.3.3 Retting condition effect on back-calculated fiber properties

The back calculated fiber modulus and tensile strength are shown in **Figure 4.4**. Similar trends in the average values as composites is seen here. Industry extracted dew fibers showed significantly lower modulus (M) of 21.3 ± 2.4 GPa and tensile strength (TS) of 266 ± 39 MPa than lab extracted dew fibers (M: 28.2 ± 3.7, TS: 457 ± 87) ($p < 0.05$). The modulus of fibers from enzyme retted groups found comparable ($p > 0.05$) (S_{L24} : 43.1 ± 6.9 GPa; S_{H6} : 41.5 ± 8.6 GPa;

S_{H24} : 40.8 ± 6.1 GPa). The tensile strength of enzyme retted fiber groups was higher and have similar trends to composites but are comparable due to high variability ($p > 0.05$) (S_{L24} : 664 ± 150 MPa; S_{H6} : 587 ± 86 MPa; S_{H24} : 454 ± 20 MPa).

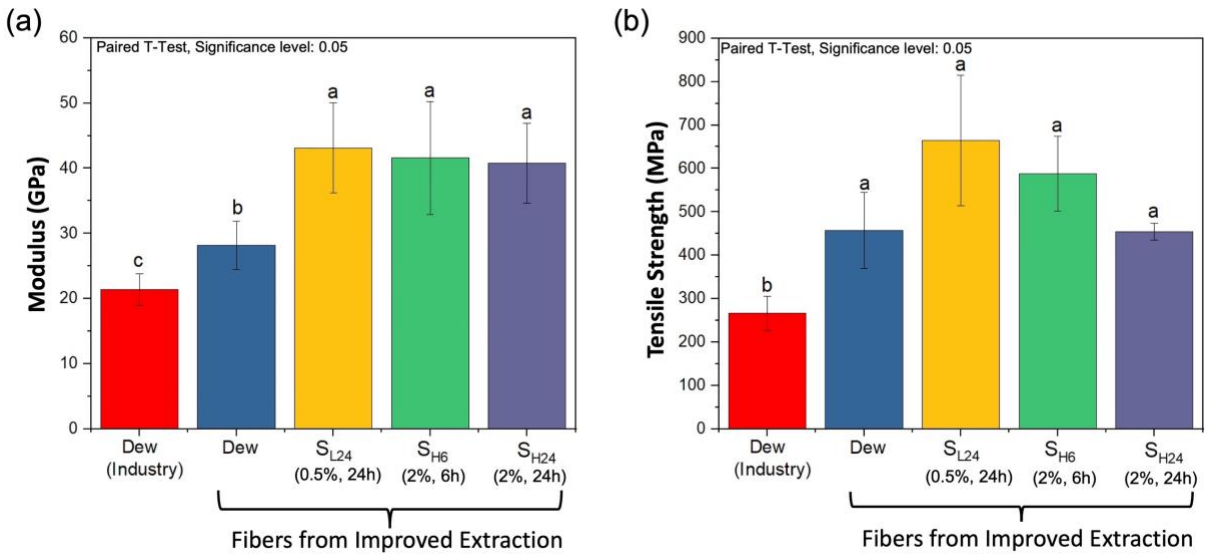

Figure 4.4 Back- calculated fiber properties using rule of mixtures

Furthermore, tensile modulus of back-calculated fibers shows a similar trend as the modulus in single fiber tests from 10 mm and 30 mm gauge lengths in chapter 2. However, the averages of back calculated tensile strength follow the trend from single fiber testing results from 30 mm gauge length. Hence, to visualize this further, the back calculated properties are plotted against single fiber tests at 30 mm in **Figure 4.5**. These back calculated properties showed slightly lower values from measured single fiber properties, and a smaller standard deviations as well, especially in S_{H24} that has the finest fibers with the least variation in diameter. Similar observations in tensile properties of back-calculated fibers are seen in the literature on big dog bone samples (200 mm x 10 mm x 2 mm) [43,106]. However, Bensadoun et al.'s study compared the back

calculated properties with the elementary fiber which is higher than technical fibers inside composites [106]. Also, the simple rule of mixture assumes perfect load transfer between the matrix and fiber interphase which is a limitation as well in determining the fiber properties from composites [106,107]. Furthermore, our study also verifies that the variations were high in the case of smaller composite samples in the IFBT study by Bensadoun et al. [106]. This is due to an increase sensitivity of measurement errors to a small sample size, such as fiber volume fraction, porosity, fiber density and cross-sectional area at failure. An example of composite cross-section in **Figure 4.6** show defects such as cracks and porosity, that leads to variability in properties of these composite samples**.** Although, the variation of back-calculated tensile properties is higher, interesting conclusions can be made. There is no statistical significance in the tensile strength of back calculated tensile properties, the averages follow the trend from single fiber testing results from 30 mm gauge length, where fiber samples from S_{H24} were weakest in tensile strength among the enzyme retted groups and comparable to dew retted fibers.

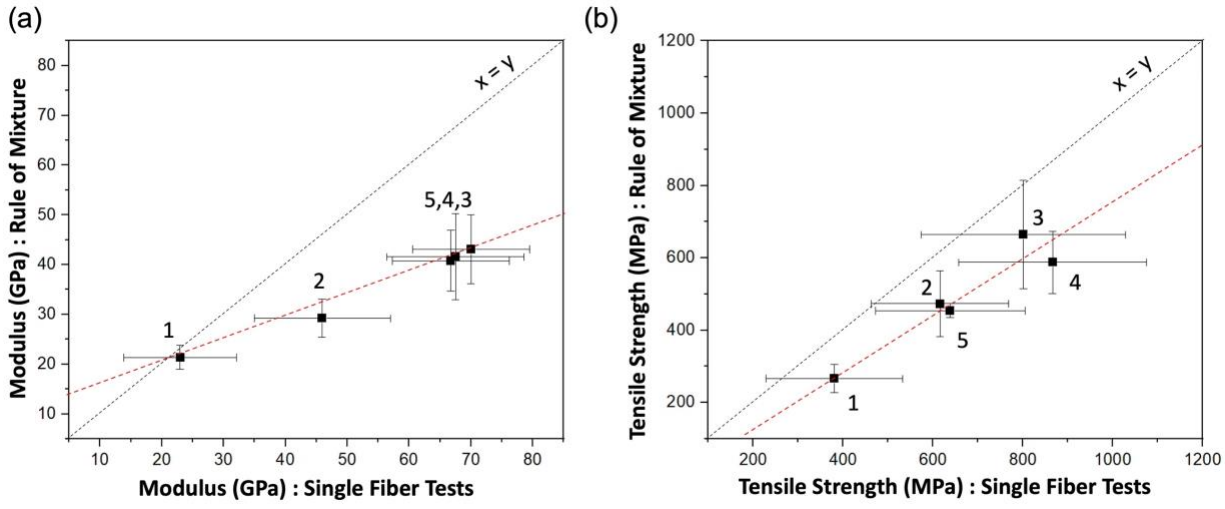

Figure 4.5 Back calculated fiber properties using rule of mixtures with respect to single fiber tests at 30 mm gauge length, where 1-Dew (industry); 2-Dew (lab); 3- S_{L24} (0.5%, 24h); 4- S_{H6} (2%, 6h); 5- S_{H24} (2%, 24h)

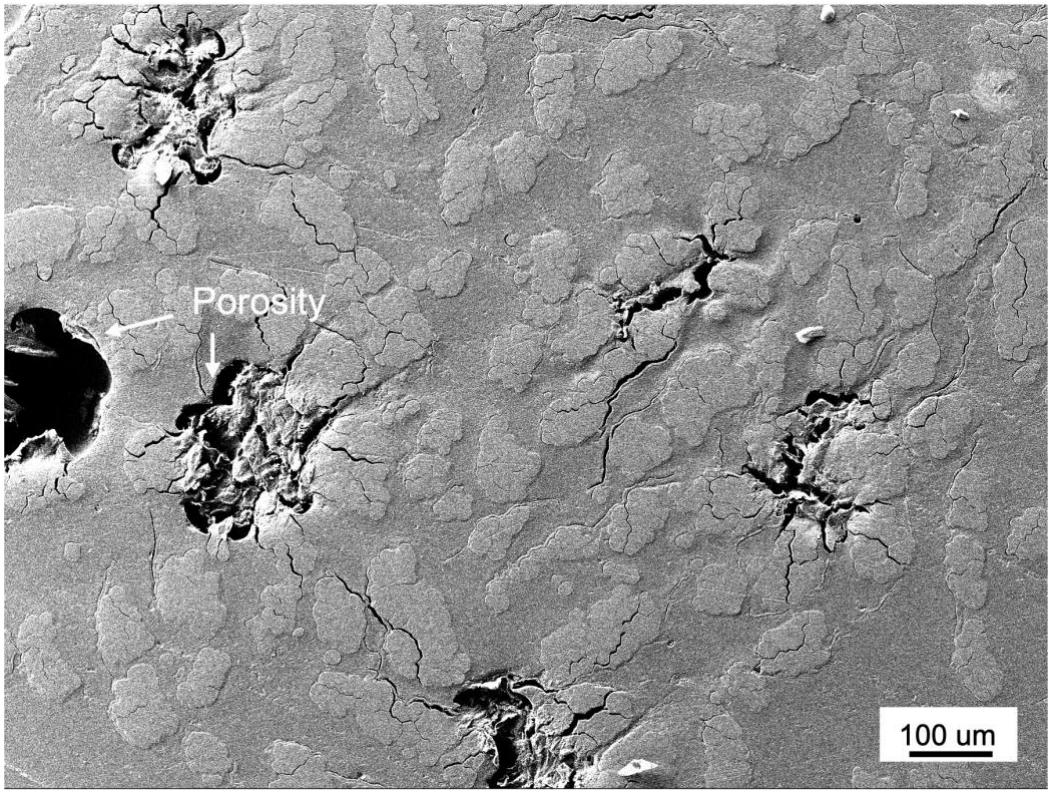

Figure 4.6 Composite cross-section for defects visualization

Lastly, it is worthwhile to mention that the method of evaluating composite and back-fiber properties used in this chapter is able to provide a quick method for evaluating fiber properties in composites. Future studies are needed to improve the fabrication method and to reduce the measurement errors of earlier mentioned sensitive parameters.

4.4 Conclusions

Technical fiber from different retting conditions were extracted with improved extraction process and used to fabricate smaller specimens of composites. Fiber yield at various steps in extraction and tensile properties of resulting composites were evaluated. It was seen that major fiber loss occurs during hackling step, leading to on average about 27 % yield with respect to initial biomass at the end of the extraction process. Composite samples from different enzyme retting

conditions shows no significant different in tensile properties, except for composite sample from highly retted fibers (S_{H24}) shows decline in tensile properties, although it showed least variation as well. Overall, these small composite samples were able to provide back calculated fiber tensile properties with lower variation and good correlation with the single technical fibers tested at gauge length of 30 mm. Still improvements in fabrication process can be made for expedited property assessment with limited fiber material.

Chapter 5
Dissertation Summary and Future Directions

5.1 Key Findings Summary

Plant based fibers such as flax have the potential to replace glass as a sustainable reinforcement in polymer composites. However, these fibers exhibit damage during the current extraction process, originally designed for textile use of these fibers, that leads to high variability in their mechanical properties, thus making it difficult to implement them in composites for structural applications. In this regard, prior literature in improving the current extraction process were found to mainly focus on fiber defect analysis or improving extraction at the industrial scale. Limited studies were found to understand the underlying fundamental mechanism of events occurring during various extraction steps within individual stems, such as fiber debonding during retting or stem fracturing during stem breaking, that leads to fiber damage. Therefore, the studies presented in this dissertation were aimed at filling those gaps in research and improving the current extraction process for extracting high quality fibers for composite application.

In Chapter 2, improvements for increased reliability & reproducibility of the current ASTM C1557 – 14 standard used for measuring cross sectional area and tensile properties of single fibers was discussed. Further, for quantitative measurement of the retting degree in terms of bond strength between bast fiber layer-woody core interphase, 90° peel test method was developed, and results expressed as peel energy in J/m^2. Specimens from a single stem were treated with different enzyme retting conditions, and the effect of enzyme concentration and incubation time (duration

of retting) on peel energy and the resulting technical fiber area was investigated through visual and statistical analysis. Single technical fiber tensile properties were evaluated at 10 mm and 30 mm gauge lengths for various enzyme retting conditions. *Some of the key findings here are as follows:*

- *The retting process divides bast fiber bundles across circumferential direction rather than dividing across the bast width.*
- *Enzymatic retting leads to uniform division of bast bundles in fine technical fibers when compared to dew retting that leads to non-uniform fibers with damage at elementary fiber level. Tensile properties were found significantly higher in case of enzyme as compared to the industry standard dew retted fibers.*
- *Both enzyme concentration and retting time significantly affects the bast-woody core bond strength, but only retting time is responsible for bast differentiation into finer technical fibers. Hence, it is possible to design an enzymatic retting process with smaller duration of incubation time to achieve desired degree of retting for later mechanical extraction steps.*
- *Over-retting even in the case of enzyme retting effects the performance of long technical fibers by degrading the interphase between elementary fibers*.
- *0.5 % enzyme concentration and 24 hours incubation time is chosen as enzyme retting condition for later mechanical extraction steps*.

In Chapter 3, fracture occurring within a retted flax stem during mechanical breaking was studied using compression and bending tests, along with visual observation of the inside woody core fracture. Bending analysis of stems under a range of tool geometries using finite element modeling (FEM) was done and used as a guide to design of an improved roller profile for a lab

scale stem breaker. A baseline roller profile was created for comparison. Fibers extracted from both breaking rollers profile was characterized for tensile properties and microscopic defect observation using scanning electron microscope (SEM). *The key findings are as follows:*

- *Non-uniform strains induce kinks and damage fibers at elementary fiber level.*
- *Observing fracturing events during compression gave insights into the ideal compression limit (~ 30-40 %) needed to optimally crush or fracture the inside woody core and avoid damage from over compression. Further, properties of single technical fibers were found unaffected at this optimal compression level.*
- *Finite element modelling (FEM) guided the novel 4-point bend design of roller profile.*
- *Crushing stems under flat rolling prior to bending under breaking rollers decreases the bending stiffness and was shown to prevent sharp bends during bending. Also, DMA bending test studies were able to provide an ideal roller gap during breaking.*
- *Comparing fiber properties with the improved breaking process using an improved roller profile showed significant improvement in tensile properties when compared to fibers extracted under high bending strains of a baseline breaker roller profile. Permanent deformations and kinks under bending were observed in case of fibers extracted from the baseline roller profile.*

In Chapter 4, fibers from different retting conditions were extracted using the improved extraction process and fiber yield at various steps in extraction was evaluated. These fibers were also used to make small composite specimens and tensile properties of resulting composites were evaluated. Further, fiber properties were back calculated using rule of mixtures and are compared with results from single fiber tensile testing. *Major key findings are as follows:*

- *Average of about 27 % (from initial stem weight) fibers yield achieved from improved extraction process, with major fiber loss occurring during hackling.*
- *Composites reinforced with enzyme retted fibers extracted from improved mechanical breaking showed significantly higher tensile properties than composites made with industry extracted fibers.*
- *The back-calculated fiber properties correlated well with single fiber test results; hence a method can be used for a quick evaluation of fiber properties in composites*.

Overall, a systematic approach in this dissertation elucidates the effect of retting conditions along with single stem fracture studies to guide the optimization of extraction process at larger scale to produce high quality natural fibers for sustainable composites.

5.2 Future Work Directions

5.2.1 Enzyme activity and Chemical composition Analysis

Tensile tests coupled with statistical analysis was able to provide an assessment for the effect of enzyme concentration and time over resulting fiber properties in Chapter 2. Still, analysis of enzyme activity over the duration of retting can provide better insights on certain aspects such as the deactivation of enzyme during that period. Also, an increasing amount of sugars compared to lower decline in peel energy was observed in Chapter 2. We hypothesize that this is due to the degradation of the pectin bond around the bast-wood interphase while the reducing sugars is still being liberating from other parts of the flax stem. A more detailed chemical composition analysis of components across the flax stem along with proportion of each individual sugar type within total reducing sugar released at various stages of enzymatic retting can provide better evidence for this hypothesis in future. Analysis of chemical composition will show degradation of components

such as cellulose leading to poor mechanical properties in case of dew retting. Methods of evaluating enzyme activities and chemical composition are established in prior literature [57,87,108]. For preliminary studies, chemical composition analysis methodology was established from Jana et al. studies and shown in **Figure 5.1** [57]. In a case of dew retted flax fibers, 5% waxes/oil, 13.57% hemicellulose, 78.71% cellulose and 4.8% lignin were found. Similar values were seen in prior literature as well [57].

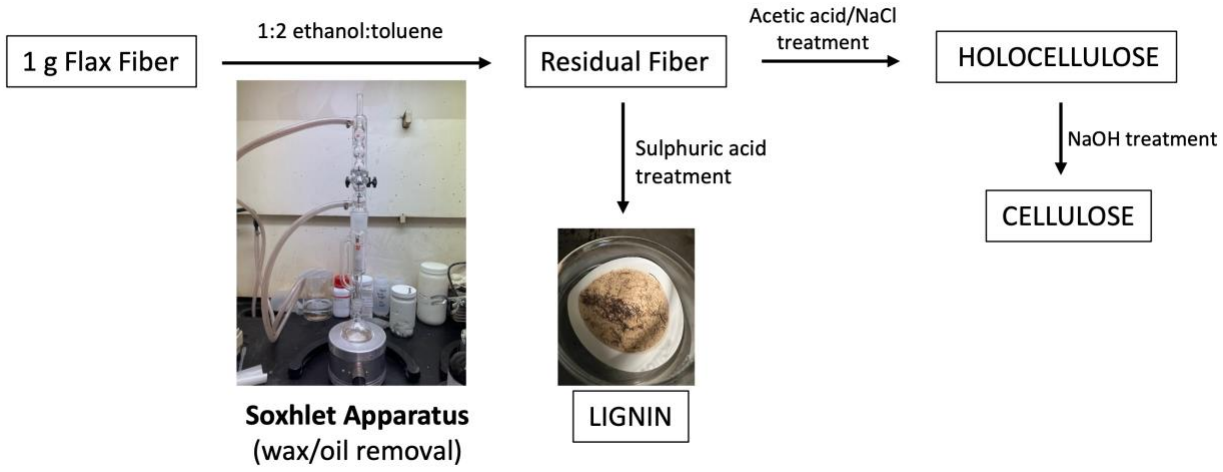

Figure 5.1 Procedure steps for evaluating chemical composition of extracted flax fibers

5.2.2 Scaling up breaking roller with multiple 4-point bends

The studies seen in Chapter 3, were able to provide a lab scale assessment of an improved breaking process with a novel 4-point bending profile of the roller. However, in this roller design, the stems were exposed to one 4-point bending at a time during rolling operation. For an industry scale operation, roller diameter is much larger, and stems can face multiple bending along its length at a time during rolling. To further explore this, a preliminary bending experiment was conducted using DMA, where, in addition to single 4-point bending case as seen in Chapter 3, the rolled

stems (35 % compressed) were subjected to two 4-point bending at a time as shown in **Figure 5.2 (b)**. Two major observations can be seen from the graph. First, as expected the maximum breaking force increased two-fold in case of multi-bending. Second, initial tool deflection is much higher prior to breaking in the case of multiple bending, indicating slipping of material in between the support spans. This gives rise to the possibility of damage occurring on the bast layer due to slippage and friction around the tool, that needs further investigation during scale up studies. And rollers with large diameter than seen in Chapter 3 are required to further observe the rolling operation from this two- 4- point bending profile.

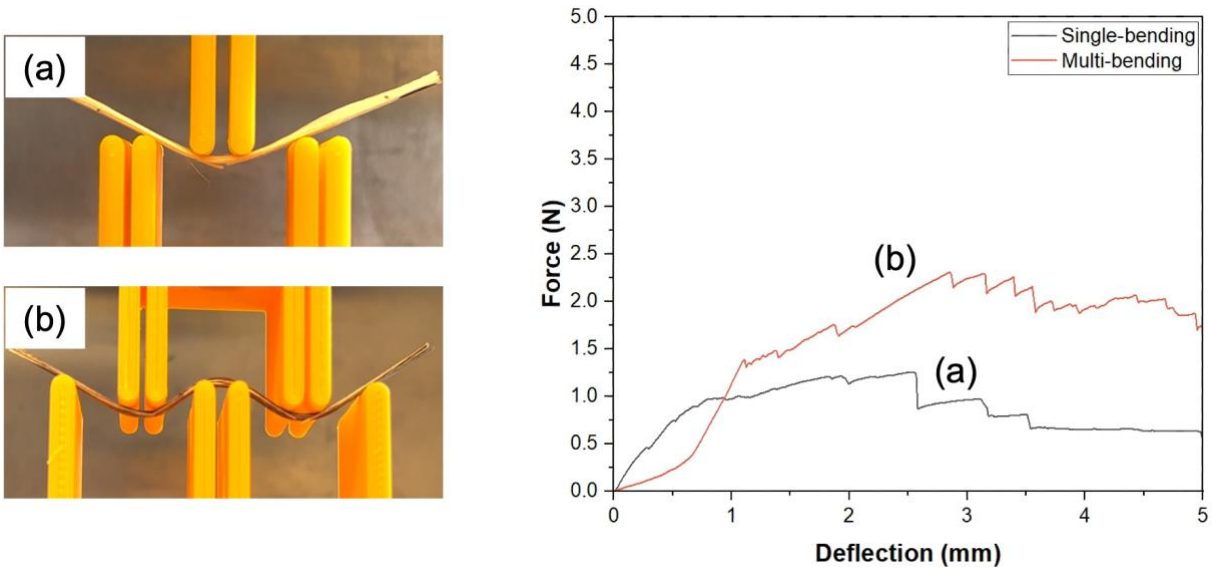

Figure 5.2 (a) Single 4-point bending comparison to (b) multiple 4-point bending

5.2.3 Improvements in composite fabrication and fiber property evaluation

The method of evaluating composite and back-fiber properties by rule of mixture used in Chapter 4 is able to provide a quick method for evaluating fiber properties in composites. Still future studies are needed to improve the fabrication method and to reduce the measurement errors

of the sensitive parameters that leads to the observed high variability. The scanning electron micrograph (SEM) of composite cross-section showed porosity, an indication that the fibers are not impregnated well by the current epoxy resin. A better choice of low viscosity resin for composite's matrix can mitigate this issue. Also, an assumption made here was that fibers from different retting conditions have the same density (1.45 g/cc), which has a direct impact over fiber volume fraction, thus affecting composite properties. Hence evaluating the fiber for correct density and volume fraction, which is combined with the improved composite fabrication for uniform dimensions and minimum porosity, can help to reduce the variations and result in a better tensile property.

Bibliography

[1] F. P. La Mantia and M. Morreale, "Green composites: A brief review," *Compos. Part A Appl. Sci. Manuf.*, vol. 42, no. 6, pp. 579–588, Jun. 2011.

[2] H. Ku, H. Wang, N. Pattarachaiyakoop, and M. Trada, "A review on the tensile properties of natural fiber reinforced polymer composites," *Compos. Part B Eng.*, vol. 42, no. 4, pp. 856–873, Jun. 2011.

[3] F. M. AL-Oqla and S. M. Sapuan, "Natural fiber reinforced polymer composites in industrial applications: feasibility of date palm fibers for sustainable automotive industry," *J. Clean. Prod.*, vol. 66, pp. 347–354, Mar. 2014.

[4] M. R. Sanjay, P. Madhu, M. Jawaid, P. Senthamaraikannan, S. Senthil, and S. Pradeep, "Characterization and properties of natural fiber polymer composites: A comprehensive review," *J. Clean. Prod.*, vol. 172, pp. 566–581, 2018.

[5] K. L. Pickering, M. G. A. Efendy, and T. M. Le, "A review of recent developments in natural fibre composites and their mechanical performance," *Compos. Part A Appl. Sci. Manuf.*, vol. 83, pp. 98–112, 2016.

[6] D. J. Carr *et al.*, "A review of recent developments in natural fibre composites and their mechanical performance," *Compos. Part A Appl. Sci. Manuf.*, vol. 83, no. 9, pp. 98–112, Feb. 2003.

[7] L. Yusriah, S. M. Sapuan, E. S. Zainudin, and M. Mariatti, "Characterization of physical, mechanical, thermal and morphological properties of agro-waste betel nut (Areca catechu) husk fibre," *J. Clean. Prod.*, vol. 72, pp. 174–180, Jun. 2014.

[8] T. P. Sathishkumar, P. Navaneethakrishnan, S. Shankar, and R. Rajasekar, "Mechanical properties and water absorption of short snake grass fiber reinforced isophthallic polyester composites," *Fibers Polym.*, vol. 15, no. 9, pp. 1927–1934, Sep. 2014.

[9] P. Wambua, J. Ivens, and I. Verpoest, "Natural fibres: Can they replace glass in fibre reinforced plastics?," *Compos. Sci. Technol.*, vol. 63, no. 9, pp. 1259–1264, 2003.

[10] G. Mehta, A. K. Mohanty, K. Thayer, M. Misra, and L. T. Drzal, "Novel Biocomposites Sheet Molding Compounds for Low Cost Housing Panel Applications," *J. Polym. Environ.*, vol. 13, no. 2, pp. 169–175, Apr. 2005.

[11] X. Li, L. G. Tabil, and S. Panigrahi, "Chemical Treatments of Natural Fiber for Use in

Natural Fiber-Reinforced Composites: A Review," *J. Polym. Environ.*, vol. 15, no. 1, pp. 25–33, Feb. 2007.

[12] B.-H. Lee, H.-J. Kim, and W.-R. Yu, "Fabrication of long and discontinuous natural fiber reinforced polypropylene biocomposites and their mechanical properties," *Fibers Polym.*, vol. 10, no. 1, pp. 83–90, Feb. 2009.

[13] A. Gore and Melcher Media., *An inconvenient truth : the planetary emergency of global warming and what we can do about it*. .

[14] E. Trujillo, M. Moesen, L. Osorio, A. W. Van Vuure, J. Ivens, and I. Verpoest, "Bamboo fibres for reinforcement in composite materials: Strength Weibull analysis," *Compos. Part A Appl. Sci. Manuf.*, vol. 61, pp. 115–125, 2014.

[15] Y. Li, H. Ma, Y. Shen, Q. Li, and Z. Zheng, "Effects of resin inside fiber lumen on the mechanical properties of sisal fiber reinforced composites," *Compos. Sci. Technol.*, vol. 108, pp. 32–40, Feb. 2015.

[16] H. Cheung, M. Ho, and F. Cardona, "Natural fibre-reinforced composites for bioengineering and environmental engineering applications," *Compos. Part B Eng.*, vol. 40, no. 7, pp. 655–663, Oct. 2009.

[17] M. G. Aruan Efendy and K. L. Pickering, "Comparison of harakeke with hemp fibre as a potential reinforcement in composites," *Compos. Part A Appl. Sci. Manuf.*, vol. 67, pp. 259–267, Dec. 2014.

[18] K. L. Pickering and M. Institute of Materials, *Properties and performance of natural-fibre composites*. CRC Press, 2008.

[19] K. L. Pickering, G. W. Beckermann, S. N. Alam, and N. J. Foreman, "Optimising industrial hemp fibre for composites," *Compos. Part A Appl. Sci. Manuf.*, vol. 38, no. 2, pp. 461–468, Feb. 2007.

[20] H. L. Bos, M. J. A. Van Den Oever, and O. C. J. J. Peters, "Tensile and compressive properties of flax fibres for natural fibre reinforced composites," *J. Mater. Sci.*, vol. 37, no. 8, pp. 1683–1692, 2002.

[21] E. Zini and M. Scandola, "Green composites: An overview," *Polym. Compos.*, vol. 32, no. 12, pp. 1905–1915, Dec. 2011.

[22] D. B. Dittenber and H. V. S. GangaRao, "Critical review of recent publications on use of natural composites in infrastructure," *Compos. Part A Appl. Sci. Manuf.*, vol. 43, no. 8, pp. 1419–1429, Aug. 2012.

[23] I. M. De Rosa, J. M. Kenny, D. Puglia, C. Santulli, and F. Sarasini, "Tensile behavior of New Zealand flax (Phormium tenax) fibers," *J. Reinf. Plast. Compos.*, vol. 29, no. 23, pp. 3450–3454, Dec. 2010.

[24] H. L. Bos., "The Potential of Flax Fibres as Reinforcement for Composite Materials," Eindhoven University of Technology, 2004.

[25] R. F. Evert, K. Esau, and K. Esau, *Esau's Plant anatomy : meristems, cells, and tissues of the plant body : their structure, function, and development*. Wiley-Interscience, 2006.

[26] A. Bourmaud, J. Beaugrand, D. U. Shah, V. Placet, and C. Baley, "Towards the design of high-performance plant fibre composites," *Prog. Mater. Sci.*, vol. 97, no. July 2017, pp. 347–408, 2018.

[27] L. Q. N. Tran, T. N. Minh, C. A. Fuentes, T. T. Chi, A. W. Van Vuure, and I. Verpoest, "Investigation of microstructure and tensile properties of porous natural coir fibre for use in composite materials," *Ind. Crops Prod.*, vol. 65, pp. 437–445, Mar. 2015.

[28] N. Defoirdt *et al.*, "Assessment of the tensile properties of coir, bamboo and jute fibre," *Compos. Part A Appl. Sci. Manuf.*, vol. 41, no. 5, pp. 588–595, May 2010.

[29] A. V. Snegireva, T. A. Gorshkova, M. V. Ageeva, M. Ebskamp, T. E. Chernova, and S. I. Amenitskii, "Intrusive growth of sclerenchyma fibers," *Russ. J. Plant Physiol.*, vol. 57, no. 3, pp. 342–355, 2010.

[30] N. Mokshina *et al.*, "Key Stages of Fiber Development as Determinants of Bast Fiber Yield and Quality," *Fibers*, vol. 6, no. 2, p. 20, Apr. 2018.

[31] V. V. Salnikov, N. N. Ibragimova, O. V. Sautkina, P. V. Mikshina, T. E. Chernova, and T. A. Gorshkova, "Development of distinct cell wall layers both in primary and secondary phloem fibers of hemp (Cannabis sativa L.)," *Ind. Crops Prod.*, vol. 117, no. January, pp. 97–109, 2018.

[32] P. S. Mukherjee and K. G. Satyanarayana, "Structure and properties of some vegetable fibres Part 1 Sisal fibre," 1984.

[33] A. . Bledzki and J. Gassan, "Composites reinforced with cellulose based fibres," *Prog. Polym. Sci.*, vol. 24, no. 2, pp. 221–274, May 1999.

[34] M. S. Zamil and A. Geitmann, "The middle lamella - More than a glue," *Phys. Biol.*, vol. 14, no. 1, p. aa5ba5, 2017.

[35] L. Taiz, E. Zeiger, I. M. (Ian M. Møller, and A. S. Murphy, *Fundamentals of plant physiology*. 2003.

[36] P. Scott, *Physiology and behaviour of plants*. John Wiley & Sons, 2008.

[37] H. L. Bos and A. M. Donald, "In situ ESEM study of the deformation of elementary flax fibres," *J. Mater. Sci.*, vol. 34, no. 13, pp. 3029–3034, 1999.

[38] C. Baley, C. Goudenhooft, P. Perré, P. Lu, F. Pierre, and A. Bourmaud, "Compressive strength of flax fibre bundles within the stem and comparison with unidirectional

flax/epoxy composites," *Ind. Crops Prod.*, vol. 130, no. December 2018, pp. 25–33, 2019.

[39] I. Van de Weyenberg, J. Ivens, A. De Coster, B. Kino, E. Baetens, and I. Verpoest, "Influence of processing and chemical treatment of flax fibres on their composites," *Compos. Sci. Technol.*, vol. 63, no. 9, pp. 1241–1246, Jul. 2003.

[40] K. H. Song and S. K. Obendorf, "Chemical and Biological Retting of Kenaf Fibers," *Text. Res. J. Artic. Text. Res. J.*, vol. 76, no. 10, pp. 751–756, 2006.

[41] W. J. M. Meijer, N. Vertregt, B. Rutgers, and M. van de Waart, "The pectin content as a measure of the retting and rettability of flax," *Ind. Crops Prod.*, vol. 4, no. 4, pp. 273–284, Dec. 1995.

[42] J. De Prez, A. W. Van Vuure, J. Ivens, G. Aerts, and I. Van de Voorde, "Enzymatic treatment of flax for use in composites," *Biotechnol. Reports*, vol. 20, p. e00294, 2018.

[43] J. De Prez, A. W. Van Vuure, J. Ivens, G. Aerts, and I. Van de Voorde, "Effect of enzymatic treatment of flax on fineness of fibers and mechanical performance of composites," *Compos. Part A Appl. Sci. Manuf.*, vol. 123, pp. 190–199, Aug. 2019.

[44] S. Hanana, A. Elloumi, V. Placet, H. Tounsi, H. Belghith, and C. Bradai, "An efficient enzymatic-based process for the extraction of high-mechanical properties alfa fibres," *Ind. Crops Prod.*, vol. 70, pp. 190–200, 2015.

[45] N. Martin, N. Mouret, P. Davies, and C. Baley, "Influence of the degree of retting of flax fibers on the tensile properties of single fibers and short fiber/polypropylene composites," *Ind. Crops Prod.*, vol. 49, pp. 755–767, Aug. 2013.

[46] R. N. Hobson, ; D G Hepworth, and ; D M Bruce, "Quality of Fibre Separated from Unretted Hemp Stems by Decortication," *J. agric. Engng Res*, vol. 78, no. 2, pp. 153–158, 2001.

[47] L. Heinrich, "Linen : from flax seed to woven cloth," p. 232, 2010.

[48] M. Atton, "Flax culture : from flower to fabric," p. 96, 1989.

[49] R. R. Franck and Textile Institute (Australia), *Bast and other plant fibres*. Woodhead, 2005.

[50] A. Le Duigou, P. Davies, and C. Baley, "Environmental Impact Analysis of the Production of Flax Fibres to be Used as Composite Material Reinforcement," *J. Biobased Mater. Bioenergy*, vol. 5, no. 1, pp. 153–165, Mar. 2011.

[51] G. Coroller *et al.*, "Effect of flax fibres individualisation on tensile failure of flax/epoxy unidirectional composite," *Compos. Part A Appl. Sci. Manuf.*, vol. 51, pp. 62–70, Aug. 2013.

[52] J. Müssig, Ed., *Industrial Applications of Natural Fibres*. Chichester, UK: John Wiley &

Sons, Ltd, 2010.

[53] M. Grégoire *et al.*, “Comparing flax and hemp fibres yield and mechanical properties after scutching/hackling processing,” *Ind. Crops Prod.*, vol. 172, p. 114045, Nov. 2021.

[54] X. Zeng, S. J. Mooney, and C. J. Sturrock, “Assessing the effect of fibre extraction processes on the strength of flax fibre reinforcement,” *Compos. Part A Appl. Sci. Manuf.*, vol. 70, pp. 1–7, 2015.

[55] A. Bourmaud, C. Morvan, A. Bouali, V. Placet, P. Perré, and C. Baley, “Relationships between micro-fibrillar angle, mechanical properties and biochemical composition of flax fibers,” *Ind. Crops Prod.*, vol. 44, pp. 343–351, Jan. 2013.

[56] H. S. S. Sharma, G. Faughey, and G. Lyons, “Comparison of physical, chemical, and thermal characteristics of water-, dew-, and enzyme-retted flax fibers,” *J. Appl. Polym. Sci.*, vol. 74, no. 1, pp. 139–143, Oct. 1999.

[57] J. De Prez, A. W. Van Vuure, J. Ivens, G. Aerts, and I. Van de Voorde, “Effect of enzymatic treatment of flax on ease of fiber extraction and chemical composition,” *BioResources*, vol. 14, pp. 1–16, 2019.

[58] V. Placet, A. Day, and J. Beaugrand, “The influence of unintended field retting on the physicochemical and mechanical properties of industrial hemp bast fibres,” *J. Mater. Sci.*, vol. 52, no. 10, pp. 5759–5777, May 2017.

[59] G. Coroller *et al.*, “Effect of flax fibres individualisation on tensile failure of flax/epoxy unidirectional composite,” *Compos. Part A Appl. Sci. Manuf.*, vol. 51, pp. 62–70, Aug. 2013.

[60] P. Ruan, V. Raghavan, J. Du, Y. Gariepy, D. Lyew, and H. Yang, “Effect of radio frequency pretreatment on enzymatic retting of flax stems and resulting fibers properties,” *Ind. Crops Prod.*, vol. 146, p. 112204, Apr. 2020.

[61] P. Ruan, J. Du, Y. Gariepy, and V. Raghavan, “Characterization of radio frequency assisted water retting and flax fibers obtained,” *Ind. Crops Prod.*, vol. 69, pp. 228–237, 2015.

[62] S. Réquilé, A. Le Duigou, A. Bourmaud, and C. Baley, “Peeling experiments for hemp retting characterization targeting biocomposites,” *Ind. Crops Prod.*, vol. 123, no. March, pp. 573–580, 2018.

[63] D. E. Akin, R. B. Dodd, and J. A. Foulk, “Pilot plant for processing flax fiber,” *Ind. Crops Prod.*, vol. 21, no. 3, pp. 369–378, May 2005.

[64] D. E. Akin, B. Condon, M. Sohn, J. A. Foulk, R. B. Dodd, and L. L. Rigsby, “Optimization for enzyme-retting of flax with pectate lyase,” *Ind. Crops Prod.*, vol. 25, no. 2, pp. 136–146, Feb. 2007.

[65] M. Alcock, S. Ahmed, S. DuCharme, and C. Ulven, “Influence of Stem Diameter on Fiber Diameter and the Mechanical Properties of Technical Flax Fibers from Linseed Flax,” *Fibers*, vol. 6, no. 1, p. 10, 2018.

[66] A. B. Bevitori, I. L. A. Da Silva, F. P. D. Lopes, and S. N. Monteiro, “Diameter dependence of tensile strength by Weibull analysis: Part II jute fiber,” *Matéria (Rio Janeiro)*, vol. 15, no. 2, pp. 117–123, 2011.

[67] C. Baley, “Influence of kink bands on the tensile strength of flax fibers,” *J. Mater. Sci.*, vol. 39, no. 1, pp. 331–334, Jan. 2004.

[68] J. Beaugrand, S. Guessasma, and J. E. Maigret, “Damage mechanisms in defected natural fibers,” *Sci. Rep.*, vol. 7, no. 1, pp. 1–7, 2017.

[69] T. Hänninen, A. Thygesen, S. Mehmood, B. Madsen, and M. Hughes, “Mechanical processing of bast fibres: The occurrence of damage and its effect on fibre structure,” *Ind. Crops Prod.*, vol. 39, no. 1, pp. 7–11, 2012.

[70] A. Hernandez-Estrada, H.-J. Gusovius, J. Müssig, and M. Hughes, “Assessing the susceptibility of hemp fibre to the formation of dislocations during processing,” *Ind. Crops Prod.*, vol. 85, pp. 382–388, Jul. 2016.

[71] S. Wang *et al.*, “Assessment system to characterise and compare different hemp varieties based on a developed lab-scaled decortication system,” *Ind. Crops Prod.*, vol. 117, no. September 2017, pp. 159–168, 2018.

[72] J. Xu, “Analysis and Design of Hemp Fibre Decorticators,” The University of Manitoba, 2010.

[73] M. Olan, A. Zaica, A. Paun, and P. Gageanu, “CONSTRUCTIVE OPTIMIZATION BY METHOD OF FINITE ELEMENT ANALYSIS OF HEMP FIBRE PROCESSING EQUIPMENT.”

[74] J. D. Wei Hu, Minh-Tan Ton-That, Florence Perrin-Sarazin, “An Improved Method for Single Fiber Tensile Test of Natural Fibers,” *Society*, pp. 1–10, 2006.

[75] F. Islam, S. Joannès, and L. Laiarinandrasana, “Evaluation of critical parameters in tensile strength measurement of single fibres,” *J. Compos. Sci.*, vol. 3, no. 3, 2019.

[76] D. Depuydt, K. Hendrickx, W. Biesmans, J. Ivens, and A. W. Van Vuure, “Digital image correlation as a strain measurement technique for fibre tensile tests,” *Compos. Part A Appl. Sci. Manuf.*, vol. 99, pp. 76–83, 2017.

[77] N. Soatthiyanon, A. Crosky, and M. T. Heitzmann, “Comparison of Experimental and Calculated Tensile Properties of Flax Fibres,” *J. Compos. Sci.*, vol. 6, no. 4, p. 100, 2022.

[78] C. Baley, M. Gomina, J. Breard, A. Bourmaud, and P. Davies, “Variability of mechanical properties of flax fibres for composite reinforcement. A review,” *Ind. Crops Prod.*, vol.

145, p. 111984, Mar. 2020.

[79] A. Bourmaud, C. Morvan, and C. Baley, “Importance of fiber preparation to optimize the surface and mechanical properties of unitary flax fiber,” *Ind. Crops Prod.*, vol. 32, no. 3, pp. 662–667, Nov. 2010.

[80] H. S. S. Sharma and C. F. van. Sumere, *The Biology and processing of flax*. M Publications, 1990.

[81] D. E. Akin, J. A. Foulk, R. B. Dodd, and D. D. McAlister, “Enzyme-retting of flax and characterization of processed fibers,” *J. Biotechnol.*, vol. 89, no. 2–3, pp. 193–203, Aug. 2001.

[82] J. De Prez, A. W. Van Vuure, J. Ivens, G. Aerts, and I. Van de Voorde, “Flax treatment with strategic enzyme combinations: Effect on fiber fineness and mechanical properties of composites,” *J. Reinf. Plast. Compos.*, vol. 39, no. 5–6, pp. 231–245, 2020.

[83] F. P. De França, J. A. Rosemberg, and A. M. De Jesus, “ Retting of Flax by Aspergillus niger ,” *Appl. Microbiol.*, vol. 17, no. 1, pp. 7–9, 1969.

[84] Y. Yu and P. Wang, “Bioprocessing of bast fibers,” *Adv. Text. Biotechnol.*, pp. 1–19, Jan. 2019.

[85] S. Anne, “Hemp fibres: enzymatic effect of microbial processing on fibre bundle structure,” 2013.

[86] S. K. Kovur, K. C. Schenzel, E. Grimm, and W. Diepenbrock, “Characterization of refined hemp fibers using NIR FT Raman micro spectroscopy and environmental scanning electron microscopy,” *BioResources*, vol. 3, no. 4, pp. 1081–1091, 2008.

[87] S. Majumdar, A. B. Kundu, S. Dey, and B. L. Ghosh, “Enzymatic retting of jute ribbons,” *Int. Biodeterior.*, vol. 27, no. 3, pp. 223–235, 1991.

[88] D. E. Akin, R. B. Dodd, W. Perkins, G. Henriksson, and K.-E. L. Eriksson, “Spray Enzymatic Retting: A New Method for Processing Flax Fibers,” *Text. Res. J.*, vol. 70, no. 6, pp. 486–494, Jun. 2000.

[89] B. Chabbert *et al.*, “Multimodal assessment of flax dew retting and its functional impact on fibers and natural fiber composites,” *Ind. Crops Prod.*, vol. 148, no. January, p. 112255, 2020.

[90] L. Bleuze, G. Lashermes, G. Alavoine, S. Recous, and B. Chabbert, “Tracking the dynamics of hemp dew retting under controlled environmental conditions,” *Ind. Crops Prod.*, vol. 123, pp. 55–63, Nov. 2018.

[91] A. Singhal, A. Langhorst, A. Bansal, M. Banu, and A. Taub, “Optimization of Retting and Extraction Through Constitutive Material Modelling of Plant Stems for Variability Reduction in Extracted Natural Fibers,” *Proc. Am. Soc. Compos. Tech. Conf. Compos.*

Mater., vol. 0, no. 0, pp. 1673–1687, 2021.

[92] A. Lefeuvre, A. Bourmaud, and C. Baley, "Optimization of the mechanical performance of UD flax/epoxy composites by selection of fibres along the stem," *Compos. Part A Appl. Sci. Manuf.*, vol. 77, pp. 204–208, 2015.

[93] J. Militký, R. Mishra, and H. Jamshaid, "Basalt fibers," *Handb. Prop. Text. Tech. Fibres*, pp. 805–840, Jan. 2018.

[94] G. L. Miller, "Use of Dinitrosalicylic Acid Reagent for Determination of Reducing Sugar," *Anal. Chem.*, vol. 31, no. 3, pp. 426–428, 1959.

[95] J. Zhang, G. Henriksson, and G. Johansson, "Polygalacturonase is the key component in enzymatic retting of flax," *J. Biotechnol.*, vol. 81, no. 1, pp. 85–89, 2000.

[96] C. Baley, M. Gomina, J. Breard, A. Bourmaud, and P. Davies, "Variability of mechanical properties of flax fibres for composite reinforcement. A review," *Ind. Crops Prod.*, vol. 145, no. September, p. 111984, 2020.

[97] L. Guzman, Y. Chen, S. Potter, W. Zhong, and M. Rahman, "Application of stochastic modelling for simulating hemp fibre peeling behaviour," *Can. Biosyst. Eng. / Le Genie des Biosyst. au Canada*, vol. 55, pp. 1–8, 2013.

[98] G. Henriksson *et al.*, "Identification and retting efficiencies of fungi isolated from dew-retted flax in the United States and europe.," *Appl. Environ. Microbiol.*, vol. 63, no. 10, pp. 3950–6, Oct. 1997.

[99] H. L. Bos, J. Müssig, and M. J. A. van den Oever, "Mechanical properties of short-flax-fibre reinforced compounds," *Compos. Part A Appl. Sci. Manuf.*, vol. 37, no. 10, pp. 1591–1604, Oct. 2006.

[100] C. A. Fuentes *et al.*, "Effect of the middle lamella biochemical composition on the non-linear behaviour of technical fibres of hemp under tensile loading using strain mapping," *Compos. Part A Appl. Sci. Manuf.*, vol. 101, pp. 529–542, 2017.

[101] B. Christophe, L. D. Antoine, B. Alain, D. Peter, and N. Michel, "Reinforcement of Polymers by Flax Fibers: Role of Interfaces," *Bio-Based Compos. High-Performance Mater.*, pp. 100–125, 2014.

[102] J. Andersons, E. Poriķe, and E. Spārniņš, "The effect of mechanical defects on the strength distribution of elementary flax fibres," *Compos. Sci. Technol.*, vol. 69, no. 13, pp. 2152–2157, Oct. 2009.

[103] B. Feigel, H. Robles, J. W. Nelson, J. M. S. Whaley, and L. J. Bright, "Assessment of mechanical property variation of as-processed bast fibers," *Sustain.*, vol. 11, no. 9, 2019.

[104] A. Ouaar, I. Doghri, L. Delannay, and J. F. Thimus, *Micromechanics of the deformation and damage of steel fiber-reinforced concrete*, vol. 16, no. 2. 2007.

[105] F. C. Campbell, *Structural Composite Materials*, Illustrate. ASM International, 2010.

[106] F. Bensadoun *et al.*, “Impregnated fibre bundle test for natural fibres used in composites,” *J. Reinf. Plast. Compos.*, vol. 36, no. 13, pp. 942–957, 2017.

[107] M. Liu *et al.*, “Controlled retting of hemp fibres: Effect of hydrothermal pre-treatment and enzymatic retting on the mechanical properties of unidirectional hemp/epoxy composites,” *Compos. Part A Appl. Sci. Manuf.*, vol. 88, pp. 253–262, 2016.

[108] W. H. Morrison, D. D. Archibald, H. S. S. Sharma, and D. E. Akin, “Chemical and physical characterization of water- and dew-retted flax fibers,” *Ind. Crops Prod.*, vol. 12, no. 1, pp. 39–46, 2000.